Loading and coating of microcontainers for oral drug delivery

Mazzoni, Chiara

Publication date:
2019

Document Version
Publisher's PDF, also known as Version of record

DTU Health Tech
Department of Health Technology

Loading and coating of microcontainers for oral drug delivery

Chiara Mazzoni, PhD Thesis January 2019

Loading and coating of microcontainers for oral drug delivery

PhD thesis

Author: Chiara Mazzoni

Supervisor: Anja Boisen
Co-supervisor: Line Hagner Nielsen

DTU Health Technology

Technical University of Denmark

January 2019

Danmarks Grundforskningsfond
Danish National Research Foundation

IDUN

VILLUM FONDEN

Preface

This thesis is presented as a partial requirement for obtaining a PhD degree from the Technical University of Denmark (DTU). The project was founded by the Danish National Research Foundation (grant no. DNRF122) and by the Villum Fonden (grant no. 9301) and was part of the Center for Intelligent Drug Delivery and Sensing Using Microcontainers and Nanomechanics (IDUN).

The research was carried out at the Department of Micro- and Nanotechnology (DTU Nanotech) which is called DTU Health Technology from the 1st of January 2019. Some of the work has been carried out at DTU Food and some at the Department of Pharmacy at the Copenhagen University. The PhD project was supervisioned by Professor Anja Boisen and co-supervised by Researcher Line Hagner Nielsen from January 2016 to January 2019.

Kongens Lyngby,
14th January 2019
Chiara Mazzoni

Acknowledgments

First of all, I would like to acknowledge my main supervisor, Prof. Anja Boisen, who has made possible all the work presented in this thesis. She has always been available, supportive, motivating; she has been a true guide through all the highs and lows. She let me dig into my uncertainties to unveil my strengths. Dr. Line Hagner Nielsen has been not only my co-supervisor, but also a mentor and a friend. She has been always present and she never forgot to ask how the experiments were going even if it was evening or the weekend. In every moment of my PhD, I could always rely on her.

I would like to thank my students: Boris, Anastasia, Jacob, Rasmus and Alvaro. It was a pleasure to supervise you and follow your progress day by day. In teaching you, I have learned more about the project and also, myself.

Thanks to the IDUN group and the whole Nanoprobes group, I had the possibility to work with a lot of colleagues and this has been one of the biggest advantages. Coming from a different background, I have learnt something from each of them. Every morning I knew that, even if the experiment did not work, I had my colleagues to ask for an opinion, help or a smile. I really enjoyed working, crying, laughing, eating, dancing, drinking and playing with all of them. A special thanks goes to Fabio with whom I shared everything (office included) since the first day and to Varadarajan and Morten who have been my pillars when I needed to be lifted up. I am grateful to Jacob, Stine, Juliane, Peter and Christoffer for proof reading the thesis and for the other times they have helped me out (of which there were a lot). Thanks to Oleksii and Roman for letting me discover the "Raman world" and being patient with me.

Everything would have been more difficult without our technicians and administrative staff: Lotte, Christina, Lars, Tine, Louise, Dorthe and Nanna. Julie, and more recently Sanne, have resolved all my doubts and helped me with documents, practicalities and much more; I would like to thank them all for their assistance. A special thanks goes to the DTU Food "family" who welcomed me in their lab and taught an engineer how to work with bacteria. It has been a great experience for me.

Thanks to all my Danish, Italian and international friends for making me feel at home even if I was in a new country. Willy, it has been priceless having an extra office when I needed to let off steam. My old friends Sara, Filippo, Luca and Cristina have supported me, visited me and made me smile even when it was not easy. Alessandra and Eugenia entered in my life and it felt as if I have always known them. To the acquired friends and family from Velo, I would like to say thanks a lot. You welcomed me in the nicest way possible and thanks for all the dinners, holidays and for letting me drive a tractor. To Marco, Corinna, Riccardo and Adele who I consider family, without our moments together I would not have survived the PhD life.

I will never be grateful enough to my mum; she has always believed in me even when I could not. Thanks for always being strong and supportive, mum, despite how far apart we have been. Without Elvira, Mario and Gabriella, life would have been tougher; you held up for me and made me realize that there is always a positive side.

A huge thanks to Matteo, my boyfriend and best friend. The PhD would have been impossible without your shoulder on which I could always rest when I needed. You are my first supporter, applauding my successes and encouraging me when I failed, and always trying to spur me on to constantly improve.

I believe I have matured both as a scientist and as a person and hope to carry this forward. I am proud of how far I have come over the past three years, of how much I have learnt, the confidence I have gained and my acquired taste of red wine and spicy food.

Contents

Abstract

Oral delivery is the most preferred route of administration of drugs by the patients. When a drug is taken orally, its absorption will occur in the small intestine as it provides a high surface area. For example, low gastric pH, enzymes and mucus layer can have a negative impact on the administered active pharmaceutical compound (API). Excipients, mucoadhesive and enteric coatings, and permeation enhancers are all common strategies to facilitate the delivery of the API. Nevertheless, these approaches are not always enough making necessary the development of new oral drug delivery systems.

Recently, microfabricated devices have been explored as alternative oral drug delivery systems to enhance release and absorption of drugs. One of these systems is microcontainers which are polymeric cylindrical microdevices fabricated in epoxy-based photoresist SU-8. They have an external diameter and height of approximately 300 µm. Contrary to the omnidirectional release that is characteristic of loaded formulation tablets, capsules and particulate systems, the unidirectional release provided by microcontainers avoids loss of the API in the lumen.

In this project, the work focused on two main aspects *i*) loading techniques for enhancing oral delivery of poorly water soluble drugs and *ii*) coating the cavity of microcontainers in order to functionalize these for increasing the oral absorption of proteins. In order to enhance the release and absorption of poorly soluble drugs, they were loaded into microcontainers with either polyvinylpyrrolidone (PVP) or polycaprolactone (PCL). It has been showed *in vitro* that the loading technique influences the release of the poorly soluble model drug ketoprofen even when loaded with the same polymer (PCL). In particular, the distribution of the ketoprofen or naproxen loaded into the PVP matrix using supercritical scCO_2 (scscCO_2) impregnation was evaluated. This was possible using a custom-made Raman system, where volumetric Raman maps of a whole microcontainer were obtained. These analyses showed that the drug was on top of the polymer even when the area exposed to the scscCO_2 was changed. Such results confirmed and explained the fast release profiles obtained by *in vitro* analyses. These studies were followed by *in vivo* experiments in rats to fully understand the behavior of the microcontainers *in vivo*. These studies showed an enhanced

relative oral bioavailability compared to control samples. For oral protein delivery, microcontainers were loaded with the model protein, lysozyme together with a permeation enhancer (sodium decanoate). The loaded microcontainers were functionalized by applying on their cavity two polymeric coatings. The idea was to enhance the protein delivery and mucoadhesion of the microcontainers. For these reasons, the first coating was poly(lactic-co-glycolic (PLGA) and on top of this either chitosan or polyethylene glycol (PEG) was applied. The functionalization was evaluated *in vitro* for morphology, drug release and mucoadhesive properties. These were coupled with *in vitro* and *ex vivo* studies using cell models and porcine intestinal tissue. This showed that microcontainers can be functionalized with bi-layer lids facilitating tunable protein release as well as improved mucoadhesion of the microcontainers.

In conclusion, techniques for loading microcontainers with poorly water soluble drugs were compared and characterized. Moreover, microcontainers were functionalized for oral delivery of protein. These results showed a promising potential for microcontainers as oral delivery system for poorly soluble drugs and proteins. Further optimization of the microcontainers and their characterization techniques are however still required in order to improve their efficacy and flexibility.

Resumé

Oral levering af lægemidler er den foretrukne administrationsvej for patienter. Når et lægemiddel indtages oralt, vil dets optagelse forekomme i tyndtarmen, da der her er et stort overfladeareal. For eksempel kan lav pH i maven, enzymer og mucus-laget have en negativ indvirkning på det administrerede lægemiddelstof. Hjælpestoffer, mucoadhæsive og enteriske overtræk og absorptionsfremmere er alle fælles strategier for at lette leveringen af et lægemiddelstof. Ikke desto mindre er disse metoder ikke altid nok, og dette gør det nødvendigt at udvikle nye orale leveringssystemer for lægemidler.

For at forbedre frigivelse og absorption af lægemidler er man for nylig begyndt at undersøge mikrofabrikerede enheder som et alternativt leveringssystem for lægemidler. Et af disse systemer er mikrocontainere, som er polymeriske cylindriske mikroenheder fremstillet i epoxybaseret fotoresist SU-8. De har en ydre diameter og en højde på ca. 300 µm. I modsætning til den omni-direktionelle frigivelse, som er karakteristisk for formuleringstabletter, kapsler og partikelformede systemer, undgår den ensrettede frigivelse, muliggjort af mikrocontainere, tab af API'en i lumen.

Dette projekt var fokuseret på to hovedaspekter *i*) Loading teknikker til forbedring af oral administrerede lægemidler med lav vandopløselighed og *ii*) Belægning af mikrocontainernes hulrum for at funktionalisere disse og dermed øge den orale absorption af proteiner. For at forbedre frigivelsen og absorptionen af lægemidler med lav vandopløselighed, blev de loaded i mikrocontainere lavet af enten polyvinylpyrrolidon (PVP) eller polycaprolacton (PCL). *In vitro* studier har vist, at forskellige loading teknikker har indflydelse på frigivelsen af det lavt-opløselige medikament ketoprofen, på trods af loading med den samme polymer (PCL). Især blev fordelingen af ketoprofen eller naproxen, loaded i PVP-matrixen med superkritisk CO_2 (scCO_2) imprægnering, evalueret. Dette var muligt ved at anvende et skræddersyet Raman-system, hvor der blev opnået volumetriske Raman-kort af hele mikrocontainere. Disse analyser viste, at lægemidlet var oven på polymeren, selvom området udsat for scCO_2 blev ændret. Disse resultater bekræftede og forklarede de hurtige frigivelsesprofiler set ved *in vitro* analyser. Disse undersøgelser blev fulgt af *in vivo* forsøg i rotter, for fuldt ud at forståmikrocontainernes funktion *in vivo*. Disse studier

viste en forbedret relativ oral biotilgængelighed sammenlignet med kontrolprøver. Til oral administration af proteiner blev mikrocontainerne fyldt med modelproteinet lysozym samt en permeationsforstærker (natriumdecanoat). De fyldte mikrocontainere blev funktionaliseret ved på førelsen af to polymere belægninger på hulrummet. Ideen var at øge mikrobeholderens proteinafgivelse og mucoadhæsion. Derfor brugte vi poly (lactic-co-glycolic (PLGA) til første overtræk, hvorefter enten chitosan eller polyethylenglycol (PEG) blev påført. Funktionaliseringen blev evalueret *in vitro* for morfologi, frigivelses- og mucoadhæsive egenskaber. Disse forsøg blev sammenkoblet med *in vitro*- og *ex vivo*-undersøgelser i cellemodeller og porcin tarmvæv. Disse forsøg viste, at mikrocontainere kan funktionaliseres med tolags overtræk, der faciliterer fleksibel proteinfrigivelse, samt forbedre mikrocontainernes mucoadhæsion.

I konklusion teknikker til loading af lægemidler med lav-vandopløselighed i mikrocontainere blev sammenlignet og karakteriseret. Desuden blev mikrocontainerne funktionaliseret til oral levering af protein. Disse resultater viste at mikrocontainere har et lovende potentiale som oral administrationsvej for dårligt opløselige lægemidler og proteiner. Yderligere optimering af mikrocontainerne og deres karakteriseringsteknikker er dog stadig nødvendig for at forbedre både effektivitet og fleksibilitet.

Publications

Paper I

Release of ketoprofen from microcontainers - influence of the loading method

F. Tentor & C. Mazzoni, L. Leonardi, P. Marizza, R.S. Petersen, S.S. Keller, A. Boisen

Submitted to Biomedical Microdevices

Paper II

Where is the drug? - Quantitative 3D distribution analyses of confined drug-loaded polymer matrices

C. Mazzoni, F. Tentor, A. Antalaki, J. Mortensen, R.D. Jacobsen, R. Slipets, O. Ilchenko, S.S. Keller, L.H. Nielsen, A. Boisen

Submitted to ACS Biomaterials Science & Engineering

Paper III

From concept to in vivo testing: Microcontainers for oral drug delivery

C. Mazzoni & F. Tentor, S.A. Strindberg, L.H. Nielsen, S.S. Keller, T.S. Alstrøm, C. Gundlach, A. Müllertz, P. Marizza, A. Boisen

Published on Journal of Controlled Release, vol. 268, pp. 343-351, October 2017

Paper IV

Polymeric Lids for Microcontainers for Oral Protein Delivery

C. Mazzoni, R.D. Jacobsen, J. Mortensen, J.R. Jørgensen, L. Vaut, J. Jacobsen, C. Gundlach, A. Müllertz, L.H. Nielsen, A. Boisen

Submitted to Macromolecular Bioscience

Contribution to the papers

Paper I

I performed part of the experimental work and data analyses in close collaboration with Fabio Tentor. I and Fabio Tentor interpreted the data and wrote the scientific article.

Paper II

I designed the study and performed part of the experiments. Together with Fabio Tentor, I supervisioned Anastasia Antalaki who partially contributed to the experimental work. Line Hagner Nielsen and I supervisioned Rasmus Due Jacobsen and Jacob Mortensen who performed part of the experimental work and the initial data treatment. I performed the final data treatment except for the volumetric Raman data which was done by Roman Slipets. I interpreted the data and wrote the paper.

Paper III

I designed, planned and performed the experiments together with Fabio Tentor. I and Fabio Tentor analyzed part of the data except for the Matlab coding which was done by Tommy Sonne Alstrøm. I interpreted the data and wrote the paper with Fabio Tentor.

Paper IV

I designed the study and the experiments. Line Hagner Nielsen and I supervisioned Rasmus Due Jacobsen and Jacob Mortensen who performed the experiments and did the initial data treatment. I performed the final data treatment, interpreted the data and wrote the paper.

Other contributions

Microcontainers for intestinal drug delivery
F. Tentor, C. Mazzoni, S. S. Keller, P. Marizza, A. Boisen

POSTER at 11th Central European Symposium on Pharmaceutical Technology (CESPT)
September 22 - 24, 2016, Belgrade, Serbia

Microcontainers as effective drug delivery vehicles: advances in the drug loading
P. Marizza, L. Leonardi, C. Mazzoni*, F. Tentor, R. Singh Petersen, Z. Abid, A. Boisen

ORAL PRESENTATION at 11th Central European Symposium on Pharmaceutical Technology (CESPT)
September 22 - 24, 2016, Belgrade, Serbia

Microcontainers for intestinal drug delivery: in vivo and ex vivo study
C. Mazzoni & F. Tentor, S. Strindberg, L. H. Nielsen, S. S. Keller, A. Müllertz, P. Marizza, A. Boisen

ORAL PRESENTATION at Non-Invasive Delivery of Macromolecules Conference 2017
February 21 - 24, 2017, San Diego, CA, USA

Loading of poorly soluble drugs by supercritical CO_2 impregnation into microcontainers for oral drug delivery
C. Mazzoni, A. Antalaki, R. D. Jacobsen, J. Mortensen, F. Tentor, R. Slipets, O. Ilchenko, S. S. Keller, L. H. Nielsen, A. Boisen

ORAL PRESENTATION at Northern Pharma Network Meeting 2018
January 29 - 31, 2018, Odense, Denmark

Loading of poorly soluble drugs by supercritical CO_2 impregnation into microcontainers for oral drug delivery
C. Mazzoni, A. Antalaki, R. D. Jacobsen, J. Mortensen, F. Tentor, R. Slipets, O. Ilchenko, S. S. Keller, L. H. Nielsen, A. Boisen

POSTER at 12th World Meeting on Pharmaceutics, Biopharmaceutics and Pharmaceutical Technology (PBP)
March 19 - 22, 2018, Granada, Spain

Distribution and quantitative analyses of poorly water soluble drugs loaded by supercritical CO_2 impregnation in microcontainers with different sizes
C. Mazzoni, F. Tentor, A. Antalaki, R. Due Jacobsen, J. Mortensen, R. Slipets, O. Ilchenko, S. S. Keller, L. H. Nielsen, A. Boisen

POSTER at 2018 Controlled Release Society Annual Meeting & Exposition (CRS)
July 22 - 24, 2018, New York, NY, USA

Distribution and quantitative analyses of poorly water soluble drugs loaded by supercritical CO_2 impregnation in microcontainers with different sizes
C. Mazzoni,F. Tentor, A. Antalaki, R. Due Jacobsen, J. Mortensen, R. Slipets, O. Ilchenko, S. S. Keller, L. H. Nielsen, A. Boisen

POSTER at Micro Nano Engineering (MNE) 2018
September 24 - 27, 2018, Copenhagen, Denmark

Biodegradable microcontainers: a new oral drug delivery platform
Z. Abid, M. M. Javed, S. Andersen, C. Mazzoni, L. H. Nielsen, C. Gundlach, L. Vaut, R. S. Petersen, A. Müllertz, A. Boisen, S. S. Keller

PAPER IN PROGRESS

List of Abbreviations

2D

Two dimensional

3D

Three dimensional

API

Active pharmaceutical ingredient

BCS

Biopharmaceutics Classification System

C10

Sodium decanoate

DBS

Dibutyl sebacate

EMA

European Medicines Agency

Fc

Fluorocarbon

FDA

Food and Drug Administration

GI

Gastrointestinal

HPLC

High performance liquid chromatography

PAA

Poly(acrylic acid)

PBS

Phosphate-buffered saline

PC

Polycarbonate

PCL

Polycaprolactone

PEG

Polyethylene glycol

PLGA

Poly(lactic-co-glycolic) acid

PLLA

Poly(lactic acid)

PMMA

Poly(methyl methacrylate)

PVP

Polyvinylpyrrolidone

RP-HPLC

Reversed phase-HPLC

scCO_2

Supercritical CO_2

SCF

Supercritical fluid

SE

Secondary electrons

SEM

Scanning electron microscopy

Si

Silicon

T_g

Glass transition temperature

UV

Ultraviolet

UV-vis

Ultraviolet-visible

WHO

World Health Organization

X-ray μCT

X-ray micro computed tomography

XRPD

X-ray powder diffraction

Chapter 1

Introduction

Oral administration is the preferred route of administration for the patient, due to its low invasiveness compared to other routes which require, for example, the use of needles [1]. Between 2013 and 2018 almost 50% of the approved pharmaceutical formulations on the market and more than 40% of the products in pipeline are for oral drug delivery [2]. These percentages indicate that there is a big market and a wide interest in oral drug delivery research.

Design of an oral drug delivery formulation can be rather complex. Despite the fact that the gastrointestinal (GI) tract has a total surface of 1000 m^2, representing a unique interface between the external environment and the interior of the body, its anatomy and physiology represent an obstacle for pathogens and toxins as well as drugs [3]. The fluids in the GI tract, the presence of mucus and the intestinal cell barrier all cause big challenges to overcome, especially for specific active pharmaceutical ingredient (API)s, like poorly water soluble drugs and therapeutic peptides and proteins [4, 5]. The most common parameter to evaluate if an oral pharmaceutical product is effective is called *oral bioavailability*. It indicates the ratio between the amount of API reaching the systemic circulation and the dose administered [6]. For all the reasons mentioned above, approximately 50% of the APIs suffer from low oral bioavailability [7]. The strategies to overcome such problems are multiple and every API requires a different formulation, with specific features to improve its oral bioavailability. The most common approaches include excipients, permeation enhancers, micro- and nanoparticulate systems, drug modification, protein inhibitors and enteric or mucoadhesive coatings [7, 8, 9, 10, 11].

All the aforementioned approaches are not always enough to enhance the oral uptake. In this project, microfabricated devices called *microcontainers* are proposed as carriers for APIs. These microdevices have a cylindrical shape and a cavity which can be used for the loading of APIs. One of the biggest and most important differences compared to traditional oral drug

delivery systems is that microcontainers allow unidirectional drug release, since only one surface of the microdevice can open. This feature can reduce the loss of API in the lumen [12]. It was observed that microcontainers engulf themselves in the intestinal mucus [13]. This phenomenon allows microcontainers to be closer to the intestinal barrier than formulations staying in the lumen. Moreover, coatings can be applied on top of the microsized cylinders to release the API in the area of interest, most often the intestine [13].

Before the start of this project, various studies have been conducted in order to discover and characterize the potential of microcontainers for oral drug delivery. The most relevant, in respect to this project, is the one carried out by Nielsen et al., which showed that microcontainers improved the relative oral bioavailalbility of furosemide (Class IV in the Biopharmaceutics Classification System (BCS)) *in vivo* compared to the drug in a capsule [13].

In the pharmaceutical field, all the loading techniques developed and commonly used are for traditional drug delivery systems, such as tablets and micro- and nanoparticles. Although microcontainers showed several advantages, their loading can be challenging, since it can be done only from the top, thus requiring great geometrical accuracy and correct alignment of the loading system. In addition, the loading technique needs to be reproducible, avoid drug degradation and waste and, for some APIs, control the solid form of the drug. Therefore, an important study for this project is related to the characterization of a loading technique for microcontainers. This allowed the loading of a poorly water soluble drug into microcontainers and the contemporary transformation of a drug into its amorphous state [14].

These studies were the starting points of this project, leading it to explore and compare different loading techniques and to use microcontainers as an oral delivery system for proteins.

1.1 Aims of the project

The aims of this PhD project were to apply microcontainers as oral delivery systems for *i*) poorly soluble drugs and *ii*) therapeutic peptides and proteins.

To improve the bioavailability of poorly soluble drugs, microcontainers should *i*) be loaded with a formulation that improves solubility and stability of the API and *ii*) be sealed with coatings preventing enzymatic degradation and release in the stomach. For these reasons, the focus was on the comparison and characterization of techniques used for the loading of microcontainers. In addition, various combinations of polymer excipients and poorly soluble drugs were evaluated.

As regards to the delivery of therapeutic peptides and proteins, microcontainers should *i*) contain a permeation enhancer to help the protein being

transported across the intestinal wall, *ii*) be functionalized to improve the release of the protein in the intestinal environment and *iii*) be coated with a mucoadhesive polymer to have a release in proximity to the intestinal barrier. In this case, the approach is directed to the functionalization of microcontainers, in order to provide mucoadhesiveness and an enhancement of the protein absorption. To this end, particular focus was devoted to the characterization of the polymers used for the double coating of the microcontainers.

To achieve these goals, two major accomplishments needed to be completed. First, loading techniques were tested and compared using, mainly, *in vitro* release studies and, in case of drug distribution analyses, Raman spectroscopy. These were followed by *in vivo* studies. Second, microcontainers needed to be functionalized for oral protein delivery. This included exploring the possibility of applying more than one coating on the microcontainers and to test them *in vitro* and *ex vivo*.

1.2 Outline of the thesis

This thesis is structured in seven chapters. This introductory chapter is followed by four chapters providing the background and an overall description of the PhD project. Specifically, Chapter 2 reports a brief description of the advantages and challenges of oral drug delivery. In Chapter 3, challenges and strategies used to orally deliver poorly water soluble drugs and therapeutic proteins are presented, followed by a description of microdevices. Chapters 4 presents microcontainers as an oral drug delivery system, describing the fabrication, loading and coating techniques. In Chapter 5, all the characterization techniques for microcontainers used during the project are illustrated. The on-going projects are briefly described in Chapter 6. The thesis is completed with the conclusions and future perspectives in Chapter 7.

In all the chapters, the terms “API” and “drug” have been used as synonyms for simplicity. Moreover, for the same reason, “therapeutic peptides and proteins” are often mentioned as either “peptides” or “proteins” according to the context.

Chapter 2

Oral drug delivery

A drug can be administered by different routes of administration. These are defined as the path by which a drug is delivered in the body. By changing this route, the number of biological barriers that the API must cross before reaching the targeted area will change. The routes of administration can be classified according to if they are invasive or not (Figure 2.1). Invasive administration refers to, for example, intravenous, intramuscular and subcutaneous routes. The non-invasive route are, for example, oral, nasal and transdermal [15, 16].

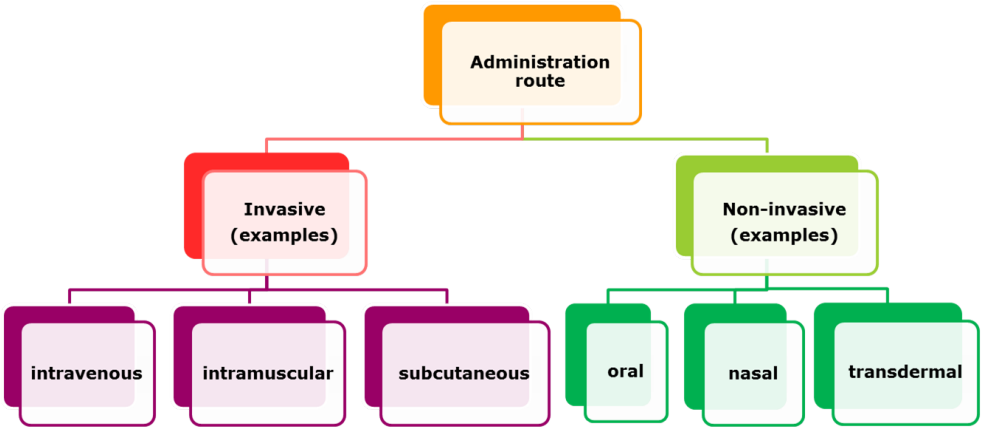

Figure 2.1: *Schematic of administration routes examples.*

Oral drug delivery is the route in which the API is taken through the mouth. Before entering into the portal circulation, from where the API will reach the desired site, the drug is exposed to different environments [15]. The advantages and disadvantages of this route will be explained in the following sections.

2.1 Advantages

The oral route of administration is the most preferred route from the point of view of the patient and therefore often leads to improved compliance [17]. The main reason for this is that swallowing a tablet is the same natural action as swallowing foods or liquids. Moreover, compared to injections, the oral route is painless and allows self-administration, with no need of training or specialized personnel [1, 18]. Formulations for oral drug delivery do not require strict sterility constraints as, for example, needles for intravenous or intramuscular dosage forms allowing to have higher degree of flexibility [19]. These formulations are also often easy to transport due to their stability. This is particularly advantageous in underdeveloped countries where the means of transport are often poor. Consequently, for all the reasons just mentioned, formulations for the oral route are most often the cheapest among all the available dosage forms [20, 21] and the most preferred way to administer APIs [17].

As mentioned in the introductory chapter, the GI tract, having a surface area of around 1000 m^2, provides a unique interface between the external environment and the interior of the body. Nevertheless, the anatomy and physiology of the GI tract present many obstacles that impair the absorption of pathogens, toxins as well as drugs [3].

2.2 Challenges

The role of the GI tract is to digest liquids and food, absorb the nutrients and excrete what is recognized as toxic for the body. Therefore, the GI tract plays an important role in the oral administration of APIs. For this reason, the drug formulation needs to be designed taking into account the physical and chemical properties of the GI tract [22].

2.2.1 Gastrointestinal tract physiology

Orally administered drugs go through the GI tract, which is divided into the upper and lower tract. The upper GI tract consists of the oral cavity, esophagus, stomach, and the small intestine, whereas the large intestine and the rectum are part of the lower GI tract (Figure 2.2) [3].

The digestion of food starts in the mouth where it is chewed and mixed with degradation enzymes. However, the transit through the mouth is fast and therefore the first organ they encounter for digestion is the stomach. Gastric acid and digestive enzymes break down the ingested food to allow it to pass through the pyloric sphincter and enter into the small intestine. The pH values in the GI tract can vary according to diet, age and sex. In the fasted state, in the stomach, the pH is below 3 (Table 2.1) and therefore only few molecules are absorbed there [23]. The small intestine is designed for

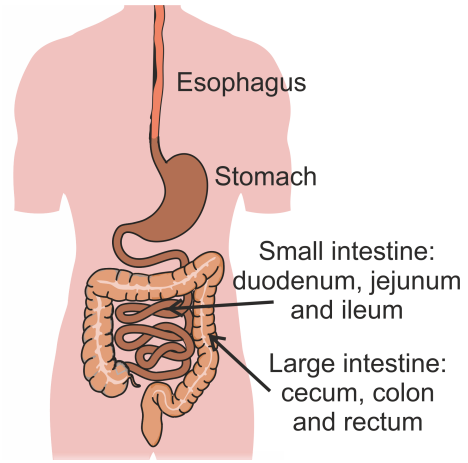

Figure 2.2: *Anatomy of the human GI tract. The main GI areas interested in the digestion and absorption are represented: esophagus, stomach, small intestine (duodenum, jejunum and ileum) and large intestine (cecum, colon and rectum).*

absorption of nutrients and is divided into duodenum, jejunum and ileum. Duodenum is the first and shortest section (Table 2.1) in which the material coming from the stomach is mixed with pancreatic digestive fluids and liver bile. The material that is not absorbed in the small intestine, is led to the colon through the ileocecal valve [24].

Table 2.1: *Biological and physical parameters of all the gastrointestinal segments. Adapted from [25, 26, 27].*

Gastrointestinal segment	**Approximate surface area**	**Approximate segment length**	**Approximate pH**
Oral cavity	100 cm^2		
Esophagus	200 cm^2	23 - 25 cm	
Stomach	3.5 m^2	0.25 cm	< 3
Duodenum	1.9 m^2	0.35 m	6.4
Jejunum	184 m^2	2.8 m	7
Ileum	276 m^2	4.2 m	7.3
Colon and rectum	1.3 m^2	1.5 m	5.7 - 6.6

In fact, 90% of the absorption takes place in the jejunum and ileum and this is due to, among others factors, the large surface area and the high density of enzymes. The internal surface of the small intestine presents three types of projections: plicae, villi and microvilli; all three increase the surface area of the small intestine by 3, 30 and 600-fold, respectively (Figure 2.3)

[28, 29]. Overall, the surface area of duodenum, jejunum and ileum is around 500 m^2 (Table 2.1). Enzymes are responsible for breaking down proteins into small peptides and amino acids, lipids into fatty acids and glycerol, and some carbohydrates into simple sugars or monosaccharides [25]. The absorption is also assisted from peristaltic movements that are particularly pronounced in the small intestine [30]. The large intestine is responsible for absorbing water and, therefore, solidification of the content into feces [30].

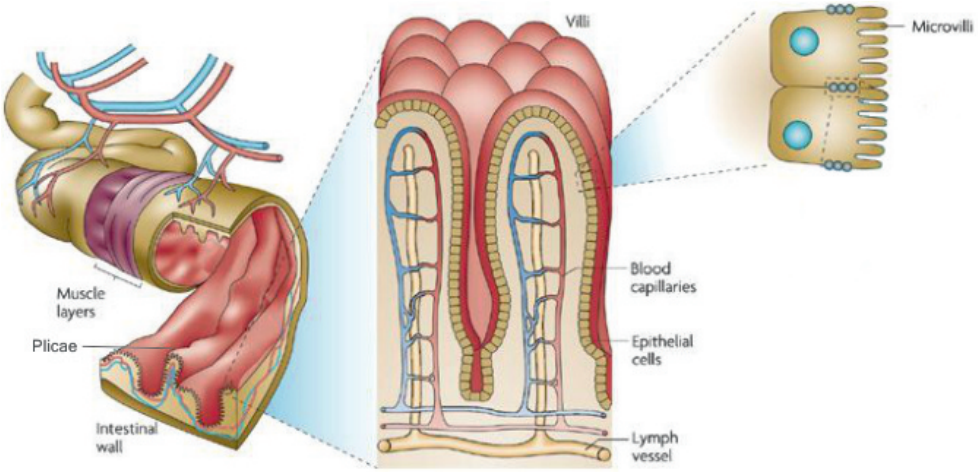

Figure 2.3: *Illustration of the composition of the small intestinal walls. From left: the plicae, villi and microvilli. They are responsible for increasing the absorption area by 3, 30 and 600 fold, respectively. Reprinted from [31] with permission.*

2.2.2 Mucus layer

The internal surface of the GI tract is covered by mucus, produced mainly by goblet cells. The mucus consists of more than 98% of water together with various mucin glycoproteins, enzymes and electrolytes [28, 32]. The most important structural component of the mucus gel are the mucin glycoproteins giving it its characteristic gel-like, adhesive and cohesive properties [33]. The mucus has different thicknesses and roles in the stomach, small intestine and colon (Figure 2.4).

In some areas, mucus is composed of two layers, one that is firmly adherent (closer to the epithelium) and one that is loosely adherent. In the small intestine, the mucus provides a diffusion barrier since it usually fills the luminal space between and on top of the villi [34]. Therefore, the designed API formulation needs to reach the epithelial layer penetrating the mucus.

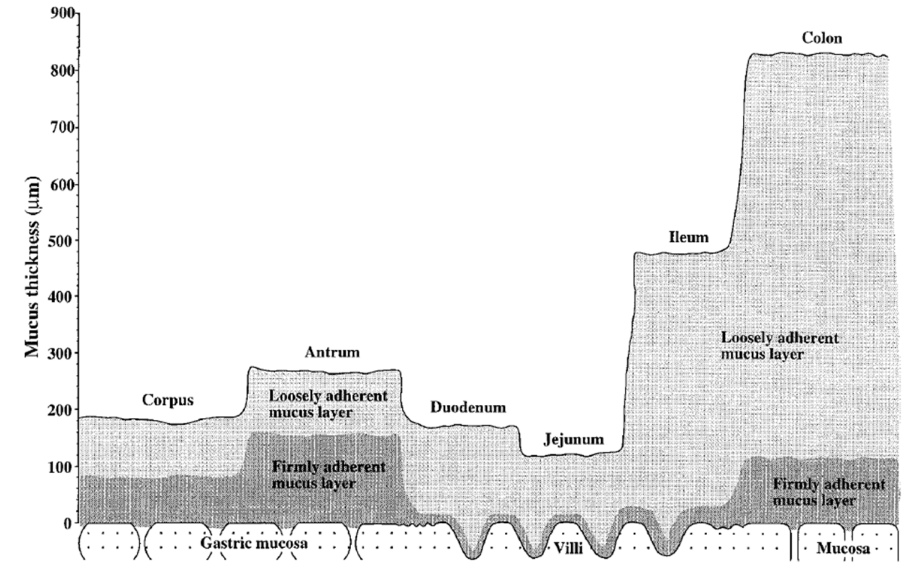

Mean mucus thickness (µm)	Corpus	Antrum	Duodenum	Jejunum	Ileum	Colon
Total	189 ± 11	274 ± 41	170 ± 38	123 ± 4	480 ± 47	830 ± 110
Firmly Adherent	80 ± 5	154 ± 16	16 ± 3	15 ± 2	29 ± 8	116 ± 51
Loosely Adherent	109 ± 12	120 ± 38	154 ± 39	108 ± 5	447 ± 47	714 ± 109
n	6	6	7	6	5 (8 firm)	11

Figure 2.4: *Schematic of the thicknesses of the loosely adherent and firmly adherent mucus layers measured in the stomach, duodenum, jejunum, ileum and colon of a rat. The adherent mucus layer is close to the epithelium and the loosely adherent layer is on top. The table shows the mean of the mucus thickness as µm ± SD. Reprinted from [34] with permission.*

2.2.3 Cellular pathways for absorption

After penetrating the mucus, the compound needs to be transported across the epithelial barrier to be able to reach the portal circulation. This barrier is composed of a single layer of epithelial cells which, depending on the GI area, vary in number. In the small intestine, the enterocytes are the most abundant cell type and they are responsible for the absorption of nutrients from the intestine into the blood stream. Other cells are interspersed together with enterocytes in the small intestine (Figure 2.5) [32]. For example, goblet cells secrete mucus and paneth cells, antibacterial peptides and proteins (Figure 2.5) [32]. All of these cell types and many others are connected with tight junctions creating a separation barrier between the luminal material and the subepithelium [35].

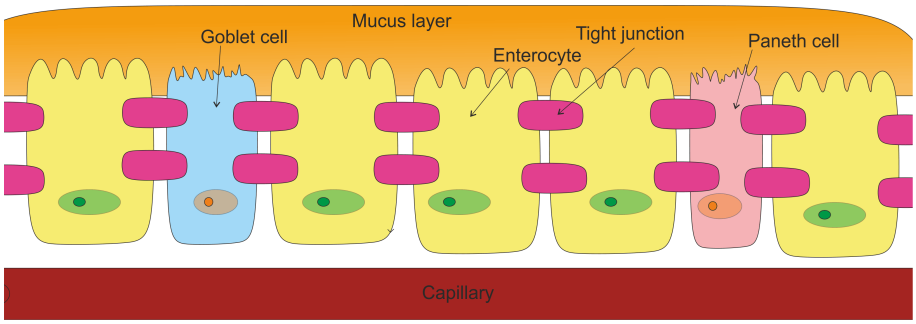

Figure 2.5: *Schematic representing the epithelial barrier showing enterocytes, goblet and paneth cells covered by mucus layer.*

There are two main pathways by which an API can pass from the intestinal lumen to the underlying tissue and into circulation; paracellular transport which is between the cells and transcellular transport where the transport is through the cells (Figure 2.6) [28, 30].

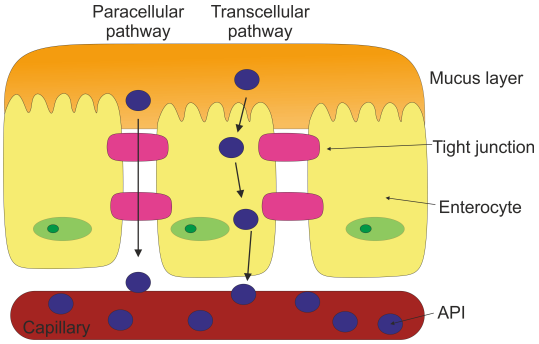

Figure 2.6: *Schematic representing the main pathways for an API to pass from the intestinal lumen to the underlying tissue and circulation: paracellular (left) and transcellular (right) pathways.*

Transcellular transport is associated with solute transport through the epithelial cells and mainly regulated by selective transporters for amino acids, electrolytes, sugars and short chain fatty acids. This pathway can also be passive when small lipophilic molecules pass through the cell membrane [36]. The paracellular transport is regulated by intercellular complexes, called tight junctions, placed at the apical-lateral membrane junction and along the lateral membrane. For this type of uptake, tight junctions have a fundamental role since they seal the intercellular space, thereby functioning as a selective paracellular barrier [37]. These junctions facilitate ions and solute passage through the intercellular space preventing, at the same time, antigens or toxins to enter [35]. The hostile acidic environment in the stomach, the high enzymatic activity in the small intestine and the intestinal mucosa barrier are inherent features that need to be kept in consideration when designing a drug formulation for oral delivery [28].

Chapter 3

Oral drug formulation

The challenges for oral drug delivery, discussed in the previous chapter, have particularly an impact on specific groups of drugs like, poorly water soluble drugs, and therapeutic proteins and peptides. In the next sections, the reasons of their low bioavailability and strategies commonly applied to improve it will be described. Moreover, microdevices will be described as an alternative and more recent way to deliver poorly soluble drugs or proteins, and to further enhance their bioavailability.

3.1 Poorly water soluble drugs

Considering that solubility and intestinal permeability are the main factors affecting oral bioavailability, the U.S. Food and Drug Administration (FDA) provided the BCS as a guide to predict the intestinal drug absorption (Figure 3.1) [38]. In general, solubility is defined as the property of a solid, liquid or gaseous chemical substance (solute) to dissolve in a solid, liquid or gaseous solvent and form a homogeneous solution of the solute in the solvent [38]. According to the BCS, a drug is classified as highly soluble, when the highest therapeutic dose of the drug is soluble in 250 mL or less of water with a pH ranging from 1 to 7.5. The intestinal permeability, instead, is a classification in which the orally administered compound is compared with the intravenous injection. The BCS divides all drugs in four classes (Figure 3.1). In case of an API with high permeability, it belongs to Class I if it is highly water soluble or in Class II if it is poorly soluble. Instead, when the drug is poorly permeable, it is part of Class III when it is highly soluble and Class IV when it is poorly soluble [39].

Regardless of the great number of novel drug molecules in pipeline, only a few of them have reached the market. This is due to several factors including lack of efficacy, safety and low bioavailability (accounting for around 40% of failures) [40]. Moreover, around 40% of marketed drugs and 70% of compounds currently under development are poorly soluble drugs meaning

that there is a huge need to enhance the solubility of these compounds [41, 42, 43]. If the solubility of the API is low, the desired concentration in the systemic circulation, and consequently, the required pharmacological response are not reached. To overcome this issue, poorly soluble drugs often require higher doses to be able to reach the therapeutic plasma concentration [38].

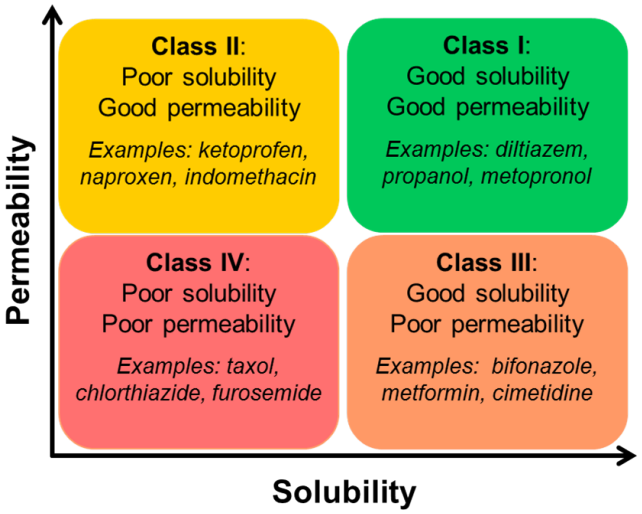

Figure 3.1: *Schematic of the Biopharmaceutics Classification System (BCS) in which drugs are divided in four classes according to their aqueous solubility and intestinal permeability.*

3.1.1 Strategies to improve bioavailability

Solving the solubility issue is one of the biggest challenges for formulation scientists. Depending on the properties of the API and its needed dosage, several techniques have been developed to enhance the solubility [44]. According to the type of modification, these techniques can be divided in three categories [45] (Figure 3.2). Physical modifications refer to changes at the particulate level as particle size reduction, amorphous systems and metastable polymorphs. When the modifications are at a molecular level, they are cassified as chemical modifications including, for example, salt formation, prodrugs, cyclodextrins and co-solvents. The third category is comprised of alterations at the colloidal level such as lipid formulations, emulsions and self-emulsifying drug delivery systems [38, 42]. Amorphous systems are one option among all the modifications (Figure 3.2). They can be easy to obtain and their missing lattice structure make them more water soluble than the ordered crystal lattice. However, these drugs are not stable in their amorphous form and tend to crystallize. One solution to stabilize them and to improve their solubility is to form solid dispersion with polymers [44].

Figure 3.2: *Schematic representing the type of modifications to enhance solubility of poorly soluble APIs and their examples.*

Solid dispersions

A solid dispersion was in 1971 defined by Chiou et al. as "the dispersion of one or more active ingredients in an inert carrier or matrix at solid state" [46]. Preparing solid dispersions is a common technique for poorly water soluble drugs since they can stabilize the amorphous form of a drug [41, 47]. This improved stability is due to the fact that the solid dispersion presents a higher glass transition temperature (T_g) that reduces the molecular mobility at storage temperature [44]. Another reason for the enhanced stability is claimed to be the polymer-drug interactions in the solid dispersion. They often form hydrogen-bond which prevents the crystal growth of the amorphous drug [44, 48].

In this project, the aim was to obtain amorphous API and to do that, poorly soluble drugs such as ketoprofen and naproxen were coupled with polymer matrixes (polyvinylpyrrolidone (PVP) or polycaprolactone (PCL)) forming a solid dispersion. In the next section, drugs and polymers used will be described.

3.1.2 Ketoprofen and naproxen

Ketoprofen and naproxen belong to Class II in the BCS and their water solubility is 15.9 mg/L (at 25 °C) and 51 mg/L (at 22 °C) [49], respectively. They are both propionic acid derivates and nonsteroidal anti-inflammatory drugs (NSAID) with anti-inflammatory, analgesic and antipyretic effects [50]. These APIs are used in the treatment of rheumatoid arthritis and

osteoarthritis. In this thesis, ketoprofen has been used as poorly water soluble model drug in Paper I, II and III, whereas naproxen has been used in Paper II.

3.1.3 Polyvinylpyrrolidone and polycaprolactone

PVP and PCL are widely used polymers in the pharmaceutical field. FDA approved PVP for oral drug delivery [51] and PCL for application used in the human body like drug delivery devices and sutures [52]. PVP is often used as an excipient in formulations due to its amorphous nature, high T_g and the ability to form hydrogen bonds with many APIs. Moreover, due to its high water solubility, it improves the solubility and stability of the drug. However, due to its hygroscopic property, care needs to be taken to avoid moisture uptake in the formulation [45].

PCL is a semicrystalline polymer with a melting temperature in the range of 59 - 64 °C depending on the crystallite size [52]. This polymer is known to be degradable at a slow rate, therefore being a good candidate for controlled release formulation or implantable long-term biostable drug delivery sytems [53]. In Paper I, PCL has been used together with ketoprofen to test two different loading techniques for microdevices. PVP was loaded with ketoprofen or naproxen to evaluate the loading technique called supercritical CO_2 (scCO_2) impregnation that will be described in the next chapter.

PCL (in Paper I) and PVP (in Paper II and III) were used as excipients in formulations for oral drug delivery of the poorly water soluble drugs ketoprofen or naproxen.

3.2 Therapeuthic peptides and proteins

Proteins are biological macromolecules able to perform vital functions in the body. They are formed by amino acids which are linked together forming a linear chain called primary protein structure. This chain can form other shapes defined as secondary, tertiary and quaternary structures [54]. Peptides are distinguished from proteins according to the number of amino acids by which they are composed. By definition, a peptide is formed by 50 or less amino acids [55].

Human insulin is one of the oldest protein and since the discovery of its recombinant form in 1978 and its FDA approval in 1982, the success of proteins has grown constantly [56, 57]. Better understanding of biochemistry and molecular biology, has opened up the enormous potential of the therapeutic use of proteins and peptides [58, 59].

Treatments with proteins are more effective compared to conventional small molecule drugs when administered for similar treatments [58] leading

to less chance of adverse effects and interference with normal biological processes. As many of the proteins used in treatments are naturally produced by the body, they are most often well-tolerated and are less prone to elicit immune responses [60]. As discussed previously, the oral route remains the most attractive route of administration for drugs [59]. In general, however, this route is not always feasible for protein-based drugs [61]. Despite their benefits, at present, protein and peptide drugs are mainly administered either subcutaneously or intramuscularly [58]. One of the reasons for this is that proteins are mostly hydrophobic and large molecules. This hinders their passive diffusion through the transcellular pathway [62]. However, passage via the paracellular pathway is usually restricted to molecules in the size range of 100-200 Da (molecular radii lower than 11 Å), by the narrow space between adjacent enterocytes. Therefore, lipophilic molecules usually utilize the transcellular pathway and hydrophilic molecules the paracellular pathway (Figure 3.3) [62].

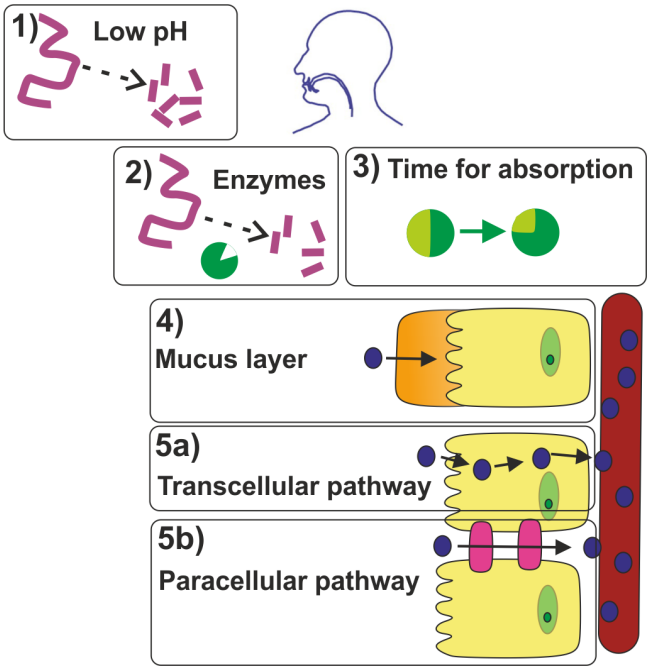

Figure 3.3: *Schematic representation of the steps for oral protein absorption. 1) Transit in the stomach: degradation in acidic environment. 2) Transit in the GI fluids: degradation by enzymes. 3) Residence time in the window of absorption. 4) Diffusion through the mucus layer. Transport across the cellular barrier through 5a) transcellular pathway or 5b) paracellular pathway.*

Generally, there is an undiminished ambition in overcoming the obstacles of oral protein delivery [63]. Thus, various strategies have been explored to target both the transcellular and paracellular pathways [63] with the use of specialised drug delivery systems [64].

3.2.1 Strategies to improve bioavailability

There are several approaches to enhance the oral bioavailability of therapeutic proteins including the use of enzyme inhibitors, absorption enhancers and mucoadhesive polymers (Table 3.1) [65].

Table 3.1: *Approches used in oral protein delivery to improve their absorption together with their outcomes and possible drawbacks.*

Approches	**Outcome for absorption**	**Drawbacks**
Enzyme inhibitors	Resist enzyme degradation occuring in the stomach and in the intestine	Induce severe side effect in chronic therapy
Absorption enhancers	Increase membrane permeation	Uptake of undesired molecules present in the GI tract
Mucoadhesive polymers	Protect drug from acid and luminal proteases in the GI tract and enhance permeation	Time limitation due to the natural mucus turnover in the intestine

As aforementioned, proteins are broken down from the digestive system into simpler molecules like amino acids and sugars that are easily absorbed. The responsibles for the cleavage of the amino acid chains are the enzymes like trypsin, chymotripsin, elastase and pepsin [66]. Enzyme inhibitors protect the protein from degradation by enzymes in the stomach and intestine. This can be a drawback in case of repeated drug delivery since protease inhibitors can prevent the absorption of other proteins and, therefore, induce toxic effects [66].

The absorption enhancers transport proteins directly through the epithelium without major effects on their solubility [67]. They can be classified as either increasing the paracellular permeability or the transcellular permeation [66]. However, one of the biggest drawbacks is that the addition of a permeation enhancer in a formulation enhances the transport of not only the desired protein but also undesired molecules present in the GI tract [65]. Bile salts and fatty acids are the most common enhancers and, in this project, sodium decanoate (C10) has been used in Paper IV. C10 is a saturated fatty acid and it is one of the most researched permeation enhancer [68]. The World Health Organization (WHO) and FDA have approved it as a food additive without daily limit. It has been shown that its effect is mainly on the paracellular pathways and that the effect is reversible preventing undesired compound from crossing the epithelium layer [69].

Mucoadhesive polymers, instead, can prolong the residence time at the site of absorption creating contact with the mucus layer and increasing the drug concentration gradient and, at the same time, reducing dilution or degradation in the lumen. However, a limitation of this approach is the natural mucus turnover in the intestine [65]. This topic will be discussed in detail in Chapter 5.

3.2.2 Lysozyme

Lysozyme is a protein formed by 129 amino acids having a molecular weight of 14.3 kDa. It is an antimicrobial enzyme and is a part of the innate immune system. It is cheap and commercially available for pharmaceutical and food applications for cancer chemotherapy and for antimicrobial approaches. This enzyme can be responsible for hydrolysis of the cell wall of a Gram-positive bacteria. Lysozyme has been used in Paper IV as a model protein.

3.3 Microdevices

Oral drug dosage forms are mainly and traditionally in powder forms and compressed to tablets [70]. In the last decades, an alternative approach has been to use micro- and nanoparticles which required the exploration of different types of polymers and techniques [65]. The main drawbacks of these particulate systems and tablets are the lack of protection from the gastric environment and the direction of release. In fact, the API is released equally in all directions, exposing the API to the lumen and not only to the cell membrane (Figure 3.4) [65].

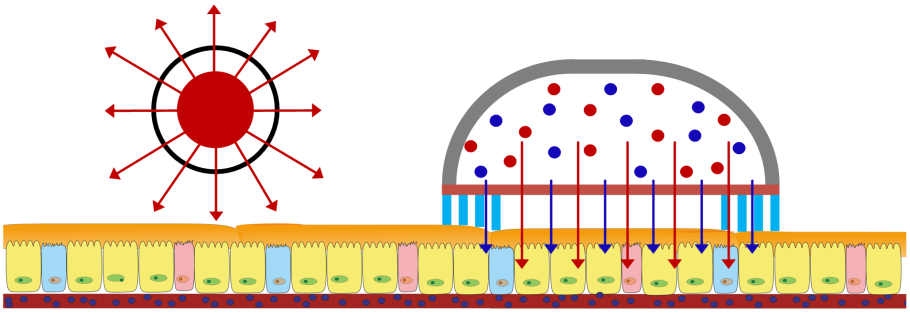

Figure 3.4: *Schematic representation of API release differences between microparticulate system (left) and microdevices (right).*

Moreover, in case of micro- or nanoparticles, the surface area exposed to the intestinal wall, due to their spherical shape, is limited. The dimensions of the particles can vary significantly and with it, the quantity of loaded API [12]. Recently, microdevices have been proposed as alternative oral drug delivery system (Figure 3.4). One of the main advantages in deploying microdevices is the unidirectional release of the loaded formulation. Moreover,

the microstructure protects the drug from three sides against, for example, low pH and enzymes, limiting the loss and degradation of the API [12].

Microdevices have been fabricated using different fabrication techniques. Depending on the material, the geometry, shape, reservoir volume and size desired, it is possible to choose among photolithography, soft lithography, hot embossing and hot punching and stamped assembly of polymers layers (Figure 3.5) [12].

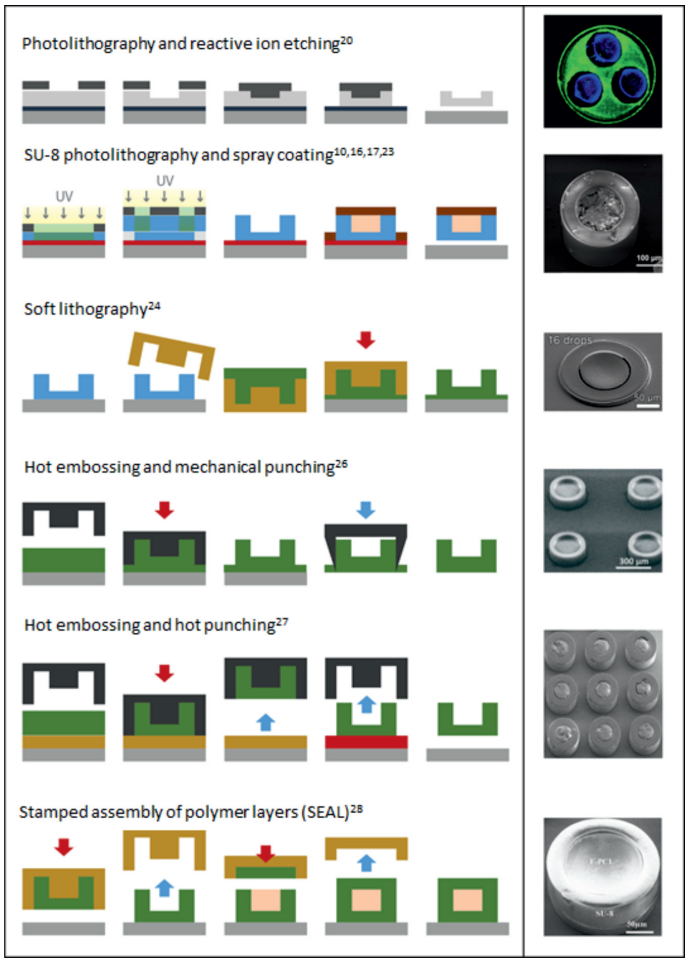

Figure 3.5: *Schematic representation of the main fabrication techniques for microdevices with images as examples. Reprint from [12] with permission.*

In the last decades, different fabrication techniques for several types of microdevices have been developed. Poly(methyl methacrylate) (PMMA) microdevices were fabricated using photolithography and lectins (proteins capable of targeting the cells on the intestinal wall) were attached to modify them chemically. The bioadhesive property was tested *in vitro* [71]. Planar microdevices for oral drug delivery were described as oral drug delivery system enhancing 4.5-fold the oral bioavailability *in vivo* of acyclovir, a

poorly water soluble drug [72]. Sealed nanostraw microdevices were made in PMMA, PCL, polycarbonate (PC) and aluminium oxide. The nanostraws facilitated API loading and enhanced the adhesion of the device to intestinal tissue [73].

Chapter 4

Microcontainers for oral drug delivery

In the previous chapters, the importance of designing an optimal formulation for oral drug delivery has been explained, as well as the strategies to enhance the oral bioavailability of formulations for poorly water soluble drugs and therapeutic proteins. In this thesis, microcontainers have been used and characterized as carriers for formulations of poorly soluble drugs and therapeutic proteins. Microcontainers are polymeric cylindrical microdevices with only the top side open (Figure 4.1) which can be loaded with a desired API using various techniques. In the next chapter, the coating of microcontainers and subsequent functionalization will be discussed.

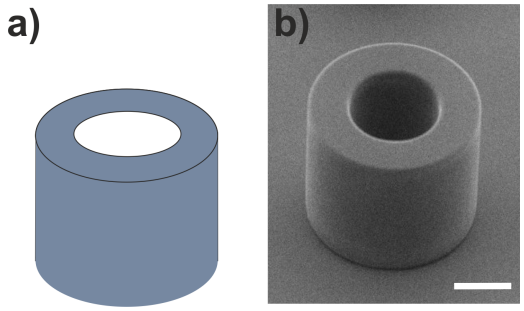

Figure 4.1: *a) Schematic and b) scanning electron microscopy (SEM) image of a microcontainer. The scale bar represents 100 µm.*

In previous works, it has been showed that microcontainers can: *i*) be fabricated in different sizes according to specific requirements [74], *ii*) stabilize the amorphous state of a loaded API [74], *iii*) enhance the oral bioavailability of furosemide [13, 75] and *iv*) be filled with PVP and loaded with ketoprofen using scCO_2 getting the drug in its amorphous form [14]. In the next section, the different steps used in this project in order to prepare formulations using microcontainers will be discussed.

4.1 Fabrication

Since the early nineties, SU-8 has been used as thick-film resist for the fabrication of microstructures with thicknesses of hundreds of micrometers. It was chosen as material for the fabrication of microcontainers due to its chemical resistance, structural stability and biocompatibility [76]. Microcontainers are fabricated with an accurate and controllable fabrication process. As shown in Figure 4.2, their fabrication is based on a two-step photolithography process of SU-8 on 4-in Si wafers.

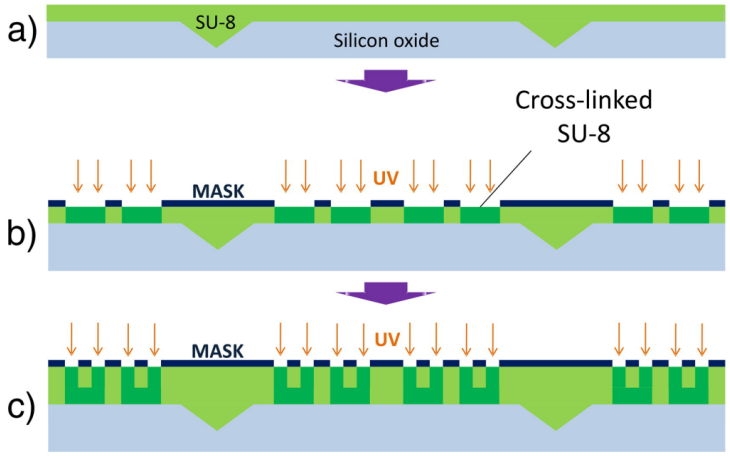

Figure 4.2: *A schematic overview of the fabrication process: a) spin coating of the resist on silicon (Si) wafer, b) mask alignment, ultraviolet (UV) exposure and development, and c) spin coating, mask alignment, exposure of the second resist layer and development. Reprinted from [77] with permission.*

At the end of the process, on each wafer, 18750 microcontainers are made and divided in smaller squares (chips) to ease subsequent handling (Figure 4.3). On every chip, there are 625 microcontainers and each squared chip has the dimensions of 12.8 x 12.8 mm^2. When not specified, microcontainers have a height and diameter of around 300 µm. However, in specific projects, the size and number of microcontainers per chip has been changed according to the needs.

For example, in Paper I, due to the chosen loading technique, the height was 100 µm. In Paper II, instead, the sizes have been changed to obtain three different sizes of microcontainers to evaluate the loading technique. In that case, their diameters varied from 200 µm (small size) to 500 µm (large size) all having 300 µm as height.

According to the type of experiment and application, it was necessary to detach the microcontainers from the Si substrate. In this case, specific materials were deposited between the Si and the SU-8 microcontainers (Figure 4.4). In Paper III, poly(acrylic acid) (PAA), being water soluble, has been used as previously described by Linder et al. as a sacrificial layer for

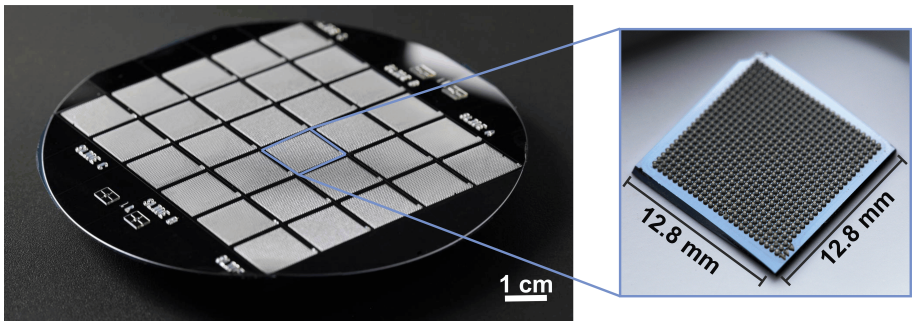

Figure 4.3: *Photo of a whole 4-inches wafer with 18750 microcontainers fabricated and zoom in of one single chip with 625 microcontainers.*

fabrication of microstructures [78]. Therefore, microcontainers detach from the Si chip when soaking the chip in water (Figure 4.4a). In Paper IV, fluorocarbon (Fc) was used as layer in between the SU-8 microcontainers and the Si (Figure 4.4b). Fc is an anti-stiction coating and it has been showed that a Fc surface has good properties for releasing SU-8 devices as cantilevers and membranes in the micrometer range [79]. Moreover, Nielsen et al. used microcontainers with this layer underneath allowing for easy manual detachment from the chip [80].

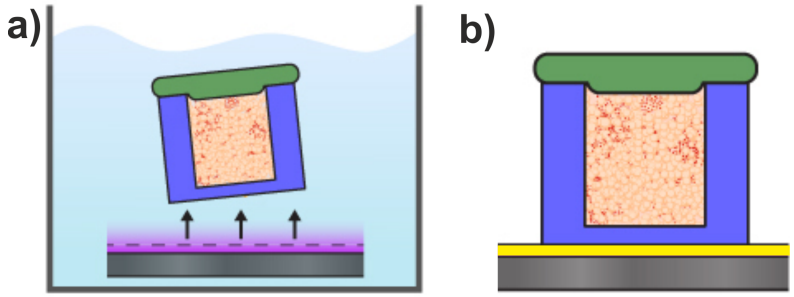

Figure 4.4: *Schematic representation of layers to detach microcontainers from the Si substrate: a) in purple the dissolving PAA layer in water detaching the microcontainer, b) in yellow a representation of the Fc anti-stiction layer.*

4.2 Loading methods

Despite all the advantages described for microcontainers, compared to traditional formulations like particulate systems or tablets, their loading can be rather complex. This is due to the fact that the loading can be made only through the cavity hole on top and needs to be quite accurate and reproducible. In case of liquids, the capillary forces may make difficult or hinder their loading. As described in the previous chapter, in case of poorly water soluble drugs, the formulation design is of fundamental importance. Therefore, it is relevant to choose the right excipients to improve solubility

and, at the same time, stabilize the amorphous state of the BCS Class II APIs. In particular, in Paper I, II and III, the focus has been on the loading techniques. Instead, in Paper IV, since the API to load was a model protein, the attention was more on the coatings and functionalization of the microcontainers.

4.2.1 Powder loading methods

Most of the commercially available APIs are in powder form and, therefore, a method for filling powder into the microcontainers is really essential. The first method used to fill microcontainers was a simple manual filling. With this method, the drug was deposited on top of the chip and with a finger or a brush, the powder was pushed into the microcontainers. To remove excess powder between the microcontainers, an air gun was used (Figure 4.5).

Figure 4.5: *Representation of the manual loading technique for loading microcontainers. The powder is pushed into the microcontainers using a brush or a finger (middle) and the excess of powder is removed using an air gun (right).*

This process can present some limitations: *i*) if the powder is sticky, it is difficult to remove it from the space between the microcontainers, *ii*) if the powder is not fine, the pressure of a finger or brush might not be enough to push it inside and *iii*) the powder can be expensive and, therefore, blowing the excess away can be costly. For these reasons, Abid et al. developed a filling method to improve the loading of powders [70]. In Figure 4.6, it is showed how the microcontainers chip (Figure 4.6b) can be placed in an alignment tool (Figure 4.6c) to allow alignment of a shadow mask on top (Figure 4.6a). The shadow mask covers the space between the microcontainers thereby reducing powder waste. In this way, the chip with the clamped mask can be placed on top of a powder layer (Figure 4.6d). Pressure can either be applied manually or by deploying a bonding press to push the powder into the microcontainers in a controllable and reproducible manner (Figure 4.6e) [70].

In Paper II and III, the simple method without mask has been used since PVP needed to be filled and its powder is dry, cheap and has a small particle size. In Paper IV, the mask was used together with a brush to reduce the waste of lysozyme between the microcontainers and to fill them applying low pressure to prevent potential denaturation of the protein.

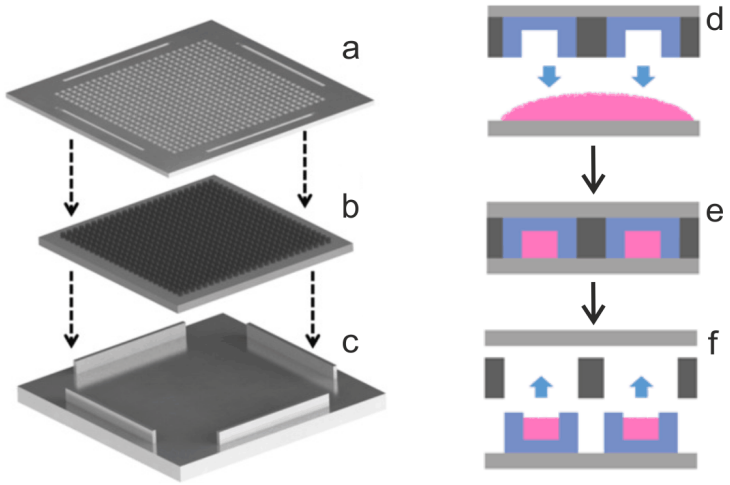

Figure 4.6: *Representation of the clamping system for the shadow mask (a) onto the chip of microcontainers (b) that is placed in an alignment tool (c). (d) The chip with the mask is placed on top of a powder layer and (e) pressed into it. (f) The mask is removed and the microcontainers are loaded. Reprinted from [70] with permission.*

4.2.2 Supercritical CO_2 impregnation

Carbon dioxide (CO_2) is non-flammable, inexpensive and chemically inert making it a widely used solvent. In addition, it is available at high purities and has low toxicity. It is defined as a "green" alternative compared to the traditional organic solvents since it is not defined as a volatile substance and does not have any restriction regarding food or pharmaceutical applications [81, 82]. ScCO_2 impregnation exploits the supercritical state of CO_2. When a substance reaches the critical point, gas and liquid merge together in a homogeneous phase called the supercritical phase (Figure 4.7) [83]. In particular, a supercritical fluid (SCF) can be defined as a substance at a temperature and pressure higher than their critical values having a density close or higher than its critical density [84]. SCFs are characterized by a density close to a liquid and viscosity and diffusivity similar to a gas.

The combination of the CO_2 and SCFs properties makes scCO_2 a good solvent for various applications [82]. The critical point of CO_2 is 73.8 bar and 31.1 °C [83]. ScCO_2 is a good solvent for many non-polar low molecular weight compounds. It alters density, diffusivity and swells polymers having, consequently, a huge plasticizer potential that usually would require higher temperatures [82]. Due to the mild conditions required, scCO_2 is suitable for thermolabile API; indeed, scCO_2 has been extensively used in the pharmaceutical industry for drug delivery systems, precipitation processes and powder processing [85].

One application is related to solid dispersions for oral drug delivery, in

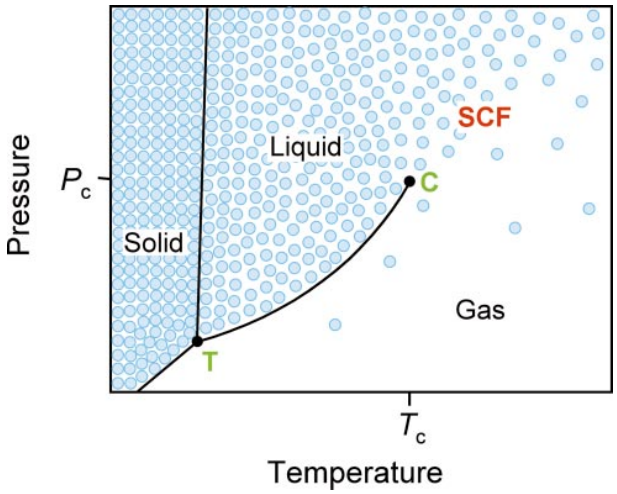

Figure 4.7: *Schematic pressure-temperature phase diagram for a pure compound showing the SCF region. The triple point T and critical point C are marked in green. The blue circles represent the variation in density of the substrate in the different regions of the phase diagram. Reprinted from [83] with permission.*

which one compound is a polymer, defined as matrix, and the other is an API that needs to be impregnated into the matrix. For this application, the polymer needs to be insoluble in scCO_2 although swelling is required to allow for the scCO_2 to permeate the matrix. To design a good formulation, it is fundamental to choose the right drug/polymer combination. For example, scCO_2 has been used to impregnate PVP microparticles with ketoprofen [86].

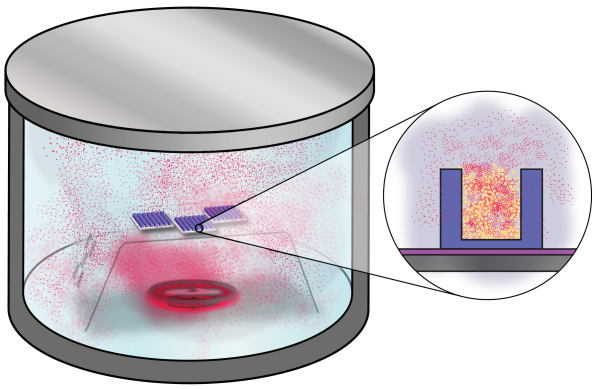

Figure 4.8: *Representation of the high pressure chamber during the scCO_2 impregnation of the PVP filled into the microcontainers with ketoprofen. Reprinted from Paper III [87] with permission.*

In the case of microcontainers, a PVP matrix (PVP) has been filled into the microcontainers and then loaded with ketoprofen using scCO_2 [14, 82]. As it can be seen in the Figure 4.8, the PVP filled microcontainers were

placed in the high pressure chamber on a grid to allow magnets to stir during the impregnation process. Together with the chips, the drug in powder form is poured into the chamber. The chamber has a heating system temperature control. Once the samples are inside, valves are opened to fill the chamber with CO_2. The pump is programmed to reach the desired pressure with a specific flow rate. When the supercritical phase is reached, a magnetic stirrer is activated to increase the movement inside the chamber. At the end of the process, the chamber is depressurized by opening the outlet valve (Figure 4.9).

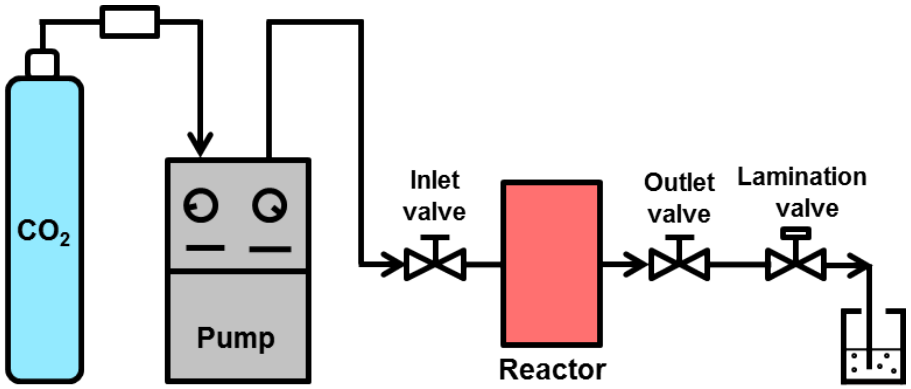

Figure 4.9: *Schematic of the scCO_2 impregnation system used in this project.*

In Paper II, this loading technique for naproxen and ketoprofen has been characterized evaluating the effect of the surface area of microcontainer cavities exposed to the scCO_2 on the API distribution and loaded amount. In Paper III, scCO_2 was used to load microcontainers for *in vivo* studies.

4.2.3 Hot-punching of polymer films

The name hot-punching indicates the combination of heating and pressure. This technique has been previously used by Petersen et al. to fabricate microstructures using biodegradable polymers like poly(lactic acid) (PLLA). The fabrication was performed by heating the polymer above its T_g and applying a pressure so that the Ni stamp could cut the polymer and obtain the desired microstructure [88, 89].

In this project, microcontainers have been used as molds to fill their cavities. The polymer or polymer+API solutions were spin coated on a Si wafer. The microcontainers were placed on top and due to heating and pressure, the microcontainer walls were able to cut the polymer layer.

From a previous study, it was shown that when ketoprofen is impregnated in PVP filled into microcontainers, its release was rapid [77]. Therefore, in Paper I, ketoprofen was loaded into PCL to evaluate if a less water soluble polymer could result in a different release of ketoprofen from the

microcontainers. In particular, in Paper I, two loading techniques were compared. In one case, microcontainers were loaded by hot-punching a layer of PCL+ketoprofen, in the second case, microcontainers were filled only with PCL by hot-punching and ketoprofen was then impregnated with scCO_2.

4.3 Coating polymers and techniques

In the previous sections, fabrication of microcontainers and different loading methods have been discussed. In Paper III and IV, the focus has also been on the coating of microcontainers. In particular, in Paper III the aim was to test *in vivo* if the microcontainers could enhance the oral bioavailability of a poorly soluble drug like ketoprofen. Microcontainers were therefore coated with a pH-sensitive polymer to prevent release of ketoprofen in the stomach. The focus in Paper IV was on how to functionalize the microcontainers for oral protein delivery. In the following section, polymers relevant for this project as well as the coating deposition technique will be introduced.

4.3.1 pH-sensitive coatings

In Chapter 1, while describing the GI tract, the difference of pH in the different segments was discussed. The values presented were from human fasted patients, but they depend on the ingested food and liquids, age, and sex [23]. In addition to that, there are differences in the pH of the GI tract among species. Therefore, it is important to consider this before designing a formulation. In Paper III, for example, we chose to test the formulation using Sprague-Dawley rats. From the pH values in the Table 4.1, it was possible to decide which polymer was relevant to use.

Table 4.1: *pH values in the stomach and in the proximal small intestine measured in rats and humans. Adapted from [90, 91].*

GI segment	pH in rats	pH in humans
Stomach	1.4 - 1.9	1.7 - 3.3
Proximal small intestine	6.7 - 7.0	5.6 - 7.8

pH-sensitive coatings are commonly used for overcoming the degradation of APIs in the stomach (Figure 4.10). Since the aim of this study was to test the microcontainers behavior *in vivo*, Eudragit L100 (Evonik, Germany) was chosen becuase it is a well tested and used polymer. The Eudragit products are synthetic polymers based on poly(meth)acrylate chemistry and, depending on the functional groups, the polymer can tune the release. In this project, since the release was aimed to happen in the intestine the Eudragit L100 has been chosen since it dissolves at pH higher than 6.

In Paper III, Eudragit L100 coating protected the loaded formulation in two occurrences: during the preparation of microcontainer formulation and during the *in vivo* experiments. Once the microcontainers had been manually filled with PVP, ketoprofen was loaded using scCO_2 impregnation. Eudragit L100 was then deposited on top to protect the load. Microcontainers needed to be detached from the chips to be filled into the capsules for oral gavage. Therefore, the chips were soaked in water in pH 3.25, at which the coating is insoluble. In this way, the PAA layer dissolved, releasing the microcontainers without compromising the coating (Figure 4.4a). Microcontainers were then filled into capsules and the formulation was ready to be dosed via oral gavage to the rats. This coating prevented the release of ketoprofen in the stomach of rats after administration (Figure 4.10). The same polymer has been used for the control formulation in order to evaluate if the microcontainers could enhance the oral bioavailability of the poorly soluble drug ketoprofen.

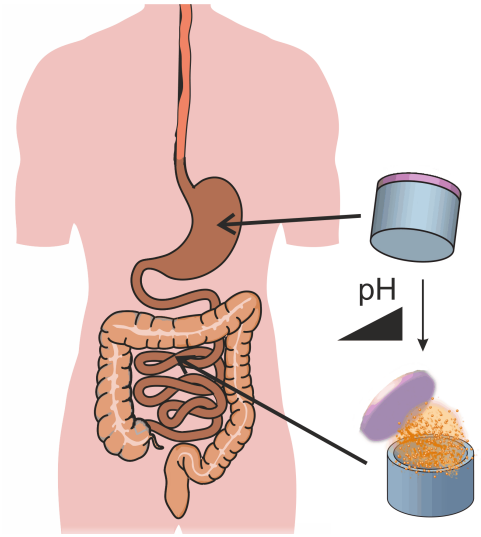

Figure 4.10: *Microcontainer with coating in the stomach and dissolution of the lid in higher pH in the small intestine where release and absorption are desired.*

4.3.2 Coatings for therapeutic proteins

In Chapter 3 and Table 3.1, different strategies to enhance the oral bioavailability of therapeutic proteins were discussed. In this section, the importance and the mechanism of mucoadhesive polymers and other coatings will be explained.

Bioadhesion is the generic word defining the state at which two materials (at least one of which biological) are held together by interfacial forces for an extended period of time. When the adhesive layer is mucus, this phenomenon is called mucoadhesion [33]. When designing a formulation for

oral drug delivery of proteins, a common strategy is the use of mucoadhesive polymers to increase the residence time at the site of absorption. These polymers keep a close contact with the intestinal mucus to increase the drug concentration gradient without degradation or dilution in the luminal fluid [65].

In Paper IV, three different polymers were chosen for microcontainer coating: chitosan, polyethylene glycol (PEG) and poly(lactic-co-glycolic) acid (PLGA). In the following sections, all of these will be described. A schematic representation of microcontainers coated with two of the chosen polymers for oral protein delivery is shown in Figure 4.11.

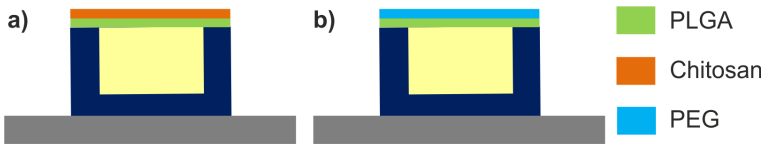

Figure 4.11: *Schematic representation of microcontainers coated with two polymer layers for oral delivery of the model protein lysozyme (Paper IV). a) Microcontainer coated with PLGA and chitosan and b) microcontainer coated with PLGA and PEG.*

Poly(lactic-co-glycolic) acid (PLGA)

PLGA is a copolymer of poly lactic acid (PLA) and poly glycolic acid (PGA) (Figure 4.12) [92]. In its dry state, PLGA is generally stable, but when exposed to aqueous environments such as the *in vivo* environment, it will degrade (Figure 4.12) [93]. This degradation occurs by hydrolysis and it is firstly broken down into small oligomers and further into its monomers. Eventually, these hydrolysis products are metabolized and cleared from the body with minimal systemic toxicity associated (Figure 4.12) [92].

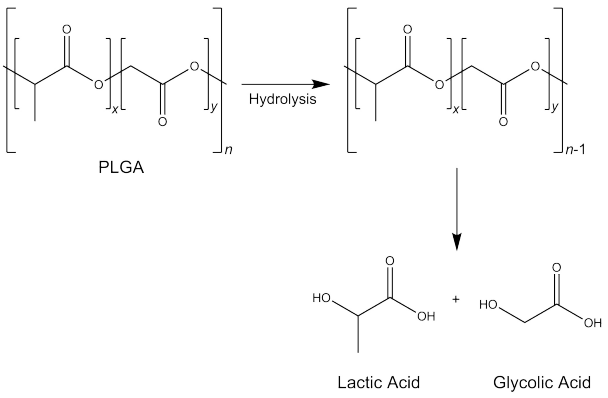

Figure 4.12: *The degradation process of PLGA into its monomers by hydrolysis.*

PLGA is considered one of the most successfully developed and used polymers owing to its very attractive properties [94]. It is biodegradable, biocompatible, approved by FDA and European Medicines Agency (EMA),

and is very well studied [95, 96]. This means that formulations and production methods are well-described in combination with different types of drugs, hydrophobic and hydrophilic small molecules, as well as macromolecules. PLGA's attributes have been utilized to protect drug molecules from degradation and facilitating sustained release. Finally, PLGA can be used to modify surface properties of biological materials [92].

Chitosan

Chitosan (Poly-(D)glucosamine) is obtained by partial or full deacylation of chitin (a long-chain polymer of N-acetylglucosamine). Chitin is a natural polysaccharide produced by a vast number of living organisms such as fungi, crustaceans and insects [97]. Chitosan exists in many molecular weights and degrees of deacetylation (40 - 98%) which influences its viscosity and solubility properties including mucoadhesion [98, 99]. The pK_a value of the primary amine of glucosamine is approximately 6.5. Consequently, chitosan is primarily protonated in acidic pH and soluble in the cationic form [100]. Therefore, generally, chitosan is soluble in aqueous acidic solutions and dimethylsulfonide [101].

Chitosan is well-known as a mucoadhesive agent, enabling longer residence time in the small intestine [102]. This property makes chitosan a popular polymer to include in drug delivery systems [102]. Chitosan's mucoadhesive properties arise from its strongly positive charge, attracting the negatively charged mucins of the mucus [103]. Chitosan has the capability to form both hydrogen bonds and covalent bonds, via its -OH and -NH_2 groups. This enables an electrostatic interaction with the negatively charged mucus components such as sialic acid [98]. In addition, hydrophobic interactions play a role in mucoadhesive properties of chitosan [104].

In Chapter 3, the importance of permeation enhancers has been discussed. In Paper IV, C10 has been loaded together with the model protein lysozyme and chitosan was one of the coating layers. In fact, its protonated form has demonstrated the ability to increase paracellular permeability across mucosal epithelia for macromolecules [98]. It does so by reversibly modulating the integrity of the epithelial tight junctions [102]. The signal mechanism by which chitosan induces opening of tight junctions has been studied and found that multiple mechanisms may be involved in the process [102, 105]. Results indicate that chitosan interacts with the transmembrane claudin protein CLDN4 to trigger the opening of tight junctions [105, 106].

Polyethylene glycol (PEG)

One of the most used polymers in drug delivery systems is the FDA approved PEG. It is a relatively chemically inert and non-biodegradable polymer. It is uncharged and amphiphilic, meaning that it is both hydrophilic

and hydrophobic in nature. Consequently, it is soluble in water and organic solvents [107]. Furthermore, PEG has good mucolytic properties, retention effects and it is widely used and studied as a mucoadhesive agent [108]. The mucoadhesive properties are believed to arise from its hydrophilic nature and ability to inter-diffuse with the mucus gel network. The molecular weight and density of PEG seem to play a role in its interaction with the mucus mesh. A high molecular weight of PEG increases mucoadhesion and a transition has shown to appear in the range of 5 to 10 kDa, where PEG changes from being mucopenetrating to mucoadhesive [109]. Higher molecular weights of PEG present longer chains resulting in better entanglement with mucins, increasing the number of intermolecular interactions such as hydrogen bonding [110].

4.3.3 Coating deposition techniques

There are different well established techniques for coating deposition. In the pharmaceutical field, the most common ones are: conventional pans, perforated pans and fluidized beds (Figure 4.13). In all cases, a polymer solution is delivered through a spray nozzle and deposited onto a sample. The coating liquid is atomized with air and the substrate moves in order to coat the whole sample surface.

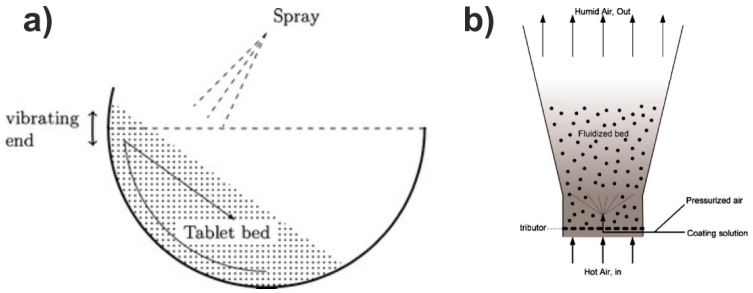

Figure 4.13: *Schematic representation of a) coating pan and b) fluidized bed coating systems. Reprinted from [111, 112] with permission.*

Although the coatings obtained with these techniques are reproducible and are used in large scale processes, they are not suitable for coating microcontainers. This is because microcontainers need to be coated only on their top, where the cavity is and, consequently, an ultrasonic coating system has been chosen in this project.

Ultrasonic coating system

In an ultrasonic coating system, the polymer solution is sprayed through an ultrasonic nozzle that moves in x-y-z directions over a sample (Figure 4.14a). The sample is placed on a heating plate in which the temperature can be controlled enhancing, for example, the solvent evaporation.

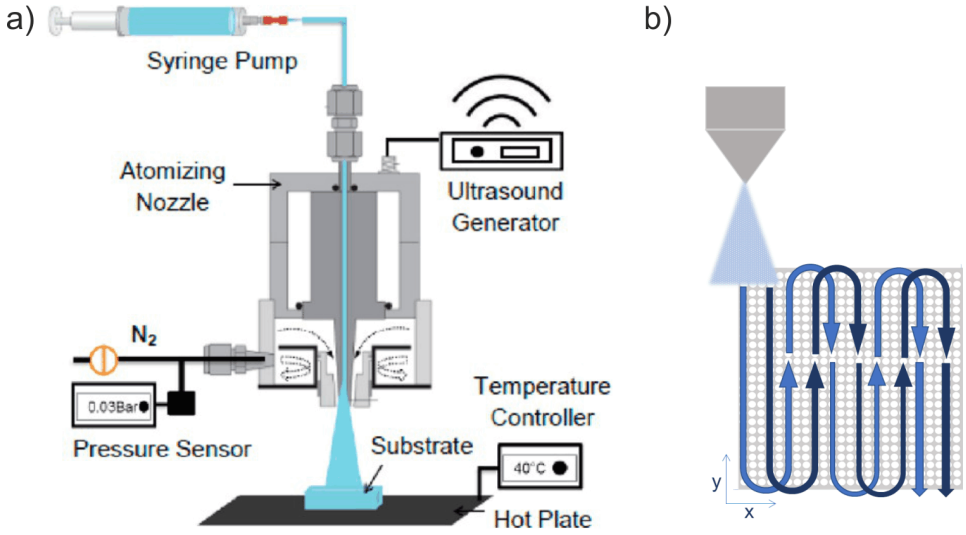

Figure 4.14: *a) Drawing of the ultrasonic coating system for coating the cavity of the microcontainers with polymers. Reprinted from [113] with permission. b) Schematic representation of the two spray paths over the microcontainer chip.*

Every coating technique has several parameters that need to be adjusted in order to obtain a uniform spray. In case of the ultrasonic coating system, these are the power of the ultrasound generator, the atomizer pressure and the syringe pump flow [113]. Once the spray is uniform, an area where the sample is placed can be defined. The nozzle moves in "arcs" as shown in Figure 4.14b. For this reason, to obtain a more homogeneous coating, in Paper III and IV, two similar areas were selected with an offset in the x direction (Figure 4.14b). Moreover, the distance between the nozzle and the sample, the nozzle speed, the temperature of the substrate and how many times the nozzle follows the two areas are all important parameters to obtain a uniform coating layer [113].

If the coating displays cracks, a plasticizer like triethyl citrate, propylene glycol or dibutyl sebacate (DBS) needs to be added to the polymer solution. A plasticizer can change thermal and mechanical properties of a polymer lowering, for example, its rigidity at room temperature [114]. For this reason, in Paper III, DBS was added to the Eudragit L100 coating solution.

Chapter 5

Characterization and evaluation techniques for microcontainers

Characterizing the microcontainers is of utmost importance to evaluate that the design and fabricated formulation provide the desired features. In the next sections, the main methods used to characterize and evaluate the microcontainers are briefly described.

5.1 Drug quantification

The amount of loaded API is commonly evaluated placing the sample in a buffer solution or biorelevant medium and measuring the drug release over time. The most common measurement method is ultraviolet-visible (UV-vis) spectrophotometry [115, 116].

The light is an electromagnetic radiation characterized by waves having different lengths or number of photons with different energy. UV-vis spectrophotometry includes the wavelength range 190 - 800 nm being from 190 to 400 nm the UV region and from 400 to 800 nm the visible range. The absorption of light happens when the energy from the photon stimulates an electron to reach a higher energy state. The capability of a molecule to absorb light as a function of wavelength is expressed in a UV-vis absorption spectrum. This ability depends on the molecular structure of the compound. The Lambert-Beer's law quantitatively describes the absorption of UV and visible light associating the absorption of light from a molecule to its concentration. The law states that the absorbed light is proportional to the number of functional groups and structural elements absorbing light present in the medium in which the light is passing through. This means that the amount of absorbed light is also proportional to the concentration of the absorbing species. The law is valid in dilute solution if the light is

monochromatic. It can be expressed with the following formula:

$$log_{10}\left(\frac{I_0}{I}\right) = log_{10}\left(\frac{1}{T}\right) = A = \varepsilon bc \tag{5.1}$$

where I_0 is the intensity of the incident light, I is the intensity of the transmitted light, T is the transmittance given by (I/I_0), A is the absorbance, ε is the molar absorption coefficient (L mol^{-1} cm^{-1}), b is the light path and c is the concentration of the absorbing molecule (mol L^{-1}) [115, 116].

5.1.1 µDiss profiler

In this project, UV spectrophotometry has been used in all Papers; in particular, the *in vitro* releases have been measured with an *in situ* UV fiber optic monitoring system (µDiss profiler, pION INC) (Figure 5.1). The system consists of a probe, which acts both as light emitter and receiver. The light detection is guaranteed by a mirror placed at the end of the probe (Figure 5.1). When the probe is submerged into the solution, the analyte absorbs some of the emitted light. As the concentration of the analyte increases, the intensity of light reflected back into the probe by the mirror decreases (Equation 5.1) [117, 118].

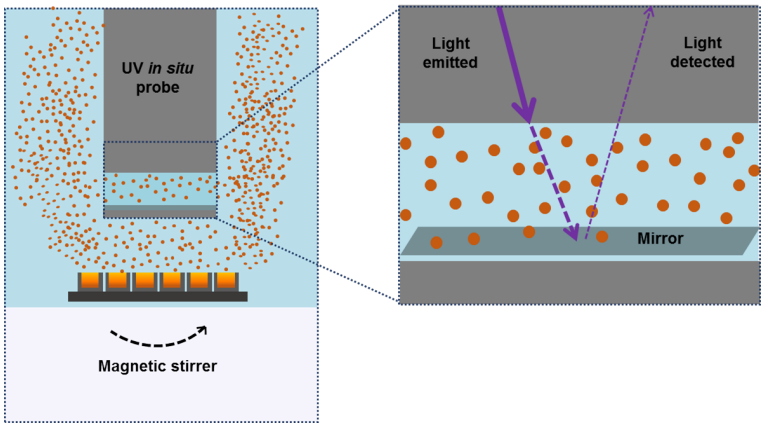

Figure 5.1: *Schematic representing a glass vial with the in situ UV probe, a magnetic stirrer and a microcontainer chip for in vitro measurements. The zoomed figure represents the release of the compound from the microcontainers and the mirror of the in situ probe for absorbance measurements.*

To determine the behavior of drugs *in vitro*, simple buffer solutions like phosphate-buffered saline (PBS) are widely used. To better simulate the *in vivo* scenario, it is important to choose media having similarities to gastrointestinal fluids. Several media have been proposed to simulate gastric and duodenal conditions and their compositions have been adjusted based on *in vivo* measurements [119]. In Paper III, to test the performance of the pH-sensitive coating, biorelevant media simulating the fasted gastric and

intestinal fluids were used (Biorelevant®). These media, containing taurocholate, phospholipids, sodium, chloride and phosphate, better represent key aspects of the GI fluids. The key features that need to be considered are, for example, osmolality, ionic strength, viscosity and surface tension [120, 121].

5.1.2 High performance liquid chromatography (HPLC)

In Paper III and IV, high performance liquid chromatography (HPLC) was used to analyze samples from *in vitro* studies, *ex vivo* transport studies, and plasma samples from *in vivo* studies. With this technique, before the detection, the sample undergoes separation. This happens in a column (Figure 5.2) where the analytes distribute between the mobile and the stationary phases thereby getting separated. The most commonly used HPLC technique is the reversed phase, in which the stationary column is more hydrophobic than the mobile phase (called reversed phase-HPLC (RP-HPLC)). With this technique, there can be different kinds of detectors such as UV, fluorescence and mass spectrometry [122, 123]. In this project, a UV detector was used.

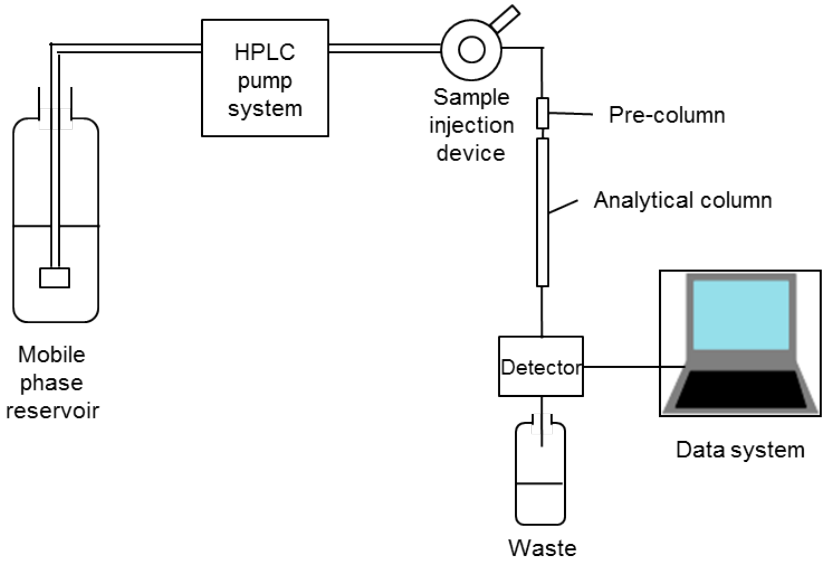

Figure 5.2: *Schematic representing a HPLC system.*

5.2 Morphology characterization

5.2.1 Scanning electron microscopy (SEM)

Since microcontainers are three dimensional (3D) structures, to evaluate their loading and coating, the use of a SEM microscope was suitable com-

pared to optical microscopy (Figure 5.3a-b). SEM is a well established technique for investigating the morphology of 3D samples like microcontainers. Scanning the sample surface, the electron beam penetrates it creating the image by collecting electrons that interact with the specimen.

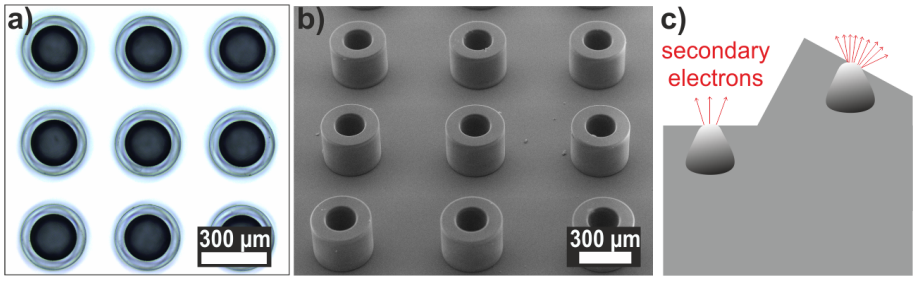

Figure 5.3: *Comparison between microcontainer images obtained with a) optical microscopy and b) SEM. c) Schematic representation of interacton of the secondary electrons with the sample surface, when it is flat and in case of a protrusion.*

The most suitable detector in the pharmaceutical field is the one collecting data from secondary electrons (SE). These electrons generate an interaction volume in the sample but only those in close vicinity (several nm) to the surface can leave the sample due to their low energy. Consequently, in protruding areas of the specimen the number of SE that leave the surface is higher than in flat areas (Figure 5.3c). In the SEM image, the protruding areas appear brighter than the others creating a 3D effect on a two dimensional (2D) image with high topography resolution (Figure 5.4) [124].

Moreover, for this project, the use of a tilted stage (30°) or the possibility of rotating it was of essential importance to be able to evaluate the level of loading and coating homogeneity on the microcontainer cavities (Figure 5.4).

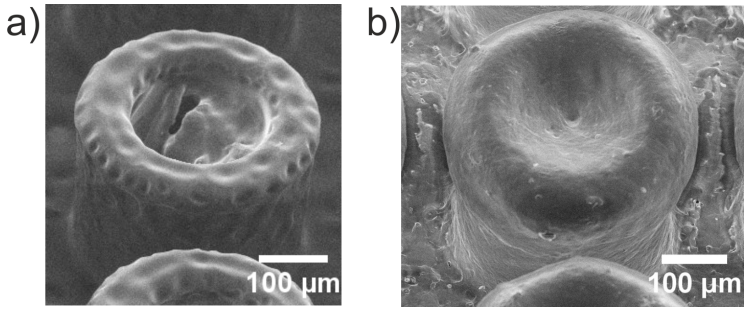

Figure 5.4: *SEM images of microcontainers that allow to evaluate a) thin and b) thick coatings.*

5.2.2 X-ray micro computed tomography (X-ray μCT)

In Paper I, III and IV, SEM images were not sufficient to evaluate various steps of the microcontainer preparation. X-ray micro computed tomography

(X-ray μCT) can be used to analyze the cross-section of a sample. In this technique, the x-rays are used to obtain the cross-section without cutting and, therefore, without destroying the sample [125, 126]. The images and videos used in this work are the result of a collaboration with the Senior Research Engineer Carsten Gundlach from DTU Physics who measured all the samples for the project. With X-ray μCT, it was possible to determine if the loading reached the bottom of the microcontainers (Paper I), to study the level of homogeneity of the coatings (Paper III and IV), and to investigate if microcontainers filled into the capsules were intact (Paper III).

5.3 Solid state characterization

In Chapter 4, the importance of the solid state of poorly soluble drugs has been described. The physical state of poorly soluble drugs can influence their solubility and dissolution rate [127]. Consequently, after characterizing the fabrication and loading of microcontainers, the solid state of the API was evaluated. In the pharmaceutical field, there are many techniques to evaluate the solid state of an API and, in this project, Raman spectroscopy and x-ray powder diffraction (XRPD) have been used in Paper I, II and III.

5.3.1 Raman spectroscopy

In the previous sections, light absorption has been described for a quantitative analyses of a compound in solution, but the light interaction with a molecule can happen either through emission or scattering [128]. The scattering phenomena can be elastic or inelastic, defined as Rayleigh and Raman scattering, respectively. The majority of photons hitting a sample undergo elastic scattering (Rayleigh) where there is no energy transfer between the photon and the sample (Figure 5.5) [129]. The remaining photons (one every 10^6 photons) will transfer energy and give rise to inelastic scattering (Raman) (Figure 5.5). The Raman signal is stronger with molecules having electrons that are easy to polarize than those held tightly since its intensity is proportional to the polarizability of the molecule [128].

A Raman spectrum represents a structural fingerprint by which it is possible to identify molecules. As most of the excipients used in the pharmaceutical field are σ-bonded molecules (e.g. starch and cellulose) and most of the APIs contain π-electrons, the Raman signal is generally strong for drugs making it a suitable technique for such investigations [130]. Raman spectroscopy for this project was even more attractive since it is very versatile allowing to measure a wide diversity of samples including the formulations loaded into microcontainers [131].

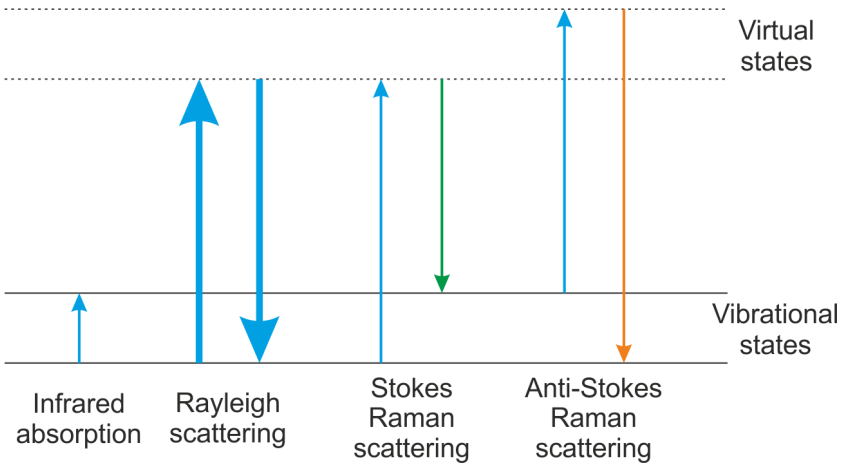

Figure 5.5: *Jablonski diagram representing energy transition for infrared absorption, Rayleight, Stokes and anti-Stokes scattering.*

5.3.2 X-ray powder diffraction (XRPD)

XRPD is one of the most straightforward analytical techniques for polymorph identification at the particulate level. It is useful for obtaining direct information on the crystalline lattice. With this technique, a diffractiogram is obtained [132]. These diffractograms consist of thousands of individual measurements of x-ray intensities, made at regular intervals along an arc that describes the angle of diffraction, 2θ, relative to the path of the incident x-ray beam [133]. Peaks in the diffractogram are a result of the diffraction of x-rays by atoms in the crystal structure and are most conveniently thought as x-ray reflections from individual lattice planes in the unit cell. These reflections are observed only if the Bragg's law is satisfied:

$$\lambda = 2dsin\theta \tag{5.2}$$

where λ is the incident x-ray wavelength, $2dsin\theta$ the path difference between two waves undergoing intereference. In principle, XRPD pattern contains information regarding the internal arrangement of the material of interest [132]. The size and shape of the unit cell can be determined by the peak positions in the diffractogram, while peak intensities can be used to determine the types of atoms present in the cell and their positions [133]. The alignment of the particles in the preferred orientation in the XRPD holder can significantly affect the location, area and intensity of the diffraction peak [133]. Thus, quantitative analysis that involves intensity ratios or areas can be greatly distorted by alignment of the crystallites in the preferred orientation. In this project, only the qualitative analysis of the solid state forms was of interest.

5.4 Drug distribution

Raman spectroscopy, together with other techniques, has been widely used to understand the distribution of compounds for example in 3D printed tablets. Trenfield et al. cut a tablet and a 2D map was measured with Raman spectroscopy obtaining information on the drug distribution [134].

The drug distribution in microcontainers after loading the drug using scCO_2 impregnation was investigated in Paper II. A line was selected on top of the microcontainer and a spectrum at each point of that line was obtained at different depths (Figure 5.6a). These analyses were performed using DXR Raman microscope (Thermo Fisher Scientific, Inc., Waltham, USA) with a signal collection time of 10 s and the signal was averaged two times, using a 50 µm confocal pinhole. All Raman spectra were recorded using a laser with a wavelength of 780 nm, power of 20 mW and a 50x objective lens. The results are shown in Figure 5.6b. The map shows the high intensity of a selected peak in red (1000 cm^{-1}). The selected wavenumber, corresponding to a characteristic peak of ketoprofen. This map shows the distribution of ketoprofen in the microcontainers after being loaded with scCO_2. A similar map was obtained selecting a wavenumber characteristic for PVP. These results showed that it was not possible to measure deeper than 50 µm as PVP was also present below according to the X-ray μCT and SEM analyses.

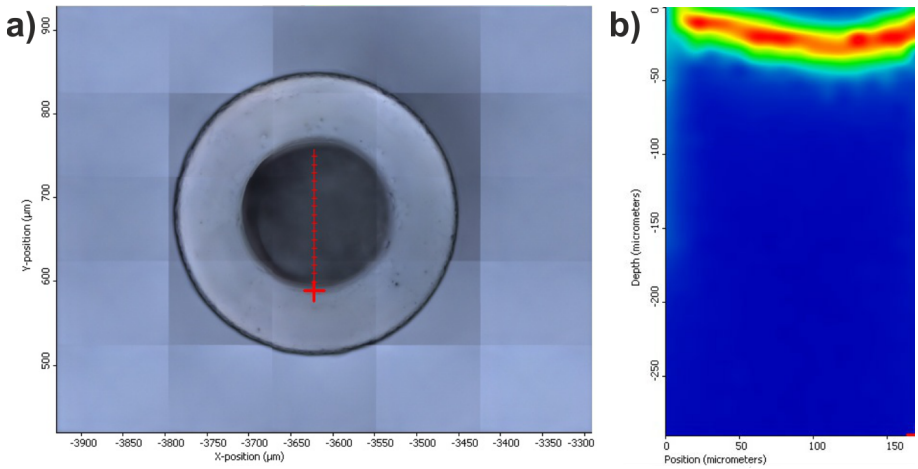

Figure 5.6: *a) Optical image of a microcontainer. The red line represents where the measurements were taken. A spectrum was collected for each point on the line at different depths ranging from 0 to 300 µm. b) Results of the measurements: Raman map in which every point represents the intensity of ketoprofen characteristic peak (1000 cm^{-1}) represented by a color scale (blue to red indicates low to high intensities).*

Since it was not possible to obtain a cross section of a microcontainer due to low transparency of the sample, a laser (microSTRUCT vario, 3D Microac AG, Chemnitz, Germany) was used to cut the microcontainers in

half (Figure 5.7a). The idea was to analyze the cross-section generated by the cut (Figure 5.7b) to obtain the full cross section of the microcontainer [134]. The cutting process was successful but the laser burned the filling materials so it was not possible to detect any material from the analyses of the samples.

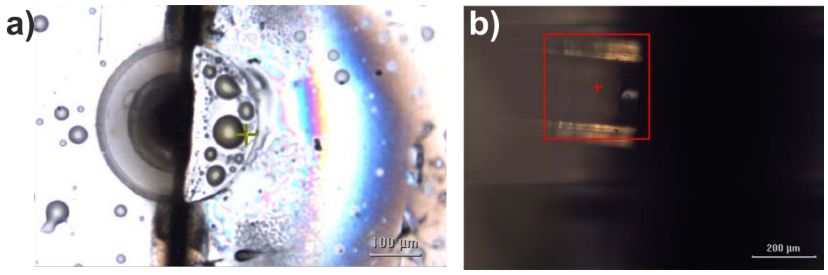

Figure 5.7: *Optical images of a microcontainer cut with a laser a) from the top and b) from the side.*

To obtain a 3D distribution of the drug, it was needed to use a custom-made highly sensitive confocal Raman microscope with a laser power of 30 mW. Due to the high laser power, a Peltier cooling system was added to control the temperature of the sample during the measurements. Moreover, a Non-Negative Least Squares (NNLS) analysis was performed to distinguish between the different components: Si, SU-8, PVP and ketoprofen or naproxen. This part of the project was done in collaboration with Dr. Oleksii Ilchenko and Roman Splipets. They designed and built the instrument, measured the samples and analyzed the data.

5.5 Intestinal drug transport investigations

5.5.1 *In vitro* cell transport studies

As explained in Chapter II, the intestinal barrier plays an important role in drug absorption. Therefore, it is a common approach to test *in vitro* whether the compound has the potential to be transported across the intestinal cells. To evaluate the amount of compound transported from the lumen to the portal circulation, a layer of cells modeling the intestinal barrier is grown on filter supports. This constitutes a cellular barrier which separates two compartments (Figure 5.8). The formulation that needs to be tested is placed on the apical side (the "lumen" side) and samples are taken from both sides over time to evaluate if it is transported to the basolateral side (Figure 5.8).

The most common cell line, which was also used for these studies, is the Caco-2 (Cancer Coli-2 or HTB-37). It was established from a human colorectal adenocarcinoma. These cells, when differentiated, express functional and morphological properties characteristic of the intestinal enterocytes such as

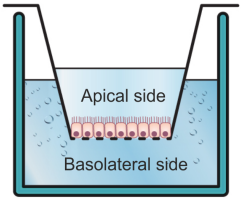

Figure 5.8: *Cell monolayers on filter support used for transepithelial transport studies, e.g. from the apical to the basolateral side.*

being polarized and acquiring the typical apical brush border with microvilli (Figure 5.9). Moreover, they express enzyme activities typical of enterocytes and they present tight junctions between adjacent cells [135, 136]. The correlation with the *in vivo* situation is particularly high if the compounds are transported by passive paracellular transport mechanisms [137, 138, 139].

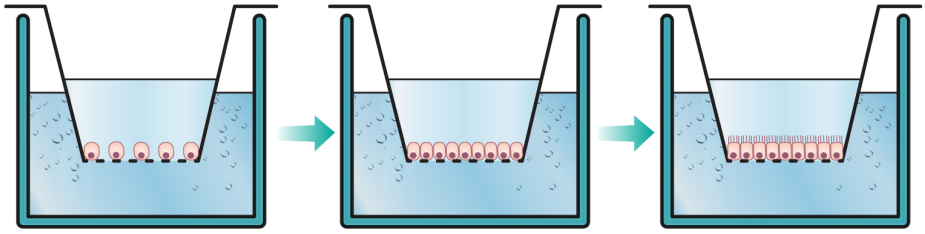

Figure 5.9: *Schematic representation of the differentiation of Caco-2 cells on a filter support. When the Caco-2 cells reach confluence (middle) they start to differentiate spontaneously, and after a period of around 21 days they will appear with dense microvilli on the apical side typical of small intestinal enterocytes (right) [136].*

One of the main drawbacks of Caco-2 cells is that, being a simple model, the diverse functions of the intestinal epithelium are not all represented. Therefore, the addition of different epithelial cell types in an *in vitro* model will better reflect the properties of the intestinal barrier. In Chapter 2, the mucus layer was described as an additional important factor acting as a barrier to the absorption of some compounds. HT29-MTX cells differentiate into mature goblet cells which secrete mucins on the apical side. For this reason, the co-culture of Caco-2/HT29-MTX cell monolayers is quite common since their combination makes a good model of the two most numerous cells in the epithelium: enterocytes and goblet cells [140]. In particular, this combination allows to study how the presence of a mucus layer affects the permeability of the tested compound in comparison to its permeability across the Caco-2 cell model.

In Paper IV, both models have been used positioning the microcontainer chip onto the cell monolayers having the coating layers in contact with the cells (Figure 5.10). The coated microcontainers filled with the model pro-

tein lysozyme were tested to evaluate the protein transport across Caco-2 and Caco-2/HT29-MTX cell monolayers. The samples taken during these experiments were analyzes with HPLC, as described above.

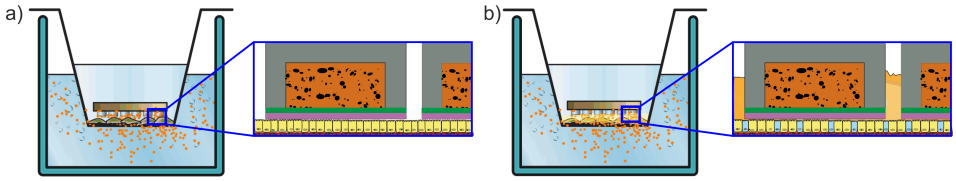

Figure 5.10: *Schematic representation of the a) Caco-2 cell monolayer and b) Caco-2/HT29-MTX cell monolayer with a microcontainer chip on top. The zoom areas represent microcontainers loaded with lysozyme+C10 and coated with two layers on top of the cells.*

5.5.2 *Ex vivo* transport studies

Even the combination of two cells type does not represent the multicellular environment of the intestinal barrier. The transport of compounds across the intestinal wall can be facilitated by other cell types and therefore, using *ex vivo* intestinal tissue segments represents a better model for the *in vivo* situation [141, 142]. The possibility of using human tissue is usually quite limited, consequently, porcine intestinal tissue is commonly used as alternative. This tissue showed high similarity with that of humans [141, 142].

A side-by-side diffusion chamber called Ussing chamber is used to investigate intestinal drug transport through excised tissue. This system is composed by two compartments (as in the cell transport studies) representing the apical and basolateral sides (Figure 5.11). Each side has a separate air/gas inlet for the circulation system. The intestinal tissue segment is mounted in vertical position between the compartments. Before mounting it, the muscle layers need to be removed from the tissue (stripping) to minimize the influence of the intrinsic neuromuscular system [143]. The compartments are then filled with buffer at 37 °C. The formulation that needs to be tested is placed in the apical side and samples are taken over time from apical and basolateral compartments.

At the end of the experiment, the tissue integrity is assessed using radioactive labelled compound as paracellular markers for passage through the tissue. One of the most common markers is D-[1-^{14}C]-mannitol since mannitol is a small hydrophilic molecule with very low cell membrane permeability. A liquid scintillation counting measures the radiolabelled molecules dissolved in an organic compound able to absorb radiant energy (scintillator). Since the energy is absorbed, excited atoms rapidly return to the ground state releasing photons. The concentration of the radioactive labelled molecule can be translated from the number of emitted photons.

In Paper IV, the functionalized microcontainers filled with the model

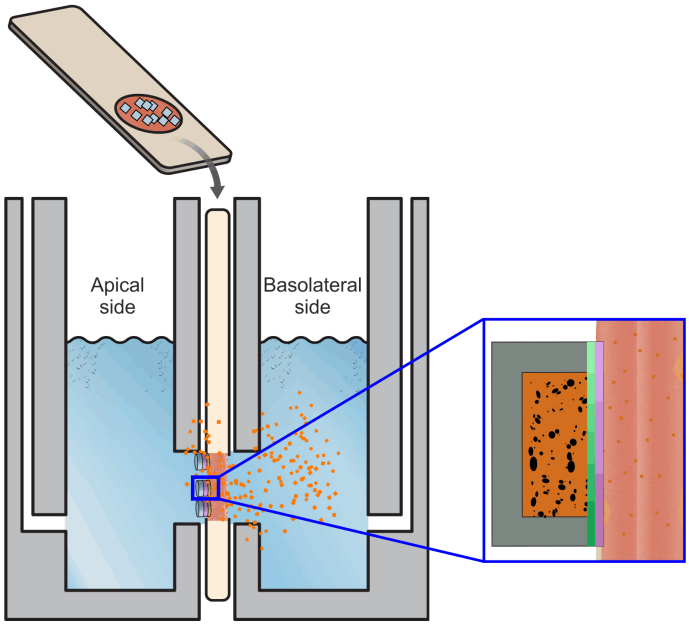

Figure 5.11: *Schematic representation of a Ussing chamber system. The zommed area represents one coated microcontainer loaded with lysozyme+C10 on the tissue. In the upper part of the figure, the slide with the intestinal tissue with randomly placed microcontainers on top is represented.*

protein lysozyme were placed on the tissue before inserting it in the chamber to evaluate the transport of lysozyme through the intestinal tissue (Figure 5.11). The samples were analyzed with HPLC.

5.6 Mucoadhesion evaluation

As introduced in the previous chapter, in Paper IV the microcontainers have been tested for oral delivery of the model protein lysozyme. For this reason, they have been functionalized by applying polymeric coatings on top and, therefore, it was necessary to verify if the mucoadhesive layers made a difference.

Numerous methods have been proposed to assess the mucoadhesive properties of formulations. These methods can be based on mechanical force determination or on particle interactions [144]. The method used in this project is rather simple; the intestinal tissue is placed on a support and when the mucoadhesive formulation is distributed on the tissue, a pump can be activated to obtain a flow of the desired buffer on the tissue to mimic the flow in the intestine [145]. In contrast to what has been found in literature, the system used to test microcontainers in Paper IV was closed in a box in which temperature and humidity could be controlled to mimic the physiological conditions (Figure 5.12a). This technique allows to measure

how the microcontainers interact with the tissue. In the experiments presented in Paper IV, a known quantity of microcontainers was placed on the tissue and a peristaltic pump was activated obtaining a PBS flow on the tissue (Figure 5.12b). At the end of the experiment, the tissue was left to dry for 24 hours in order to be able to count the number of microcontainers that adhered (Figure 5.12c).

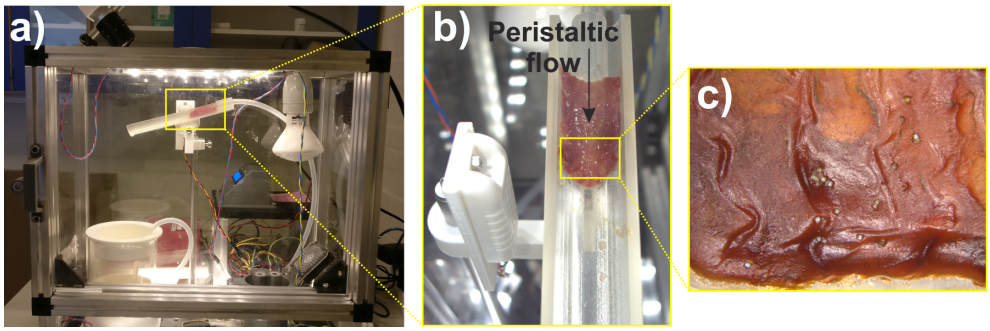

Figure 5.12: *Picture of a) the mucoadhesion setup, b) tissue with the peristaltic flow and c) dry tissue with microcontainers that adhered showing mucoadhesive properties.*

Chapter 6

Conclusions and future perspectives

The first aim of this project was to compare and characterize loading techniques for microfabricated devices for oral drug delivery such as microcontainers.

Two loading techniques for microcontainers were compared (**Paper I**): *i*) hot punching of a PCL film coupled with loading of ketoprofen using scCO_2 and *ii*) hot punching of a PCL + ketoprofen film. The drug loading techniques were evaluated by means of *in vitro* release studies, profilometry, SEM and X-ray μCT. XRPD and Raman spectroscopy showed no differences in the solid state form of ketoprofen, resulting in an amorphous form for both loading techniques. Instead, a pronounced difference between the two loading techniques was exhibited, due to a difference in the release kinetics. This observation highlighted how the choice of the loading technique is important if a certain release is desired.

Since the scCO_2 technique showed a very fast release despite the low solubility of the chosen excipient (PCL), it was necessary to understand the spatial distribution of the drug after the loading using this technique (**Paper II**). Three different sizes of microcontainers were fabricated to compare if the area exposed to scCO_2 was affecting the distribution of the API loaded into the polymer matrix. A custom-made Raman microscope allowed to obtain volumetric Raman maps of an entire microcontainer filled with PVP and scCO_2-impregnated with either naproxen or ketoprofen. For all microcontainer sizes, the drugs were only detected in the top layer of the polymer matrix, explaining the fast release obtained in the *in vitro* studies. Using XRPD and Raman spectroscopy, the solid state form of the drugs was evaluated, showing how ketoprofen was amorphous in all microcontainer sizes, while naproxen was not crystalline.

After comparing and characterizing the loading techniques, microcontainers were tested *in vivo* as an oral drug delivery system for the poorly

water soluble model drug ketoprofen (**Paper III**). This study showed 180% improvement in the relative oral bioavailablity compared to a control prepared with the same materials as the microcontainer formulation. Before the *in vivo* studies, all the preparation steps were characterized using SEM, X-ray μCT, *in vitro* release studies and Raman spectroscopy.

The second aim of the project was the exploration of the possible use of microcontainers as an oral delivery system for proteins. Therefore, the microcontainers were functionalized to further enhance their features for this purpose (**Paper IV**). The functionalization was made by applying two polymeric layers on top of the microcontainers loaded with the model protein lysozyme and the permeation enhancer C10. The functionalized microcontainers were characterized *in vitro* for morphology, drug release and mucoadhesive properties. These were coupled with *in vitro* and *ex vivo* studies using Caco-2 and Caco-2/HT29-MTX-E12 cell monolayers, and porcine intestinal tissue.

From all the results above, in this project, it was shown that: *i*) the loading technique influences, among others, the release profile of the drug, *ii*) it is possible to use a custom-made Raman microscope to obtain a 3D map of an entire microcontainer and evaluate the distribution of the loaded drug in a polymer matrix, *iii*) microcontainers enhance the oral delivery of a poorly soluble model drug *in vivo* and *iv*) it is possible to functionalize the microcontainers to enhance mucoadhesiveness and tune the release in case of protein delivery.

Starting from the results obtained in this project, there are still many directions to explore in order to fully understand the behavior of microcontainer as oral drug delivery system. In particular, the delivery of prodrugs using microcontainers as a delivery system showed preliminary positive results. In the future, the experimental setup needs to be improved and eventually followed by *in vivo* rat study. For example, this will allow to assess if the microcontainers can limit the prodrug transformation in the GI fluids and reach the intestinal barrier for an improved transport of the prodrug to its target.

Regarding delivering probiotics, microcontainers have the potential to ensure a better establishment and colonization of the microorganisms compared to the commercially available technologies available today. In this regard, the microcontainer fabrication can be adjusted to obtain two cavities: one for the probiotics and the other one for prebiotics or antibiotics. If the target area for probiotics is the colon, another possible aspect that needs to be further addressed is the microcontainer coating. As discussed in the thesis, the pH values and transit times in the GI tract are affected from dif-

ferent factors, so the coating characterization will be of utmost importance for the release in the colon.

As a final remark, there is a need for understanding if amorphous indomethacin is stable in different shapes. This will allow to understand if the stability depends only on the fact that the API is confined or if it is a combination of rounded shape and confinement.

Bibliography

[1] C. Loh, A. MacRobert, J. Bedwell, J. Regula, N. Krasner, and S. Bown, "Oral versus intravenous administration of 5-aminolaevulinic acid for photodynamic therapy," *British Journal of Cancer*, vol. 68, no. 1, pp. 41–51, 1993.

[2] K. Sedo and T. Kararli, "GLOBAL REPORT - 2017 Global Drug Delivery & Formulation Report: Part 4, The Drug Delivery & Formulation Pipeline," *Drug Development & Delivery*, 2018.

[3] S. Hooser and D. Earnest, "Introduction: The Gastrointestinal Tract," *Comprehensive Toxicology*, pp. 1–2, 2018.

[4] U. Wais, A. W. Jackson, T. He, and H. Zhang, "Nanoformulation and encapsulation approaches for poorly water-soluble drug nanoparticles," *Nanoscale*, vol. 8, no. 4, pp. 1746–1769, 2016.

[5] A. Patel, M. Patel, X. Yang, and A. K. Mitra, "Recent Advances in Protein and Peptide Drug Delivery: A Special Emphasis on Polymeric Nanoparticles," *Protein and peptide letters*, vol. 21, no. 11, pp. 1102–1120, 2014.

[6] T. Hetal, P. Bindesh, and T. Sneha, "A REVIEW ON TECHNIQUES FOR ORAL BIOAVAILABILITY ENHANCEMENT OF DRUGS," *International Journal of Pharmaceutical Sciences Review and Research*, vol. 4, no. 3, pp. 203–223, 2010.

[7] C. B. Fox, J. Kim, L. V. Le, C. L. Nemeth, H. D. Chirra, and T. A. Desai, "Micro/nanofabricated platforms for oral drug delivery," *Journal of Controlled Release*, vol. 219, pp. 431–444, 2015.

[8] H. D. Chirra and T. A. Desai, "Emerging microtechnologies for the development of oral drug delivery devices," *Advanced Drug Delivery Reviews*, vol. 64, no. 14, pp. 1569–1578, 2012.

[9] P. Li and L. Zhao, "Developing early formulations: Practice and perspective," *International Journal of Pharmaceutics*, vol. 341, no. 1-2, pp. 1–19, 2007.

[10] U. Agrawal, R. Sharma, M. Gupta, and S. P. Vyas, "Is nanotechnology a boon for oral drug delivery?," *Drug Discovery Today*, vol. 19, no. 10, pp. 1530–1546, 2014.

[11] U. Schwarz, T. Gramatté, J. Krappweis, R. Oertel, and W. Kirch, "P-glycoprotein inhibitor erythromycin increases oral bioavailability of talinolol in humans," *Int. Journal of Clinical Pharmacology and Therapeutics*, vol. 38, no. 04, pp. 161–167, 2000.

[12] L. H. Nielsen, S. S. Keller, and A. Boisen, "Microfabricated devices for oral drug delivery," *Lab on a Chip*, vol. 18, no. 16, pp. 2348–2358, 2018.

[13] L. H. Nielsen, A. Melero, S. S. Keller, J. Jacobsen, T. Garrigues, T. Rades, A. Müllertz, and A. Boisen, "Polymeric microcontainers improve oral bioavailability of furosemide," *International Journal of Pharmaceutics*, vol. 504, no. 1-2, pp. 98–109, 2016.

[14] P. Marizza, L. Pontoni, T. Rindzevicius, J. Alopaeus, K. Su, J. Zeitler, S. Keller, I. Kikic, M. Moneghini, N. De Zordi, D. Solinas, A. Cortesi, and A. Boisen, "Supercritical impregnation of polymer matrices spatially confined in microcontainers for oral drug delivery: Effect of temperature, pressure and time," *The Journal of Supercritical Fluids*, vol. 107, pp. 145–152, 2016.

[15] A. C. Anselmo, Y. Gokarn, and S. Mitragotri, "Non-invasive delivery strategies for biologics," *Nature Reviews Drug Discovery*, 2018.

[16] A. C. Anselmo, "An overview of clinical and commercial impact of drug delivery systems," *Journal of Controlled Release*, vol. 190, pp. 15–28, 2014.

[17] K. Thanki, R. P. Gangwal, A. T. Sangamwar, and S. Jain, "Oral delivery of anticancer drugs: Challenges and opportunities," *Journal of Controlled Release*, vol. 170, no. 1, pp. 15–40, 2013.

[18] G. Liu, E. Franssen, M. I. Fitch, and E. Warner, "Patient preferences for oral versus intravenous palliative chemotherapy.," *Journal of Clinical Oncology*, vol. 15, no. 1, pp. 110–115, 1997.

[19] P. Viswanathan, Y. Muralidaran, and G. Ragavan, "Challenges in oral drug delivery: a nano-based strategy to overcome," *Nanostructures for Oral Medicine*, pp. 173–201, 2017.

[20] L. A. Mandell, M. G. Bergeron, M. J. Gribble, P. J. Jewesson, D. E. Low, T. J. Marrie, and L. E. Nicolle, "Sequential Antibiotic Therapy: Effective Cost Management and Patient Care," *Canadian Journal of Infectious Diseases*, vol. 6, no. 6, pp. 306–315, 1995.

[21] F. Sevinc, J. M. Prins, R. P. Koopmans, P. N. J. Langendijk, P. M. Bossuyt, J. Dankert, and P. Speelman, "Early switch from intravenous to oral antibiotics: guidelines and implementation in a large teaching hospital," *Journal of Antimicrobial Chemotherapy*, vol. 43, no. 4, pp. 601–606, 1999.

[22] P. M. Treuting, M. J. Arends, and S. M. Dintzis, "11. Upper Gastrointestinal Tract," *Comparative Anatomy and Histology*, pp. 191–212, 2017.

[23] E. L. McConnell, H. M. Fadda, and A. W. Basit, "Gut instincts: Explorations in intestinal physiology and drug delivery," *International Journal of Pharmaceutics*, vol. 364, no. 2, pp. 213–226, 2008.

[24] W. F. Boron and E. L. Boulpaep, *Medical physiology: a cellular and molecular approach*. Elsevier, 2012.

[25] P.-A. Billat, E. Roger, S. Faure, and F. Lagarce, "Models for drug absorption from the small intestine: where are we and where are we going?," *Drug Discovery Today*, vol. 22, no. 5, pp. 761–775, 2017.

[26] J. Fallingborg, L. A. Christinsen, M. Ingeman-Nielsen, B. A. Jacobsen, K. Abildgaard, and H. H. Rasmussen, "pH-Profile and regional transit times of the normal gut measured by a radiotelemetry device," *Alimentary Pharmacology & Therapeutics*, vol. 3, no. 6, pp. 605–614, 2007.

[27] P. V. Balimane, S. Chong, and R. A. Morrison, "Current methodologies used for evaluation of intestinal permeability and absorption," *Journal of Pharmacological and Toxicological Methods*, vol. 44, no. 1, pp. 301–312, 2000.

[28] A. L. Daugherty and R. J. Mrsny, "Transcellular uptake mechanisms of the intestinal epithelial barrier Part one," *Pharmaceutical Science & Technology Today*, vol. 2, no. 4, pp. 144–151, 1999.

[29] P. V. Balimane and S. Chong, "Cell culture-based models for intestinal permeability: A critique," *Drug Discovery Today*, vol. 10, no. 5, pp. 335–343, 2005.

[30] B. Greenwood-Van Meerveld, A. C. Johnson, and D. Grundy, *Gastrointestinal Physiology and Function*. Springer, Cham, 2017.

[31] V. K. Viswanathan, K. Hodges, and G. Hecht, "Enteric infection meets intestinal function: how bacterial pathogens cause diarrhoea," *Nature Reviews Microbiology*, vol. 7, no. 2, pp. 110–119, 2009.

[32] T. Pelaseyed, J. H. Bergström, J. K. Gustafsson, A. Ermund, G. M. H. Birchenough, A. Schütte, S. van der Post, F. Svensson, A. M. Rodríguez-Piñeiro, E. E. L. Nyström, C. Wising, M. E. V. Johansson, and G. C. Hansson, "The mucus and mucins of the goblet cells and enterocytes provide the first defense line of the gastrointestinal tract and interact with the immune system.," *Immunological reviews*, vol. 260, no. 1, pp. 8–20, 2014.

[33] J. D. Smart, "The basics and underlying mechanisms of mucoadhesion," *Advanced Drug Delivery Reviews*, vol. 57, no. 11, pp. 1556–1568, 2005.

[34] L. M. Ensign, R. Cone, and J. Hanes, "Oral drug delivery with polymeric nanoparticles: The gastrointestinal mucus barriers," *Advanced Drug Delivery Reviews*, vol. 64, no. 6, pp. 557–570, 2012.

[35] K. R. Groschwitz and S. P. Hogan, "Intestinal barrier function: molecular regulation and disease pathogenesis.," *The Journal of allergy and clinical immunology*, vol. 124, no. 1, pp. 3–22, 2009.

[36] P. Fonte, F. Araújo, S. Reis, and B. Sarmento, "Oral insulin delivery: how far are we?," *Journal of diabetes science and technology*, vol. 7, no. 2, pp. 520–31, 2013.

[37] J. Hochman and P. Artursson, "Mechanisms of absorption enhancement and tight junction regulation," *Journal of Controlled Release*, vol. 29, no. 3, pp. 253–267, 1994.

[38] K. T. Savjani, A. K. Gajjar, and J. K. Savjani, "Drug solubility: importance and enhancement techniques," *ISRN pharmaceutics*, vol. 2012, pp. 1–10, 2012.

[39] G. L. Amidon, H. Lennernäs, V. P. Shah, and J. R. Crison, "A theoretical basis for a biopharmaceutic drug classification: the correlation of in vitro drug product dissolution and in vivo bioavailability.," *Pharmaceutical research*, vol. 12, no. 3, pp. 413–20, 1995.

[40] A. Mullard, "Re-assessing the rule of 5, two decades on," *Nature Reviews Drug Discovery*, vol. 17, no. 11, p. 777, 2018.

[41] S. V. Jermain, C. Brough, and R. O. Williams, "Amorphous solid dispersions and nanocrystal technologies for poorly water-soluble drug delivery - An update," *International Journal of Pharmaceutics*, vol. 535, no. 1-2, pp. 379–392, 2018.

[42] G. Poovi and N. Damodharan, "Lipid nanoparticles: A challenging approach for oral delivery of BCS Class-II drugs," *Future Journal of Pharmaceutical Sciences*, 2018.

[43] L. Padrela, M. A. Rodrigues, A. Duarte, A. M. Dias, M. E. Braga, and H. C. de Sousa, "Supercritical carbon dioxide-based technologies for the production of drug nanoparticles/nanocrystals - A comprehensive review," *Advanced Drug Delivery Reviews*, vol. 131, pp. 22–78, 2018.

[44] T. Vasconcelos, B. Sarmento, and P. Costa, "Solid dispersions as strategy to improve oral bioavailability of poor water soluble drugs," *Drug Discovery Today*, vol. 12, no. 23-24, pp. 1068–1075, 2007.

[45] Y. Perrie and T. Rades, "Immediate-release drug delivery system I: increasing the solubility and dissolution rate of drugs," in *Pharmaceutics: drug delivery and targeting*, ch. 2, pp. 25–58, Pharmaceutical Press, 2 ed., 2012.

[46] W. L. Chiou and S. Riegelmant, "Pharmaceutical Applications of Solid Dispersion," *Journal of Pharmaceutical Sciences*, vol. 60, no. 9, pp. 1281–1302, 1971.

[47] Y. Huang and W.-G. Dai, "Fundamental aspects of solid dispersion technology for poorly soluble drugs," *Acta Pharmaceutica Sinica B*, vol. 4, no. 1, pp. 18–25, 2014.

[48] J. E. Patterson, M. B. James, A. H. Forster, R. W. Lancaster, J. M. Butler, and T. Rades, "The Influence of Thermal and Mechanical Preparative Techniques on the Amorphous State of Four Poorly Soluble Compounds," *Journal of Pharmaceutical Sciences*, vol. 94, no. 9, pp. 1998–2012, 2005.

[49] S. Yalkowski, S. Banerjee, and M. Dekker, "Aqueous Solubility: Methods of Estimation for Organic Compounds," in *Journal of Dispersion Science and Technology*, p. 583, 1992.

[50] T. Hložek, M. Bursová, and R. Čabala, "Fast ibuprofen, ketoprofen and naproxen simultaneous determination in human serum for clinical toxicology by GC-FID," *Clinical Biochemistry*, vol. 47, no. 15, pp. 109–111, 2014.

[51] S. Kalepu and V. Nekkanti, "Insoluble drug delivery strategies: review of recent advances and business prospects," *Acta Pharmaceutica Sinica B*, vol. 5, no. 5, pp. 442–453, 2015.

[52] C. G. Pitt, "Poly-Caprolactone and Its Copolymers," in *Biodegradable Polymers as Drug Delivery Systems* (M. Chasin and R. Langer, eds.), ch. 3, pp. 71–120, New York, NY: Marcel Dekker, IND., 1990.

[53] G. S. Kwon and D. Y. Furgenson, "Biodegradable polymers for drug delivery systems," *Biomedical Polymers*, pp. 83–110, 2007.

[54] J. Murray, N. Laurieri, and R. Delgoda, "Proteins," in *Pharmacognosy* (S. Badal and R. Delgoda, eds.), ch. 24, pp. 477–494, Academic Press, 2017.

[55] A. D. McNaught and A. Wilkinson, "Compendium of Chemical Terminology," in *IUPAC Compendium of Chemical Terminology*, Blackwell Scientific Publications, Oxford, 2nd ed., 1997.

[56] M. S. Kinch, "An overview of FDA-approved biologics medicines," *Drug Discovery Today*, vol. 20, no. 4, pp. 393–398, 2015.

[57] J. L. Lau and M. K. Dunn, "Therapeutic peptides: Historical perspectives, current development trends, and future directions," *Bioorganic & Medicinal Chemistry*, vol. 26, no. 10, pp. 2700–2707, 2018.

[58] H. R. Lakkireddy, M. Urmann, M. Besenius, U. Werner, T. Haack, P. Brun, J. Alié, B. Illel, L. Hortala, R. Vogel, and D. Bazile, "Oral delivery of diabetes peptides - Comparing standard formulations incorporating functional excipients and nanotechnologies in the translational context," *Advanced Drug Delivery Reviews*, vol. 106, pp. 196–222, 2016.

[59] A. Fasano, "Innovative strategies for the oral delivery of drugs and peptides," *Trends in Biotechnology*, vol. 16, no. 4, pp. 152–157, 1998.

[60] P. Varamini and I. Toth, "Recent advances in oral delivery of peptide hormones," *Expert Opinion on Drug Delivery*, vol. 13, no. 4, pp. 507–522, 2016.

[61] A. Banerjee, K. Ibsen, T. Brown, R. Chen, C. Agatemor, and S. Mitragotri, "Ionic liquids for oral insulin delivery.," *Proceedings of the National Academy of Sciences of the United States of America*, vol. 115, no. 28, pp. 7296–7301, 2018.

[62] Y.-W. Huang and S. Barua, "ORAL DRUG DELIVERY SYSTEMS FOR GASTROINTESTINAL CANCER THERAPY," pp. 187–218, 2018.

[63] J. A. Al-Lawati, "Diabetes Mellitus: A Local and Global Public Health Emergency!," *Oman medical journal*, vol. 32, no. 3, pp. 177–179, 2017.

[64] E. Caffarel-Salvador, A. Abramson, R. Langer, and G. Traverso, "Oral delivery of biologics using drug-device combinations," *Current Opinion in Pharmacology*, vol. 36, pp. 8–13, 2017.

[65] K. Park, I. C. Kwon, and K. Park, "Oral protein delivery: Current status and future prospect," *Reactive and Functional Polymers*, vol. 71, no. 3, pp. 280–287, 2011.

[66] A. Muheem, F. Shakeel, M. A. Jahangir, M. Anwar, N. Mallick, G. K. Jain, M. H. Warsi, and F. J. Ahmad, "A review on the strategies for oral delivery of proteins and peptides and their clinical perspectives," *Saudi Pharmaceutical Journal*, vol. 24, no. 4, pp. 413–428, 2016.

[67] D. J. Brayden and R. J. Mrsny, "Oral peptide delivery: prioritizing the leading technologies," *Therapeutic Delivery*, vol. 2, no. 12, pp. 1567–1573, 2011.

[68] F. McCartney, J. P. Gleeson, and D. J. Brayden, "Safety concerns over the use of intestinal permeation enhancers: A mini-review.," *Tissue barriers*, vol. 4, no. 2, p. e1176822, 2016.

[69] S. M. Krug, M. Amasheh, I. Dittmann, I. Christoffel, M. Fromm, and S. Amasheh, "Sodium caprate as an enhancer of macromolecule permeation across tricellular tight junctions of intestinal cells," *Biomaterials*, vol. 34, no. 1, pp. 275–282, 2013.

[70] Z. Abid, C. Gundlach, O. Durucan, C. von Halling Laier, L. H. Nielsen, A. Boisen, and S. S. Keller, "Powder embossing method for selective loading of polymeric microcontainers with drug formulation," *Microelectronic Engineering*, vol. 171, pp. 20–24, 2017.

[71] A. Ahmed, C. Bonner, and T. a. Desai, "Bioadhesive microdevices with multiple reservoirs: a new platform for oral drug delivery," *Journal of Controlled Release*, vol. 81, no. 3, pp. 291–306, 2002.

[72] H. D. Chirra, L. Shao, N. Ciaccio, C. B. Fox, J. M. Wade, A. Ma, and T. A. Desai, "Planar Microdevices for Enhanced In Vivo Retention and Oral Bioavailability of Poorly Permeable Drugs," *Advanced Healthcare Materials*, vol. 3, no. 10, pp. 1648–1654, 2014.

[73] C. B. Fox, Y. Cao, C. L. Nemeth, H. D. Chirra, R. W. Chevalier, A. M. Xu, N. A. Melosh, and T. A. Desai, "Fabrication of Sealed Nanostraw Microdevices for Oral Drug Delivery," *ACS Nano*, vol. 10, no. 6, pp. 5873–5881, 2016.

[74] L. H. Nielsen, S. S. Keller, K. C. Gordon, A. Boisen, T. Rades, and A. Müllertz, "Spatial confinement can lead to increased stability of amorphous indomethacin," *European Journal of Pharmaceutics and Biopharmaceutics*, vol. 81, no. 2, pp. 418–425, 2012.

[75] L. H. Nielsen, J. Nagstrup, S. Gordon, S. S. Keller, J. Østergaard, T. Rades, A. Müllertz, and A. Boisen, "pH-triggered drug release from biodegradable microwells for oral drug delivery," *Biomedical Microdevices*, vol. 17, no. 3, pp. 1–7, 2015.

[76] S. Keller, G. Blagoi, M. Lillemose, D. Haefliger, and A. Boisen, "Processing of thin SU-8 films," *Journal of Micromechanics and Microengineering*, vol. 18, no. 12, p. 125020, 2008.

[77] P. Marizza, S. S. Keller, A. Müllertz, and A. Boisen, "Polymer-filled microcontainers for oral delivery loaded using supercritical impregnation.," *Journal of Controlled Release*, vol. 173, pp. 1–9, 2014.

[78] V. Linder, B. D. Gates, D. Ryan, B. A. Parviz, and G. M. Whitesides, "Water-soluble sacrificial layers for surface micromachining," *Small*, vol. 1, no. 7, pp. 730–736, 2005.

[79] S. Keller, D. Haefliger, and A. Boisen, "Optimized plasma-deposited fluorocarbon coating for dry release and passivation of thin SU-8 cantilevers," *Journal of Vacuum Science & Technology B: Microelectronics and Nanometer Structures*, vol. 25, no. 6, p. 1903, 2007.

[80] L. H. Nielsen, T. Rades, B. Boyd, and A. Boisen, "Microcontainers as an oral delivery system for spray dried cubosomes containing ovalbumin," *European Journal of Pharmaceutics and Biopharmaceutics*, vol. 118, pp. 13–20, 2017.

[81] J. L. Panza and E. J. Beckman, "Supercritical Fluid Technology for Drug Product Development," in *Supercritical Fluid Technology for Drug Product Development* (P. York, U. B. Kompella, and B. Y. Shekunov, eds.), ch. 1, pp. 1–26, 2005.

[82] S. P. Nalawade, F. Picchioni, and L. Janssen, "Supercritical carbon dioxide as a green solvent for processing polymer melts: Processing aspects and applications," *Progress in Polymer Science*, vol. 31, no. 1, pp. 19–43, 2006.

[83] A. I. Cooper, "Polymer synthesis and processing using supercritical carbon dioxide," *Journal of Materials Chemistry*, vol. 10, no. 2, pp. 207–234, 2000.

[84] J. A. Darr and M. Poliakoff, "New Directions in Inorganic and Metal-Organic Coordination Chemistry in Supercritical Fluids," *Chemical review*, vol. 99, no. 2, pp. 495–542, 1999.

[85] N. De Zordi, I. Kikic, M. Moneghini, and D. Solinas, "Solubility of pharmaceutical compounds in supercritical carbon dioxide," *The Journal of Supercritical Fluids*, vol. 66, pp. 16–22, 2012.

[86] L. Manna, M. Banchero, D. Sola, A. Ferri, S. Ronchetti, and S. Sicardi, "Impregnation of PVP microparticles with ketoprofen in the presence of supercritical CO2," *The Journal of Supercritical Fluids*, vol. 42, no. 3, pp. 378–384, 2007.

[87] C. Mazzoni, F. Tentor, S. A. Strindberg, L. H. Nielsen, S. S. Keller, T. S. Alstrøm, C. Gundlach, A. Müllertz, P. Marizza, and A. Boisen, "From concept to in vivo testing: Microcontainers for oral drug delivery," *Journal of Controlled Release*, vol. 268, no. September, pp. 343–351, 2017.

[88] R. S. Petersen, R. Mahshid, N. K. Andersen, S. S. Keller, H. N. Hansen, and A. Boisen, "Hot embossing and mechanical punching of biodegradable microcontainers for oral drug delivery," *Microelectronic Engineering*, vol. 133, pp. 104–109, 2015.

[89] R. S. Petersen, S. S. Keller, and A. Boisen, "Hot punching of high-aspect-ratio 3D polymeric microstructures for drug delivery.," *Lab on a chip*, vol. 15, no. 12, pp. 2576–9, 2015.

[90] C. A. Bergström, R. Holm, S. A. Jørgensen, S. B. Andersson, P. Artursson, S. Beato, A. Borde, K. Box, M. Brewster, J. Dressman, K.-I. Feng, G. Halbert, E. Kostewicz, M. McAllister, U. Muenster, J. Thinnes, R. Taylor, and A. Mullertz, "Early pharmaceutical profiling to predict oral drug absorption: Current status and unmet needs," *European Journal of Pharmaceutical Sciences*, vol. 57, pp. 173–199, 2014.

[91] Y. Tanaka, T. Hara, R. Waki, and S. Nagata, "Regional differences in the components of luminal water from rat gastrointestinal tract and comparison with other species," *Journal of Pharmacy and Pharmaceutical Sciences*, vol. 15, no. 4, pp. 510–518, 2012.

[92] F. Danhier, E. Ansorena, J. M. Silva, R. Coco, A. Le Breton, and V. Préat, "PLGA-based nanoparticles: An overview of biomedical applications," *Journal of Controlled Release*, vol. 161, no. 2, pp. 505–522, 2012.

[93] C. L. Stevenson, C. A. Rhodes, and S. J. Prestrelski, "Delivery of Peptides and Proteins via Long Acting Injections and Implants," in *Long Acting Injections and Implants* (J. C. Wright and D. J. Burgess, eds.), pp. 409–427, Boston, MA: Springer US, 2012.

[94] A. Kumari, S. K. Yadav, and S. C. Yadav, "Biodegradable polymeric nanoparticles based drug delivery systems," *Colloids and Surfaces B: Biointerfaces*, vol. 75, no. 1, pp. 1–18, 2010.

[95] A. Prokop and J. M. Davidson, "Nanovehicular Intracellular Delivery Systems," *Journal of Pharmaceutical Sciences*, vol. 97, no. 9, pp. 3518–3590, 2008.

[96] M. Vert, J. Mauduit, and S. Li, "Biodegradation of PLA/GA polymers: increasing complexity," *Biomaterials*, vol. 15, no. 15, pp. 1209–1213, 1994.

[97] M. Rinaudo, "Chitin and chitosan: Properties and applications," *Prog. Polym. Sci*, vol. 31, pp. 603–632, 2006.

[98] T. M. M. Ways, W. M. Lau, and V. V. Khutoryanskiy, "Chitosan and Its Derivatives for Application in Mucoadhesive Drug Delivery Systems," *Polymers*, vol. 10, no. 3, p. 267, 2018.

[99] J. A. S. Moreno, A. C. Mendes, K. Stephansen, C. Engwer, F. M. Goycoolea, A. Boisen, L. H. Nielsen, and I. S. Chronakis, "Development of electrosprayed mucoadhesive chitosan microparticles," *Carbohydrate Polymers*, vol. 190, pp. 240–247, 2018.

[100] C. K. S. Pillai, W. Paul, and C. P. Sharma, "Chitin and chitosan polymers: Chemistry, solubility and fiber formation," *Progress in Polymer Science*, vol. 34, pp. 641–678, 2009.

[101] A. Jain, A. Gulbake, S. Shilpi, A. Jain, P. Hurkat, and S. K. Jain, "A New Horizon in Modifications of Chitosan: Syntheses and Applications," *Critical Reviews in Therapeutic Drug Carrier Systems*, vol. 30, no. 2, 2013.

[102] L.-W. Hsu, P.-L. Lee, C.-T. Chen, F.-L. Mi, J.-H. Juang, S.-M. Hwang, Y.-C. Ho, and H.-W. Sung, "Elucidating the signaling mechanism of an epithelial tight-junction opening induced by chitosan," *Biomaterials*, vol. 33, no. 26, pp. 6254–6263, 2012.

[103] M. Mohammed, J. Syeda, K. Wasan, E. Wasan, M. A. Mohammed, J. T. M. Syeda, K. M. Wasan, and E. K. Wasan, "An Overview of Chitosan Nanoparticles and Its Application in Non-Parenteral Drug Delivery," *Pharmaceutics*, vol. 9, no. 4, p. 53, 2017.

[104] I. A. Sogias, A. C. Williams, and V. V. Khutoryanskiy, "Why is chitosan mucoadhesive?," *Biomacromolecules*, vol. 9, no. 7, pp. 1837–1842, 2008.

[105] T.-H. Yeh, L.-W. Hsu, M. T. Tseng, P.-L. Lee, K. Sonjae, Y.-C. Ho, and H.-W. Sung, "Mechanism and consequence of chitosan-mediated reversible epithelial tight junction opening," *Biomaterials*, vol. 32, no. 26, pp. 6164–6173, 2011.

[106] J. Smith, E. Wood, and M. Dornish, "Effect of Chitosan on Epithelial Cell Tight Junctions," *Pharmaceutical Research*, vol. 21, no. 1, pp. 43–49, 2004.

[107] K. Knop, R. Hoogenboom, D. Fischer, and U. S. Schubert, "Poly(ethylene glycol) in Drug Delivery: Pros and Cons as Well as Potential Alternatives.," *ChemInform*, vol. 42, no. 3, pp. no–no, 2011.

[108] M. Liu, J. Zhang, W. Shan, and Y. Huang, "Developments of mucus penetrating nanoparticles," *Asian Journal of Pharmaceutical Sciences*, vol. 10, no. 4, pp. 275–282, 2015.

[109] Y.-Y. Wang, S. K. Lai, J. S. Suk, A. Pace, R. Cone, and J. Hanes, "Addressing the PEG Mucoadhesivity Paradox to Engineer Nanoparticles that "Slip" through the Human Mucus Barrier," *Angewandte Chemie International Edition*, vol. 47, no. 50, pp. 9726–9729, 2008.

[110] Q. Xu, L. M. Ensign, N. J. Boylan, A. Schön, X. Gong, J.-C. Yang, N. W. Lamb, S. Cai, T. Yu, E. Freire, and J. Hanes, "Impact of Surface Polyethylene Glycol (PEG) Density on Biodegradable Nanoparticle Transport in Mucus ex Vivo and Distribution in Vivo," *ACS Nano*, vol. 9, no. 9, pp. 9217–9227, 2015.

[111] R. Kumar and C. Wassgren, "Angular circulation speed of tablets in a vibratory tablet coating pan.," *AAPS PharmSciTech*, vol. 14, no. 1, pp. 339–51, 2013.

[112] F. L. Laksmana, P. J. A. Hartman Kok, H. Vromans, H. W. Frijlink, and K. Van der Voort Maarschalk, "Development and application of a process window for achieving high-quality coating in a fluidized bed coating process.," *AAPS PharmSciTech*, vol. 10, no. 3, pp. 732–42, 2009.

[113] S. Bose, S. S. Keller, T. S. Alstrøm, A. Boisen, and K. Almdal, "Process Optimization of Ultrasonic Spray Coating of Polymer Films," *Langmuir*, vol. 29, no. 23, pp. 6911–6919, 2013.

[114] E. H. Immergut and H. F. Mark, "Principles of Plasticization," in *Plasticization and Plasticizer Processes* (N. A. J. Platzer, ed.), ch. 1, pp. 1–26, Washington: AMERICAN CHEMICAL SOCIETY, 1965.

[115] J. Østergaard, "UV/Vis Spectrophotometry and UV Imaging," in *Analytical techniques in the pharmaceutical sciences* (A. Müllertz, Y. Perrie, and T. Rades, eds.), ch. 1, pp. 3–27, Springer, New York, NY, 2016.

[116] J. Østergaard, "UV imaging in pharmaceutical analysis," *Journal of Pharmaceutical and Biomedical Analysis*, vol. 147, pp. 140–148, 2018.

[117] A. Avdeef and O. Tsinman, "Miniaturized Rotating Disk Intrinsic Dissolution Rate Measurement: Effects of Buffer Capacity in Com-

parisons to Traditional Wood's Apparatus," *Pharmaceutical Research*, vol. 25, no. 11, pp. 2613–2627, 2008.

[118] X. Lu, R. Lozano, and P. Shah, "In-Situ Dissolution Testing Using Different UV Fiber Optic Probes and Instruments," *Dissolution Technologies*, pp. 6–15, 2003.

[119] P. Christophersen, M. Fano, L. Saaby, M. Yang, H. Nielsen, and H. Mu, "Characterization of Particulate Drug Delivery Systems for Oral Delivery of Peptide and Protein Drugs," *Current Pharmaceutical Design*, vol. 21, no. 19, pp. 2611–2628, 2015.

[120] S. Klein, "The use of biorelevant dissolution media to forecast the in vivo performance of a drug.," *The AAPS journal*, vol. 12, no. 3, pp. 397–406, 2010.

[121] J. F. Christfort, S. Strindberg, J. Plum, J. Hall-Anderesen, C. Janfelt, L. H. Nielsen, and A. Müllertz, "Simulated gastric and intetsinal rat media improve in vitro in vivo relation," *European journal of pharmaceutics and biopharmaceutics*.

[122] S. H. Hansen, "HPLC/UHPLC," in *Analytical techniques in the pharmaceutical sciences* (A. Müllertz, Y. Perrie, and T. Rades, eds.), ch. 13, pp. 413–437, Springer, New York, NY, 2016.

[123] P. K. Sahu, N. R. Ramisetti, T. Cecchi, S. Swain, C. S. Patro, and J. Panda, "An overview of experimental designs in HPLC method development and validation," *Journal of Pharmaceutical and Biomedical Analysis*, vol. 147, pp. 590–611, 2018.

[124] L. Reimer, "Image Contrast and Signal Processing," in *Scanning Electron Microscopy*, pp. 207–251, Springer, Berlin, Heidelberg, 1998.

[125] I. Akseli, S. Iyer, H. P. Lee, and A. M. Cuitiño, "A quantitative correlation of the effect of density distributions in roller-compacted ribbons on the mechanical properties of tablets using ultrasonics and X-ray tomography.," *AAPS PharmSciTech*, vol. 12, no. 3, pp. 834–53, 2011.

[126] M. L. Bouxsein, S. K. Boyd, B. A. Christiansen, R. E. Guldberg, K. J. Jepsen, and R. Müller, "Guidelines for assessment of bone microstructure in rodents using micro-computed tomography," *Journal of Bone and Mineral Research*, vol. 25, no. 7, pp. 1468–1486, 2010.

[127] L. H. Nielsen, S. S. Keller, A. Boisen, A. Müllertz, and T. Rades, "A slow cooling rate of indomethacin melt spatially confined in microcontainers increases the physical stability of the amorphous drug without influencing its biorelevant dissolution behaviour," *Drug Delivery and Translational Research*, vol. 4, no. 3, pp. 268–274, 2014.

[128] K. C. Gordon and S. J. Fraser-Miller, "Raman Spectroscopy," in *Analytical Techniques in the Pharmaceutical Sciences* (A. Müllertz, Y. Perrie, and T. Rades, eds.), ch. 4, pp. 139–169, Springer, New York, NY, 2016.

[129] R. L. McCreery, *Raman spectroscopy for chemical analysis*. John Wiley & Sons, 2000.

[130] S. Assi, "Raw material identification using dual laser handheld Raman spectroscopy," *European Pharmaceutical Review*, vol. 18, no. 5, pp. 25–31, 2013.

[131] A. Paudel, D. Raijada, and J. Rantanen, "Raman spectroscopy in pharmaceutical product design," *Advanced Drug Delivery Reviews*, vol. 89, pp. 3–20, 2015.

[132] L.-l. Ooi, *Principles of x-ray crystallography*. Oxford University Press, 2010.

[133] K. D. M. Harris, M. Tremayne, and B. M. Kariuki, "Contemporary Advances in the Use of Powder X-Ray Diffraction for Structure Determination," *Angewandte Chemie International Edition*, vol. 40, no. 9, pp. 1626–1651, 2001.

[134] S. J. Trenfield, A. Goyanes, R. Telford, D. Wilsdon, M. Rowland, S. Gaisford, and A. W. Basit, "3D printed drug products: Non-destructive dose verification using a rapid point-and-shoot approach," *International Journal of Pharmaceutics*, vol. 549, no. 1-2, pp. 283–292, 2018.

[135] M. Engle, G. Goetz, and D. Alpers, "Caco-2 cells express a combination of colonocyte and enterocyte phenotypes," *Journal of Cellular Physiology*, vol. 174, no. 3, pp. 362–369, 1998.

[136] T. Lea, "Caco-2 Cell Line," in *The Impact of Food Bioactives on Health*, pp. 103–111, Cham: Springer International Publishing, 2015.

[137] P. Artursson and J. Karlsson, "Correlation between oral drug absorption in humans and apparent drug permeability coefficients in human intestinal epithelial (Caco-2) cells," *Biochemical and Biophysical Research Communications*, vol. 175, no. 3, pp. 880–885, 1991.

[138] K.-C. Cheng, C. Li, and A. S. Uss, "Prediction of oral drug absorption in humans - from cultured cell lines and experimental animals," *Expert Opinion on Drug Metabolism & Toxicology*, vol. 4, no. 5, pp. 581–590, 2008.

[139] H. Sun, E. C. Chow, S. Liu, Y. Du, and K. S. Pang, "The Caco-2 cell monolayer: usefulness and limitations," *Expert Opinion on Drug Metabolism & Toxicology*, vol. 4, no. 4, pp. 395–411, 2008.

[140] A. Wikman-Larhed and P. Artursson, "Co-cultures of human intestinal goblet (HT29-H) and absorptive (Caco-2) cells for studies of drug and peptide absorption," *European Journal of Pharmaceutical Sciences*, vol. 3, no. 3, pp. 171–183, 1995.

[141] J. K. Patterson, X. G. Lei, and D. D. Miller, "The Pig as an Experimental Model for Elucidating the Mechanisms Governing Dietary Influence on Mineral Absorption," *Experimental Biology and Medicine*, vol. 233, no. 6, pp. 651–664, 2008.

[142] E. M. Walters, Y. Agca, V. Ganjam, and T. Evans, "Animal models got you puzzled?: think pig," *Annals of the New York Academy of Sciences*, vol. 1245, no. 1, pp. 63–64, 2011.

[143] L. L. Clarke, "A guide to Ussing chamber studies of mouse intestine.," *American journal of physiology. Gastrointestinal and liver physiology*, vol. 296, no. 6, pp. G1151–66, 2009.

[144] C. Woertz, M. Preis, J. Breitkreutz, and P. Kleinebudde, "Assessment of test methods evaluating mucoadhesive polymers and dosage forms: An overview," *European Journal of Pharmaceutics and Biopharmaceutics*, vol. 85, no. 3, pp. 843–853, 2013.

[145] K. V. R. Rao and P. Buri, "A novel in situ method to test polymers and coated microparticles for bioadhesion," *International Journal of Pharmaceutics*, vol. 52, no. 3, pp. 265–270, 1989.

Appendix A

Paper I

Release of ketoprofen from microcontainers - influence of the loading method

F. Tentor & C. Mazzoni, L. Leonardi, P. Marizza, R.S. Petersen, S.S. Keller, A. Boisen

Submitted to Biomedical Microdevices

Appendix B

Paper II

Where is the drug? - Quantitative 3D distribution analyses of confined drug-loaded polymer matrices

C. Mazzoni, F. Tentor, A. Antalaki, J. Mortensen, R.D. Jacobsen, R. Slipets, O. Ilchenko, S.S. Keller, L.H. Nielsen, A. Boisen

Submitted to ACS Biomaterials Science & Engineering

Appendix C

Paper III

From concept to in vivo testing: Microcontainers for oral drug delivery

C. Mazzoni & F. Tentor, S.A. Strindberg, L.H. Nielsen, S.S. Keller, T.S. Alstrøm, C. Gundlach, A. Müllertz, P. Marizza, A. Boisen

Published on Journal of Controlled Release, vol. 268, pp. 343-351, October 2017

Journal of Controlled Release 268 (2017) 343–351

Contents lists available at ScienceDirect

Journal of Controlled Release

journal homepage: www.elsevier.com/locate/jconrel

From concept to *in vivo* testing: Microcontainers for oral drug delivery

Chiara Mazzoni[a,*,1], Fabio Tentor[a,*,1], Sophie Andersen Strindberg[b], Line Hagner Nielsen[a], Stephan Sylvest Keller[a], Tommy Sonne Alstrøm[c], Carsten Gundlach[d], Anette Müllertz[b], Paolo Marizza[a], Anja Boisen[a]

[a] Department of Micro- and Nanotechnology, Technical University of Denmark, Ørsteds Plads 345C, 2800 Kgs. Lyngby, Denmark
[b] Department of Pharmacy, Faculty of Health and Medical Sciences, University of Copenhagen, Universitetsparken 2, 2100 Copenhagen O, Denmark
[c] Department of Applied Mathematics and Computer Science, Technical University of Denmark, Richard Petersens Plads 324, 2800 Kgs. Lyngby, Denmark
[d] Department of Physics, NEXMAP, Technical University of Denmark, Fysikvej 311, 2800 Kgs. Lyngby, Denmark

ARTICLE INFO

Keywords:
Enteric coating
Supercritical impregnation
Oral drug delivery
Microtechnology

ABSTRACT

This work explores the potential of polymeric micrometer sized devices (microcontainers) as oral drug delivery systems (DDS). Arrays of detachable microcontainers (D-MCs) were fabricated on a sacrificial layer to improve the handling and facilitate the collection of individual D-MCs. A model drug, ketoprofen, was loaded into the microcontainers using supercritical CO_2 impregnation, followed by deposition of an enteric coating to protect the drug from the harsh gastric environment and to provide a fast release in the intestine. *In vitro*, *in vivo* and *ex vivo* studies were performed to assess the viability of the D-MCs as oral DDS. D-MCs improved the relative oral bioavailability by 180% within 4 h, and increased the absorption rate by 2.4 times compared to the control. This work represents a significant step forward in the translation of these devices from laboratory to clinic.

1. Introduction

Oral administration of drugs is preferred by patients [1] due to its inherently reduced invasiveness compared to injections and minimal need for trained personnel [2,3]. Moreover, the effective healthcare costs can be diminished avoiding the usage of drugs administered by injections [4,5].

Following oral administration, drug absorption will occur in the gastro-intestinal (GI) tract; primarily in the small intestine due to ahigh surface area provided by the presence of villi and microvilli [6,7]. When delivering drugs through the GI tract, care needs to be taken due to the presence of enzymes and a low gastric pH (1–3.5 in fasted state and 3–6 in fed state) [8]. Both of these can have a negative impact on the administered drug, thereby limiting the effect of the oral formulation.

Traditional oral dosage forms, such as tablets or capsules, can be designed to target the intestine. Enteric coatings can be used to protect the dosage form during transit of the stomach and facilitate the delivery of the drug to the intestinal epithelium for systemic absorption [9,10]. Tablets, capsules as well as micro- and nanoparticulate systems (*i.e.* vesicles, polymeric particles and dendrimers) [11–13], manifest an omni-directional release of the drug in the intestinal lumen. Omni-directional release entails an inevitable loss of the drug in the lumen and therefore a reduction of the drug absorbed into the systemic circulation. Recent and promising approaches focus on reservoir-based microdevices serving as drug carriers, potentially bringing the drug to the desired place of absorption by unidirectional release from the device. An example of such microdevices is microcontainers. Here a polymeric cylinder is situated on a flat surface, defining a container structure with a cavity in the micrometer size [14,15]. Microcontainers provide unidirectional drug release due to their design and a protection of the drug formulation from the acidic environment of the stomach. Previously, they have been suggested as a promising oral drug delivery system, for instance maintaining indomethacin in its amorphous state [16,17] and being suitable for the confinement of spray dried lipid nanoparticles [18]. Furthermore, microcontainers have shown to improve the oral bioavailability of an amorphous salt of furosemide (a class IV drug in the Biopharmaceutics Classification System (BCS)), compared to the same drug loaded into a capsule. It was speculated by the authors that this could be due to the protection of the drug during the passage through the stomach and because of an engulfment of the microcontainers in the intestinal mucus, resulting in a prolonged absorption period [19]. Chirra et al. have illustrated the beneficial effect of using microdevices to improve the relative oral bioavailability of the BCS class III drug, acyclovir compared to a solution of the same drug [20]. Moreover, Fox et al. have shown that nanostraw membranes (porous

* Corresponding authors.
E-mail addresses: chimaz@nanotech.dtu.dk (C. Mazzoni), fabt@nanotech.dtu.dk (F. Tentor).
[1] The authors contributed equally to the work.

http://dx.doi.org/10.1016/j.jconrel.2017.10.013
Received 5 September 2017; Received in revised form 11 October 2017; Accepted 12 October 2017
Available online 18 October 2017
0168-3659/

nanostructured delivery substrates) increase adhesion to the mucus and facilitate the drug loading *via* diffusion [21]. So far, the presented works have only covered part of a device development and/or characterization and, in most cases, not reporting on *in vivo* studies and not characterizing the devices and drugs after individual processing steps. For example, we have previously reported on drug loading of polymer filled microcontainers using supercritical carbon dioxide ($scCO_2$) [22]. However, these containers were not detachable and thus, never used in animal studies. Likewise, we have reported on microcontainers loaded with powder of furosemide [19] where the filled containers were mechanically removed from the carrier substrate introducing a risk of damaging the containers.

Here we present, for the first time, the complete process of developing and characterizing a microcontainer-based oral delivery system. The aim of this work was to translate detachable microcontainers (D-MCs) filled with drug and sealed with a lid, from the concept to the final oral DDS suitable for *in vivo* and *ex vivo* studies. For this purpose, D-MCs have been fabricated on a sacrificial layer, improving handling and facilitating detachment and collection of the individual filled and coated D-MCs. D-MCs were loaded with the BCS class II model drug ketoprofen utilizing $scCO_2$ followed by an enteric coating to prevent release of the formulation during handling, detachment and transit through the stomach. The loaded and coated D-MCs were investigated *in vitro* to assess the functionality of the enteric lid, and *in vivo* and *ex vivo*, to evaluate the potential of microcontainers as an oral DDS.

2. Materials and methods

2.1. Fabrication of detachable microcontainers (D-MCs)

Silicon (Si) wafers (4-in. b100N n-type) were supplied by Okmetic (Vantaa, Finland). SU-8 2075 and SU-8 developer were purchased from Microresist Technology GmbH (Berlin, Germany). Polyacrylic acid 35 wt% aqueous solution (PAA, Mw 100,000) was purchased from Sigma Aldrich (St. Louis, USA) and neutralized with NaOH. A 15 μm thick film of PAA was spin coated on a Si wafer and dried at 80 °C for 10 min. The PAA film served as a water soluble release layer after completed detachable microcontainers (D-MCs) fabrication [23]. D-MCs were fabricated with epoxy-based photoresist SU-8 using a procedure similar to the one described earlier [15,16]. After fabrication, the wafers were cut into square chips containing 625 D-MCs using a laser (microSTRUCT vario, 3D Microac AG, Chemnitz, Germany). The dimensions of the D-MCs were measured using an Alpha-Step IQ Stylus Profilometer (KLA-Tencor Corporation, Milpitas, USA) and optical microscopy.

2.2. Loading of drug formulation into the microcontainers

D-MCs sitting on a Si chip were manually loaded with polyvinylpyrrolidone (PVP) (Mw = 10,000, Sigma Aldrich, St. Louis, USA) blowing away the excess in between the D-MCs using an air gun in a similar setup as described previously [18,19]. The chips were weighted before and after and placed within a supercritical CO_2 chamber (3 chips at a time, see Fig. 1), together with 14.2 ± 0.1 mg (n = 15, SD) of ketoprofen powder (≥ 98% racemate, Sigma Aldrich, St. Louis, USA). The impregnation of the polymer was conducted by bringing CO_2 over its supercritical state at 100 bar and 40 °C, keeping it under stirring for 1 h. During this process ketoprofen solubilizes in supercritical CO_2 and diffuses into the polymer matrix. The pressurization and depressurization rate were 3.9 bar/min and 2.5 bar/min, respectively.

2.3. Enteric coating deposition

A pH sensitive polymer, Eudragit® L100 (Evonik, Darmstad, Germany) was employed for the enteric coating on the cavity of the D-MCs. A solution of 2% w/v Eudragit® L100 and 5% w/w in relation to the polymer of dibutyl sebacate (Sigma Aldrich, St. Louis, USA) was dissolved in isopropanol (Sigma Aldrich, St. Louis, USA).

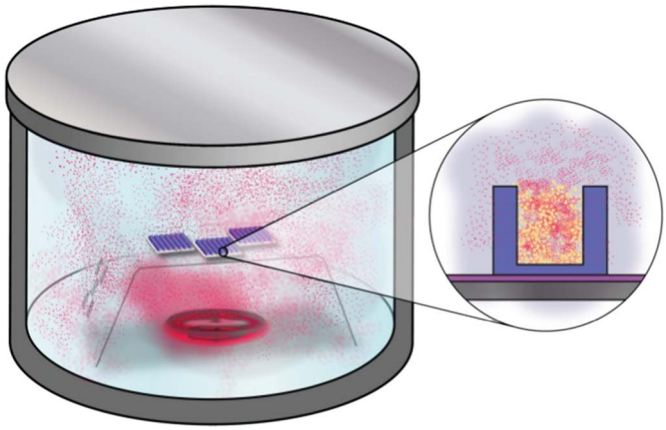

Fig. 1. Schematic representation of the supercritical CO_2 impregnation process. Within the chamber the loading of three D-MCs chips due to the solubilization of ketoprofen in the supercritical CO_2 is depicted. On the right, a zoom in of one D-MC during the loading process is represented.

The solution was sprayed over a chip of drug-loaded microcontainers using an ultrasonic spray coater equipped with an accumist nozzle operating at 120 kHz (Sono-Tek, USA). During the procedure, the flow rate was kept at 0.1 mL/min, together with a 1.5 W generator power. The shaping air was set to 0.02 bar, and the speed of the nozzle was maintained at 5 mm/s, keeping a distance between the tip and the sample of 6.5 cm. The nozzle of the spray coater was positioned above the chip containing loaded D-MCs, following a path in the x-y axis to cover an area defined by the corners of the chip, previously identified using an integrated camera. Each chip was coated with two alternating wavy line spray paths having an offset of 2 mm, resulting in a total of 100 passages. The chips were kept at 40 °C during the spray coating process.

2.4. Morphology characterization

X-ray micro computed tomography (X-ray μCT, Zeiss Xradia 410 versa, Pleasanton, USA) was applied to assess the filling level of the ketoprofen:PVP formulation into the D-MCs and the coating morphology on the cavity of the D-MCs. The 3D tomographic reconstruction was done with the software, provided with the system, based on a FDK algorithm [24]. The chip with D-MCs was investigated using a high voltage of 60 kV and having an effective pixel size of 19.33 μm, taking 1601 projection images. For examining smaller parts of the chip with a higher resolution 60 kV as high voltage and an effective pixel size of 3.02 μm with 3201 projection images was utilized. Three areas from each sample were analyzed to obtain a more representative image of the whole chip.

Capsules filled with D-MCs were scanned to assess the effect of the collection of the D-MCs after their detachment, to assess if they were separated one to each other and if the coating was still intact. For this purpose, scans were recorded with a voltage of 40 kV with a pixel size of either 10.23 μm or 3.36 μm, taking 1601 projection images.

The quality of both the loading and the coating of the D-MCs was investigated using a Zeiss Supra 40VP Field Emission Scanning Electron Microscope (SEM, Carl Zeiss Microscopy GmbH, Jena, Germany). The samples were placed over metallic holders and tilted to 30° prior the analyses, both low and high vacuum modes were used with a variable energy between 4 and 8 keV.

The coating thickness of Eudragit® L100 was measured by contact profilometry (Alpha-Step IQ Stylus Profilometer, KLA-Tencor Corporation, Milpitas, USA). Eudragit® L100 films were sprayed on a SU-8 covered flat silicon chip as described in the above section 'Enteric

coating deposition'. The profiles were measured using a 15.6 mg tip force with a scan speed of 20 μm/s and a sampling rate of 50 Hz.

2.5. Solid state characterization of ketoprofen

X-Ray powder diffraction (XRPD) was used to determine the solid state form of ketoprofen in the D-MCs and of the controls. An X'Pert PRO X-ray diffractometer (PANalytical, Almelo, The Netherlands, MPD PW3040/60 XRD; Cu KR anode, λ = 1.541 Å, 45 kV, 40 mA) was utilized. A starting angle of 5° 2θ and an end angle of 30° 2θ were employed for the scans with a scan speed of 0.67335° 2θ/min and a step size of 0.0262606° 2θ. Data were collected using X'Pert Data Collector software (PANalytical B.V.). The diffractogram of loaded and coated D-MCs was compared to that of crystalline ketoprofen, coated D-MCs loaded with crystalline ketoprofen and D-MCs loaded with 1:4 crystalline ketoprofen:PVP. The diffractograms of D-MCs on the PAA layer, PVP and Eudragit® L100 were also investigated for comparison (data not shown). Moreover, XRPD was used to verify the amorphous form of ketoprofen in the control samples for the *in vivo* studies (described in the 'Capsules preparation' section).

In addition, the solid state form of ketoprofen impregnated into the D-MCs and of control formulations was assessed by means of Raman spectroscopy using a DXR Raman microscope (Thermo Fisher Scientific, Inc., Waltham, USA). The microscope was coupled to a single grating spectrometer with 5 cm^{-1} FWHM spectral resolution and ± 2 cm^{-1} wavenumber accuracy. All spectra were collected using a laser with a wavelength of 780 nm, with a 50× objective and an estimated laser spot of 3.6 μm diameter. A 50 μm slit was utilized when analyzing bulk powder, whereas a 25 μm pinhole was deployed to analyze the ketoprofen inside the microcontainers the laser power was equal to 10 and 20 mW, respectively. The spectra of: i) pure ketoprofen, ii) pure PVP and iii) microcontainers filled with PVP and impregnated with ketoprofen were compared.

2.6. Release of ketoprofen from D-MCs

The efficacy of the coating and its resistance after the detachment of the D-MCs was evaluated determining the release of the impregnated ketoprofen, both in a Fasted State Simulated Gastric Fluid (FaSSGF pH 1.65 – Biorelevant®, London, UK) and Fasted State Simulated Intestinal Fluid (FaSSIF pH 6.5 – Biorelevant®, London, UK). Impregnated chips either coated or uncoated were individually immersed in 2 mL of deionized water (pH 3.25) to allow the solubilization of the PAA layer (avoiding the coating to dissolve) and hence, the detachment of the D-MCs. Suspended D-MCs were transferred into dialysis bags (MW cut off: 14,000) and placed in 20 mL of FaSSGF in an orbital shaking water bath at 37 °C, 150 rpm (Grant Instrument Ltd., model OLS26, Cambridge, UK) for 2 h. Afterwards, the bags were removed, rinsed with FaSSIF and placed in 20 mL of fresh FaSSIF at 37 °C, 150 rpm for 6 h. 20 μL were collected at 0, 5, 10, 20, 40, 60, 120 min during the release in FaSSGF and after 1, 2, 5, 10, 20, 40, 60, 120, 240 and 360 min during the release in FaSSIF. Samples were analyzed using the UV–Vis spectrophotometer (NanoDrop 2000c, Thermo Fisher Scientific Inc., UK) at 258 nm. The amount of ketoprofen loaded in the D-MCs chips was also investigated as described in the section '*In vitro* release of ketoprofen from coated D-MCs'. The release curves were performed at least in triplicates (n = 3 for the coated and n = 6 for the uncoated D-MCs).

2.7. Capsules preparation

Three chips of D-MCs were impregnated together and coated individually as described above. The solubilization of the sacrificial layer and the subsequent detachment from the Si chip were obtained soaking the chips into 5 mL of deionized water (pH 3.25). After 5 min, the water was removed and the D-MCs were dried at 37 °C for 15 min. Gelatin capsules (Torpac® size 9, Fairfield, USA) were filled with individual D-MCs (258 ± 31 D-MCs per capsule, as visible in Fig. S5 in the Supplementary information) and weighted before and after filling. The concentration of ketoprofen in the capsules was assessed *in vitro* by placing 14 capsules in 20 mL of phosphate buffered saline (PBS, Sigma Aldrich, St. Louis, USA) and kept under stirring (150 rpm) at 37 °C for 24 h. Measurements were done through UV–Vis spectroscopy as described before at a wavelength of 258 nm.

The preparation for the control for the *in vivo* study started with a physical mixture of ketoprofen and PVP powders with the same weight ratio (1:4) as in the D-MCs. The mixture was prepared by heating it up to 120 °C on a heating plate gently mixing the two compounds during the melting of the drug. The heated mixture was immediately quenched using liquid nitrogen followed by grinding to a fine powder. The amorphous form of ketoprofen was confirmed using XRPD as previously described. Gelatin capsules were loaded with 922.4 ± 11.5 μg of the grinded powder, an amount corresponding to that of the D-MCs formulation. Subsequently, the capsules were coated with a solution of 5% w/v Eudragit® L100 and 5% w/w dibutyl sebacate in relation to the polymer in isopropanol. The capsules were coated by dipping half of it into the coating solution and dried for 15 min before coating the other half. This procedure was repeated three times for each capsule.

2.8. In vivo and ex vivo studies

All animal care and experimental studies were performed according to Danish and European laws, guidelines and policies for animal housing, care and experiments at the University of Copenhagen. The *in vivo* experiment was carried out at the Department of Experimental Medicine, University of Copenhagen and approved by the local institutional Animal Welfare Committee under the license number 2015-15-0201-00454. The *ex vivo* study was performed at the Department of Pharmacy, University of Copenhagen under the license number 2016-15-0201-00892. Both studies were carried out in compliance with the Danish laws regulating experiments on animals and EC Directive 2010/63/EU.

Male Sprague-Dawley rats were housed in pairs in cages to acclimatize for a period of one week with a light/dark period of 12/12 h and a temperature of 22 °C with a relative humidity of 55 ± 10%. During this period, the rats had free access to standard pellets and water.

For the *in vivo* study the rats with a weight ranging from 373 to 436 g were randomly divided into two groups. One group was dosed with capsules loaded with D-MCs (n = 11), the second group was dosed with capsules containing the control formulation (n = 6). Both types of capsules were given using a polyurethane feeding tube (Instech Laboratories Inc., Plymouth Meeting, USA), one capsule was dosed per rat. The rats were fastened for 1 h before and after the dosing, and for the rest of period they had free access to water and standard pellets. Blood (200 μL) was sampled through the lateral tail vein at 15, 30, 45, 60, 75, 90, 120 min, 4, 6, 8 and 24 h post dosing and collected in ethylenediaminetetraacetic acid tripotassium salt dihydrate (EDTA, Sigma-Aldrich, St. Louis, USA) coated tubes. Plasma was obtained by immediately spinning the blood samples at 1500 *g* for 10 min. Plasma was stored at − 20 °C until further analyses.

For the *ex vivo* study, two male Sprague–Dawley rats weighting 316 and 319 g were used and were fasted 1 h prior to dosing.

Capsules filled with D-MCs (see the section 'Capsules preparation') were administered to the rats by oral gavage as described previously. After 90 min post-dosing, the rats were sacrificed, and opened at the *linea alba* for retrieving the stomach and small intestine. These were immediately cut open and examined for localizing the D-MCs using a stereo microscope (SteReo Discovery V8, Carl Zeiss MicroImaging GmbH, Jena, Germany).

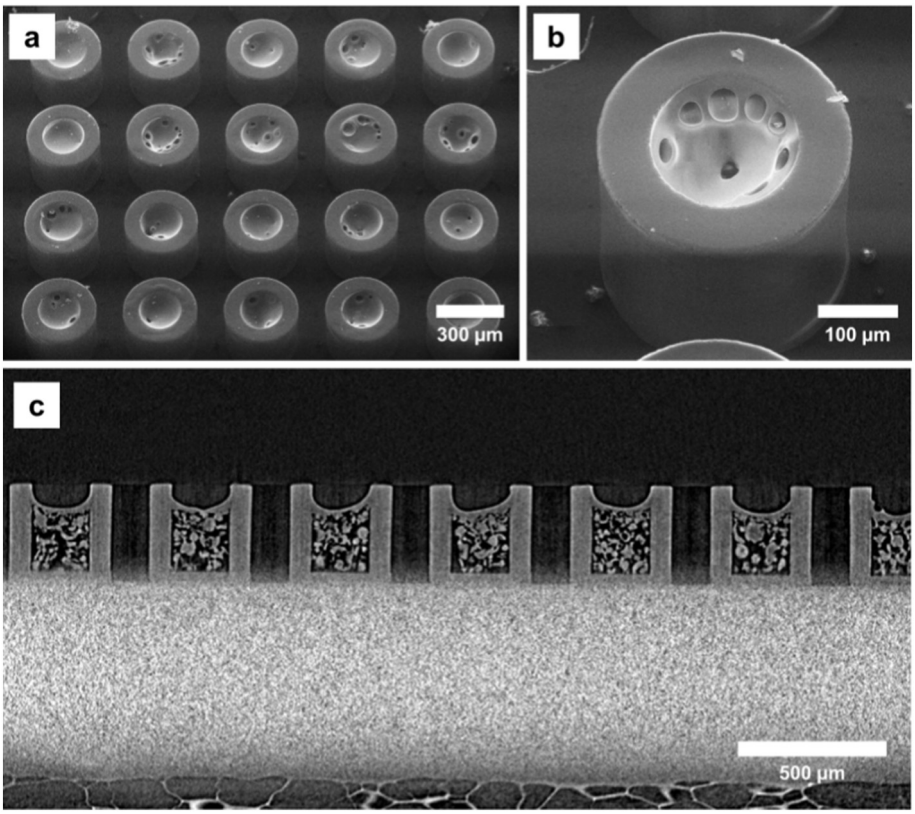

Fig. 2. Morphological characterization of drug loaded D-MCs. (a) and (b): SEM images of D-MCs first manually loaded with PVP and then impregnated with ketoprofen in supercritical CO_2 at 40 °C and 100 bar for 1 h. (c):X-ray µCT cross-sectional view of the loaded D-MCs.

2.9. High Pressure Liquid Chromatography (HPLC) analysis of plasma samples

HPLC analyses were performed using a Dionex Ultimate 3000 Pump equipped with a Dionex ASI-100 Automated Sample Injector and with a UV-VIS lamp.

Ketoprofen was extracted from the plasma samples using a method described elsewhere [25] with minor modifications. Briefly, methanol was added in a 3:1 v/v ratio to the plasma and, after vortexing the mixtures, the samples were centrifuged at 15,000 *g* for 6 min and the supernatants were transferred into HPLC vials.

The HPLC was run in isocratic mode using a method already described in literature with slight modifications [25]. The mobile phases constituted of (A): deionized water with 1% v/v trifluoroacetate (Sigma Aldrich, St. Louis, USA) and (B): 100% acetonitrile (Sigma Aldrich, St. Louis, USA). The ratio of the mobile phase A:B was equal to 45:55 v/v. Samples were run over a Kinetex 5.0 µm XB-C18 100 Å, 100 × 4.6 mm column (Phenomenex ApS, Nordic Region, Værløse, Denmark) at 22 °C. The injected volume was 40 µL with a flow rate of 1 mL/min and a total run time per sample of 10 min. The absorbance was measured at 258 nm.

2.10. Statistics

For the *in vivo* studies, all results were normalized for the averages of rat mass and of the ketoprofen dosed.

To calculate the standard error for the area under the curve (AUC, Table 1), the standard error of the mean of correlated variables is used

$$SE_{\overline{AUC}} = \sqrt{\frac{\sum_{i=1}^{M} var[A_i] + \sum_{i=1}^{M}\sum_{j\neq i}^{M} cov(A_i, A_j)}{N}}$$

where A_i is the AUC for region *i*.

To calculate the average amount of PVP inside a capsule, and the associated standard error, the following formula is derived. To derive the formula, it is assumed that the amount of PVP in each D-MCs in the filling process are independently distributed.

$$SE_{\overline{PVP}} = \sqrt{\frac{1}{N_c}\left(\frac{1}{NM} var[X]\, var[Y] + \frac{1}{N} var[X] E[Y]^2 + \frac{1}{M} var[Y] E[X]^2\right)}$$

where N_c is the total amount of microcontainers per chip, X is the total amount of PVP measured N times, and Y is the number of microcontainers contained inside a capsule, measured M times.

The raw data of the *in vivo* studies can be found in the Supplementary information (Fig. S4).

Moreover, as the sample sizes are different the effect sizes reported in Table 1 uses the Hedges g effect size defined as $g = (M_1 - M_2)/SD_{pooled}$ where SD_{pooled} is the weighted standard deviation of the two groups [26–28].

All of the data are expressed as mean and the usage of standard deviation (SD) or standard error of the mean (SE) is defined within the text. Where appropriate, statistical analysis was carried out using Student *t*-tests using GraphPad Prism version 6.05. P-values below 5% ($p < 0.05$) were considered statistically significant.

3. Results

3.1. Fabrication of microcontainers on a sacrificial layer

D-MCs were successfully fabricated in SU-8 on a water soluble layer of PAA. D-MCs had a height of 304 ± 12 µm (n = 8, SD) and a diameter equal to 329 ± 5 µm (n = 8, SD). The inner reservoir had a depth of 272 ± 6 µm (n = 8, SD) and a diameter of 188 ± 4 µm (n = 8, SD) resulting in a container volume of 7.5 ± 0.3 nL (n = 8, SD). D-MCs were adhering well to the PAA layer not impairing the handling. D-MCs were arranged in arrays of 25 × 25 devices on quadratic chips with a side length of 12.8 mm.

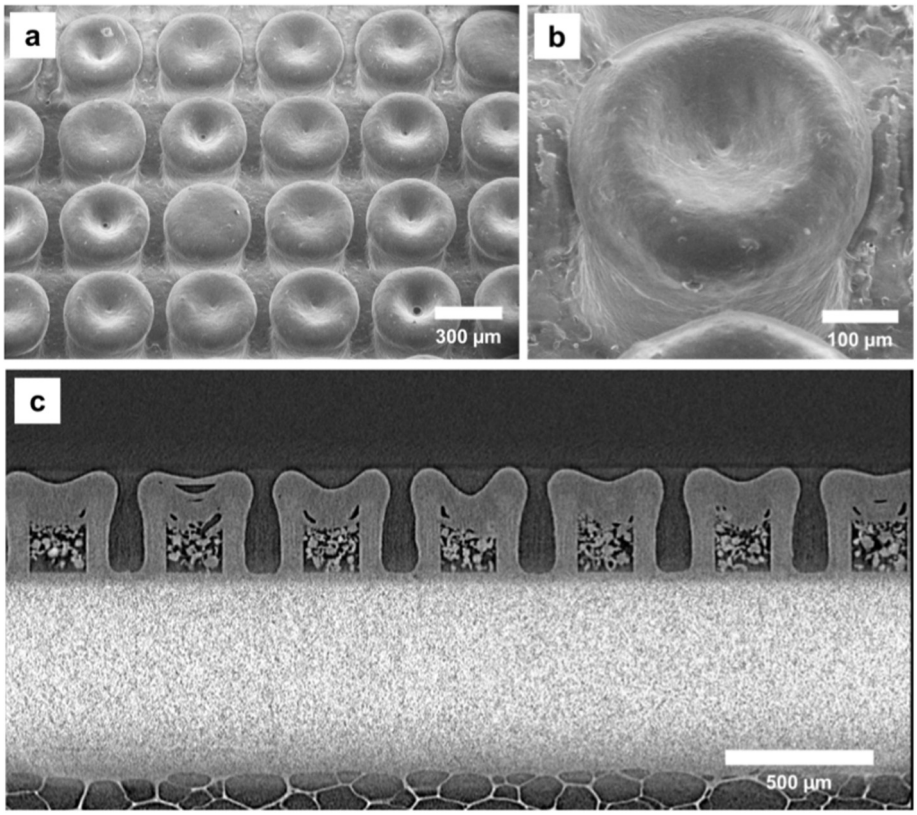

Fig. 3. Morphological characterization of loaded and coated D-MCs. (a) and (b):SEM images of D-MCs coated with Eudragit® L100 onto the cavity of the drug-loaded D-MCs. (c): X-ray µCT cross-sectional view of the drug-loaded and coated D-MCs.

3.2. Loading of D-MCs

Every chip with D-MCs was manually filled with 1.79 ± 0.21 mg (n = 54 chips, SD) of PVP powder followed by loading ketoprofen into the polymer matrix using $scCO_2$. All chips underwent the same supercritical treatment at 40 °C and 100 bar for 1 h. The filled D-MCs on chips were visualized using a SEM (Fig. 2a, b). The cross-sectional X-ray µCT image of the D-MCs loaded with PVP and ketoprofen is shown in Fig. 2c.

3.3. Enteric coating deposition onto drug-loaded D-MCs

The spray coated gastro-resistant lid of Eudragit® L100 was, initially, characterized using contact profilometry to define the coating thickness on two chips. This resulted in thicknesses of 123.0 ± 1.9 and 118.7 ± 3.3 µm (SD describes the roughness of the surface of the coating). X-Ray µCT and SEM were utilized to assess the morphology of the coatings after their deposition on the cavity of the D-MCs. The coatings were homogenous (Fig. 3a, b) and well distinguishable from the impregnated PVP and ketoprofen (Fig. 3c).

3.4. In vitro release of ketoprofen from coated D-MCs

The detachment of the drug-loaded and coated D-MCs from the PAA layer was accomplished by soaking chips in deionized water at pH 3.25 for about 5 min.

The release of ketoprofen was evaluated in human FaSSGF for 120 min (simulating the residence time in the stomach) followed by investigation of the drug release in human FaSSIF for 360 min (simulating the transit time of the small intestine). After 120 min in FaSSGF, 56 ± 14% of the loaded ketoprofen from uncoated D-MCs was released compared to 16 ± 3% from the coated D-MCs (Fig. 4). Upon changing to FaSSIF, a burst release with a significant immediate concentration difference was noticed for the coated microcontainers (p-value = 0.0022). After 6 h in FaSSIF, 100% of the loaded ketoprofen

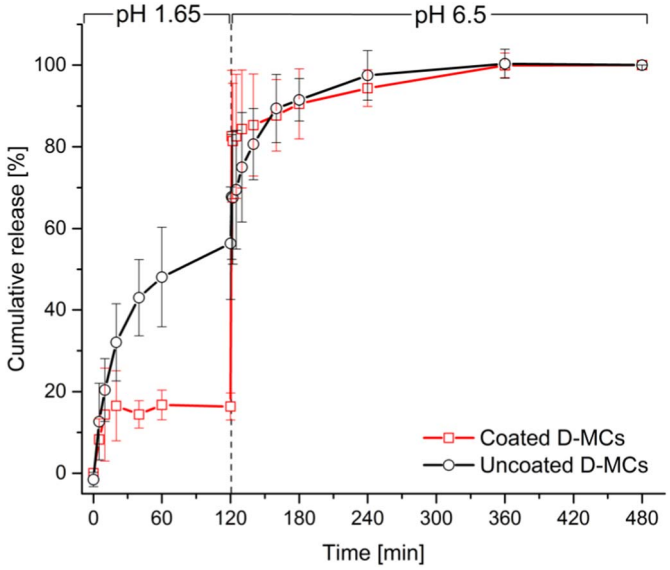

Fig. 4. *In vitro* cumulative release of ketoprofen. Coated (red line) and uncoated (black line) D-MCs. For the first 120 min, the chips were placed in FaSSGF and subsequently in FaSSIF for 360 min. Each release curve is calculated as mean ± standard deviation (n = 6 for the uncoated D-MCs, n = 3 for the coated D-MCs). For the individual profiles refer to Fig. S3 in the Supplementary information. (For interpretation of the references to colour in this figure legend, the reader is referred to the web version of this article.)

was released from both the coated and uncoated D-MCs. The release profile of ketoprofen for the uncoated D-MCs did not present a burst release, but instead followed a first order kinetic. Consequently, statistical significance (p-value = 0.002) was noticeable for the release of ketoprofen after 2 h between coated and uncoated D-MCs. The total amount of ketoprofen loaded into a single chip with 625 D-MCs was 424 ± 10 µg (n = 14, SE) corresponding to a weight ratio of

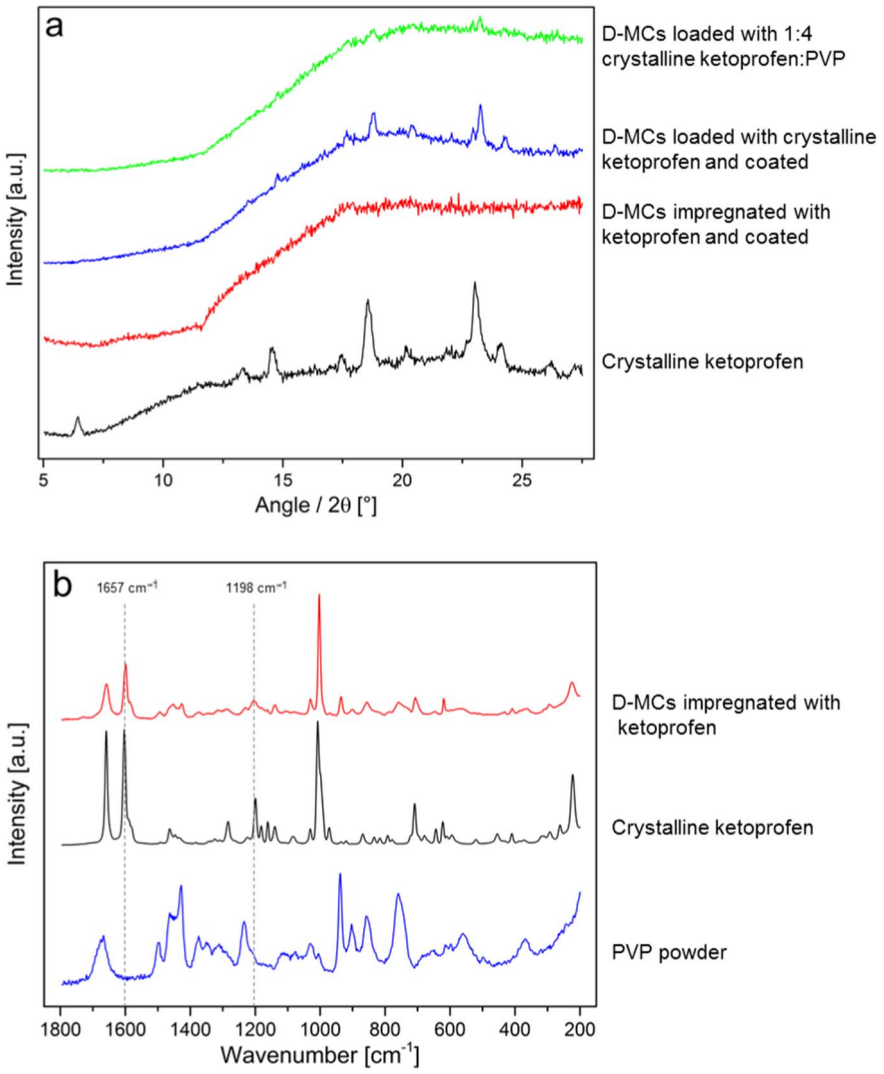

Fig. 5. Solid state characterization of ketoprofen in D-MCs. (a) XRPD diffractograms of crystalline ketoprofen (black), D-MCs impregnated with ketoprofen and coated (red), D-MCs loaded with crystalline ketoprofen and coated (blue) and D-MCs loaded with 1:4 crystalline ketoprofen:PVP (green). (b) Raman scattering profiles of PVP powder (blue), crystalline ketoprofen (black) and D-MCs impregnated with ketoprofen (red). (For interpretation of the references to colour in this figure legend, the reader is referred to the web version of this article.)

ketoprofen to PVP of approximately 1:4 (see the 'Formulation preparation for *in vivo* and *ex vivo* studies' section). The total amount of ketoprofen loaded into the coated and uncoated D-MCs were seen to be very similar. No significant difference was found (p-value = 0.2542).

3.5. Solid state characterization of ketoprofen in D-MCs

The solid state form of ketoprofen in the D-MCs both after $scCO_2$ impregnation and after additional enteric coating deposition was evaluated by means of XRPD. By comparing the diffractograms (Fig. 5a), it was found that the distinct peaks of crystalline ketoprofen were not visible in the final $scCO_2$ impregnated and coated microcontainers. This, together with the typical scattering halo (Fig. 5a, red), indicated the maintenance of ketoprofen in its amorphous form within the D-MCs. The two controls (coated D-MCs loaded with crystalline ketoprofen and D-MCs with a crystalline ketoprofen:PVP mixture in the ratio 1:4) demonstrated that it was possible to measure through the coating and to detect crystalline ketoprofen in the D-MCs in the same quantity as seen in the $scCO_2$ impregnated and coated microcontainers (Fig. 5a, blue and green).

It is worth mentioning that the melted and quenched mixture of ketoprofen:PVP 1:4 (used as control for the *in vivo* studies) was also found to be amorphous in the XRPD diffractograms (see in Supplementary information Fig. S1).

The XRPD results were corroborated by Raman spectroscopy comparing the spectra of pure crystalline ketoprofen, pure PVP and microcontainers filled with PVP and impregnated with ketoprofen (Fig. 5b). As noticeable from the Raman spectra, the characteristic vibrational patterns of ketoprofen were also visible in the impregnated D-MCs. Briefly, the intensity of the peak at 1657 cm^{-1}, which is attributed to the vibrational stretch of the carbonyl ν(C═O), decreased compared to that of crystalline ketoprofen. Moreover, the broadening of the band around 1198 cm^{-1} (CH ring plane bending) together with the lowering of the peak intensities between 1500 cm^{-1} and 1100 cm^{-1}, supported the hypothesis of ketoprofen amorphization due to the impregnation process [29].

3.6. Formulation preparation for in vivo and ex vivo studies

Gelatin capsules were filled with 258 ± 31 (n = 54, SE) $scCO_2$ loaded and coated D-MCs corresponding to 176 ± 14 μg (n = 14, SE) of ketoprofen and 741 ± 52 μg (n = 54, SE) of PVP.

X-ray μCT was employed to visualize the microcontainers inside the capsule. It can be seen that the coating was preserved through all preparation steps and that the microcontainers were intact and separated from each other (Fig. 6).

3.7. In vivo studies

Capsules filled with D-MCs or with the control formulation were

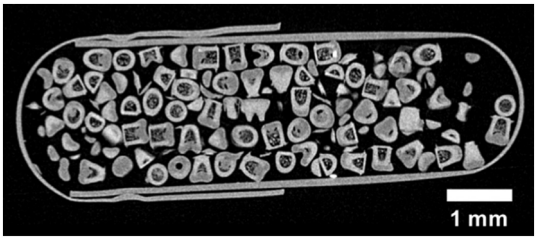

Fig. 6. X-ray μCT image of a gelatine capsule filled with loaded and coated D-MCs.

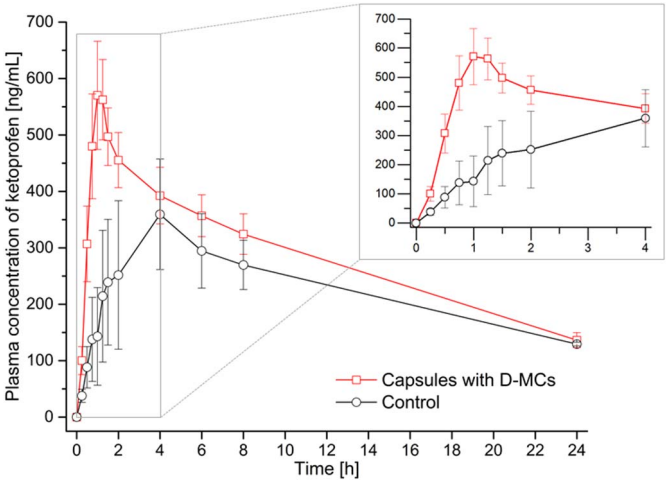

Fig. 7. Plasma concentration of ketoprofen over time. (Red line), capsules with loaded and coated D-MCs (n = 11, SE). (Black line), control capsules filled with melted ketoprofen and PVP and coated (n = 6, SE). The inset represents the same profiles zoomed in the first 4 h. For the individual profiles refer to Fig. S4 in the Supplementary information. (For interpretation of the references to colour in this figure legend, the reader is referred to the web version of this article.)

dosed by oral gavage to rats. The measured plasma concentration of ketoprofen over time is presented in Fig. 7 and key results are summarized in Table 1. The maximum plasma concentrations (C_{max}) are similar for D-MCs and the control. The values were found to be 657 ± 78 ng/mL and 488 ± 105 ng/mL for the formulation with D-MCs and for the control, respectively (p-value = 0.2191). The AUC from 0 to 24 h ($AUC_{0\text{-}24h}$) was calculated to be 406 ± 40 min·ng/mL for the D-MCs formulation and 320 ± 49 min·ng/mL for the control, thereby, no significant difference was observed between the two groups (p-value = 0.2041). The relative bioavailability from 0 to 24 h for ketoprofen in D-MCs compared to the control was found to be 127 ± 23%. However, statistically relevant difference (p-value = 0.0279) was found for the time corresponding to the maximum plasma concentration (T_{max}) when comparing the two formulations (93 ± 17 min for the D-MC and 212 ± 60 min for the control). The $AUC_{0\text{-}4h}$ for the D-MCs formulation was 99 ± 10 min·ng/mL and 55 ± 18 min·ng/mL for the control resulting in a statistically significant difference between the two groups (p-value = 0.0387). According to this, the oral relative bioavailability from 0 to 4 h was 180 ± 62% for the D-MC formulation compared to the control. The absorbance rate of ketoprofen (C_0 to C_{max}) for the rats dosed with D-MCs was 10 ± 2 $ng \cdot min^{-1} \cdot mL^{-1}$, which is significantly higher than for the control (4 ± 1 $ng \cdot min^{-1} \cdot mL^{-1}$) (p-value = 0.0430, Fig. 7, top right).

3.8. Ex vivo study

In order to understand the mechanism of action of the D-MCs, their position in the GI tract of the rats at T_{max} (90 min) was assessed. No D-MCs were found in the stomach of the rats at T_{max}, whereas many were found in the mid-jejunum (see Fig. S2 in the Supplementary information). This indicates that the enteric coating protected the formulation until the intestine was reached, where the ketoprofen was released and absorbed.

4. Discussion

Micro- and nanotechnologies are enabling new possibilities in the world of oral drug delivery. It is a highly complex and multidisciplinary field with focus on fabrication and on the possibilities to integrate novel functionalities into drug delivery systems. *In vivo* studies proving their actual performances [21,30–32] are, however, not always carried out.

In this work, an oral DDS based on microcontainers has been further developed compared to previous ones [19,33]. The complete process, starting from the fabrication of the new D-MCs to the loading and coating, highlighting the subsequent results from the *in vivo* and *ex vivo* investigations, is presented.

D-MCs were filled with PVP in a simple and reproducible manner and $scCO_2$ was used to load the D-MCs with the model drug ketoprofen with a final 1:4 weight ratio of drug to polymer. A single D-MC has a cavity of 7.5 ± 0.3 nL, 178 times larger compared to other similar DDS [34], and each one was loaded with 0.68 μg of ketoprofen, which is considerably more compared to the data presented by Chirra et al. (1.54 ng) [20]. The amount of ketoprofen in a single D-MC corresponds to 1.3% w/w of the total weight of the microdevice. The technique of $scCO_2$ impregnation was preferred over inkjet printing due to the low spotting reproducibility and low loading capacity of the printing process [35,36].

In the loading process, $scCO_2$ acts as a solvent for ketoprofen, but not for PVP, which only swells [22]. The porosity of PVP increased during the impregnation allowing ketoprofen to access the D-MCs. CO_2, in its supercritical state, has a density similar to a liquid, whereas the viscosity and diffusivity are closer to the ones of a gas. These features are exploited during the impregnation process, where ketoprofen is used in relatively high concentration and diffuses easily with the CO_2 into the D-MCs.

Table 1
Non-compartmental model of the *in vivo* study of ketoprofen in D-MCs (n = 11, SE) and for the control formulation (n = 6, SE).

	Capsule with loaded and coated D-MCs	Coated capsules with 1:4 ketoprofen:PVP amorphous mixture (control)	Effect size[b]
C_{max} [ng/mL]	657 ± 78	488 ± 105	0.65
T_{max} [min]	93 ± 17[a]	212 ± 60[a]	1.24
$AUC_{0\text{-}4h}$ [min·ng/mL]	99 ± 10[a]	55 ± 18[a]	1.16
$AUC_{0\text{-}24h}$ [min·ng/mL]	406 ± 40	320 ± 49	0.68
Relative oral bioavailability [%]			
0–4 h	180 ± 62%		
0–24 h	127 ± 23%		

[a] p-value < 0.05.
[b] *Effect size* = $(M_1 - M_2)/SD_{pooled}$ where M_1 and M_2 are the averages of the two populations and SD_{pooled} is the weighted standard deviation of the two groups.

During the $scCO_2$ impregnation, a solid state transition of ketoprofen from its crystalline to its amorphous form was obtained. Ketoprofen is a BCS class II drug meaning that it has a poor solubility in water. Therefore, its aqueous solubility can be increased by exploiting the amorphous form [37–40]. The XRPD diffractograms and the Raman spectra (Fig. 5a and b, respectively) suggested that the amorphous form of ketoprofen was present after impregnation into the D-MCs, confirming previous results [33].

Ketoprofen was kept in its amorphous form for at least 7 days (data not shown) due to the use of $scCO_2$ and to its affinity with PVP [29,41,42]. PVP is a water soluble polymer and has unique properties in prolonging the stability of amorphous forms of drugs, thereby increasing their dissolution rate and solubility [41]. Microcontainers can additionally stabilize the amorphous form of drugs by spatially confining the drug molecules, leading to an improved physical stability of the amorphous drugs [16,17].

In order to avoid premature release of ketoprofen, D-MCs were coated with the gastro-resistant polymer Eudragit® L100. The *in vitro* dissolution studies (Fig. 4) confirmed that this polymer successfully protected the drug during transit through the gastric environment and dissolved quickly upon arrival in the small intestine (where the pH is generally above 6) [19,43–46]. Spray coating by an ultrasonic nozzle was selected as the technology to deposit the coating onto the cavity of the D-MCs. The morphology of PVP and ketoprofen after impregnation (Fig. 2) was suitable for the coating deposition as there was still space for the coating in the top of the cavity of the D-MCs. The deposition of the lid was simple and straightforward, and has the potential of being scaled up. D-MCs were detached from the fabrication platform by soaking them into acidified water. This approach maintains the integrity of the gastro-resistant lid (Fig. 6) and it is a gentler and more controlled procedure than using, for example, mechanical forces. SEM images and X-ray μCT scans of coated D-MCs showed that after spray coating no agglomerates of polymer were present between adjacent microcontainers and that the D-MCs were not attached to each other after dissolution of the PAA sacrificial layer (Figs. 3 and 6).

The *in vitro* release of ketoprofen from the D-MCs in gastric and intestinal simulated media demonstrated the efficacy of the coating. The immediate release of 16 ± 3% of ketoprofen from the coated D-MCs in FaSSGF can be explained by the presence of small pores in the coating (Fig. 3) and/or the possible variation of the polymer morphology (refer to the video in the Supplementary Information for a more detailed view). For the uncoated D-MCs, 56 ± 14% of ketoprofen was released in FaSSGF, showing that nothing efficiently hindered the drug release. Coated D-MCs showed a very significant burst release upon changing to FaSSIF due to the dissolution of Eudragit® L100 followed by a fast release of ketoprofen, together with dissolution of PVP (Fig. 4).

In vivo studies are necessary when testing new drug delivery systems as they provide indications on possible bioavailability improvements after oral administration compared to a control formulation [47,48].

The control formulation used in these studies was designed to have the same ratio of ketoprofen:PVP (1:4) and a total amount of drug and polymer as for the D-MCs formulation to obtain information on the behavior of the D-MCs. The solid state form of a drug has a large influence on the dissolution rate, and can therefore, be of great importance for the bioavailability [49]. It was found that ketoprofen in the D-MCs after $scCO_2$ impregnation was amorphous and consequently, the ketoprofen in the control formulation was also brought to its amorphous form. This was obtained by melting the ketroprofen together with PVP followed by a fast cooling, which is a common method for preparing the amorphous form of a drug, as reported by Enfalt et al. [50].

Compared to the control, the D-MCs formulation did not provide a higher C_{max}. However, a faster T_{max} was observed for the D-MCs formulation being roughly 2.3 times faster than the control. This significant difference resulted in a large value for the effect size (Table 1), in accordance with the classification proposed by Choen [28], where the intervals 0.00–0.20, 0.20–0.50 and 0.50–0.80 correspond to a small, medium or large effect, respectively. This indicates that D-MCs have a large effect on the time of absorption. For the first 4 h of the plasma concentration-time profile (Fig. 7), the absorption of ketoprofen was significantly higher than for the control, again resulting in a large effect size value (Table 1). This difference resulted in a relative oral bioavailability of 180 ± 62% for the first 4 h. In accordance with the difference between the T_{max} values, the absorption rate was significantly higher for the rats administered with D-MCs compared to the control rats. This supports the conclusion that the D-MCs provided a much faster absorption of ketoprofen compared to the control. It can be hypothesized that this, to some extent, is caused by a faster gastric emptying of the rats dosed with the D-MCs compared to the control. Indeed, D-MCs were most likely released from the gelatin capsule in the stomach as no coating was applied to the entire capsule, conversely to the control formulation. From the plasma concentration curve (Fig. 7), it is noticeable that after 4 h the two formulations show more similar kinetics, and the $AUC_{0\text{-}24h}$ is not significantly different. This is reflected in the relative bioavailability of ketoprofen in the D-MCs formulation compared to the control being 127 ± 23%. Choi et al. [51] evaluated the intestinal absorption of a suspension of ketoprofen in rats administering a 2.3 times higher dosage compared to the one used in the present study. The authors report a higher C_{max} (6.12 ± 1.02 μg/mL) and a faster T_{max} (0.42 ± 0.29 h). Indeed, these results might be attributed to the higher dosage and to the fact that ketoprofen was dosed in a suspension form, thus, partially pre-solubilized. An important difference comparing these two studies is the plasma concentration decay over time. The decrease is slower for the D-MCs, indicating a prolonged drug release and absorption time. A possible explanation for this might be provided by the results of our *ex vivo* study where at the time in which the T_{max} was reached (93 ± 17 min), D-MCs were spread in the small intestine, and most of them were found in the mid-jejunum embedded deep into the mucus. This pronounced engulfment might indeed have resulted in a slower release and at the same time allowed prolonged absorption of ketoprofen. It has previously been shown in intestinal perfusion studies in rats that SU-8 microcontainers have mucoadhesive properties showing *i.e.* a high tendency to be engulfed by the mucus [19].

5. Conclusions

In this work, we demonstrated that D-MCs are a promising oral drug delivery system providing a 2.3 times faster T_{max} and a 180% increased $AUC_{0\text{-}4h}$ when compared to the control. These features can be of high importance as it could imply that the administered dose could be reduced. The BCS class II model drug ketoprofen was successfully loaded into D-MCs exploiting the features of $scCO_2$ impregnation maintaining the API in its amorphous form. Enteric coating was employed to protect the drug from the stomach environment and to release ketoprofen in the intestine, as proven by the *in vitro* study. All preparation steps are designed to be compatible with each other maintaining ketoprofen in its amorphous state. *In vivo* and *ex vivo* analyses finally show the potentials of using D-MCs as an oral drug delivery system.

Supplementary data to this article can be found online at https://doi.org/10.1016/j.jconrel.2017.10.013.

Acknowledgments

The authors would like to acknowledge the Danish National Research Foundation (DNRF122) and Villum Fonden (Grant No. 9301) for Intelligent Drug Delivery and Sensing Using Microcontainers and Nanomechanics (IDUN). The 3D Imaging Centre at The Technical University of Denmark is gratefully acknowledged. Line Hagner Nielsen would like to acknowledge Danish Research Council for Technology and Production (FTP), Project DFF 4004-00120B for financial support.

The authors would also like to acknowledge Professor Massimo Borelli, School of PhD Programmes, University 'Magna Graecia', Catanzaro, Italy for his suggestion on the statistical analysis. Nanna Bild, Technical University of Denmark, is acknowledged for the drawing of the schematics.

References

[1] K. Thanki, R.P. Gangwal, A.T. Sangamwar, S. Jain, Oral delivery of anticancer drugs: challenges and opportunities, J. Control. Release 170 (2013) 15–40.
[2] G. Liu, E. Franssen, M.I. Fitch, E. Warner, Patient preferences for oral versus intravenous palliative chemotherapy, J. Clin. Oncol. 15 (1997) 110–115.
[3] C.S. Loh, A.J MacRobert, J. Bedwell, J. Regula, N. Krasner, S.G Bown, Oral versus intravenous administration of 5-aminolaevulinic acid for photodynamic therapy, Br. J. Cancer 68 (1993) 41–51.
[4] Lionel A. Mandell, Michel G. Bergeron, Marie J. Gribble, Peter J. Jewesson, E. Donald, Thomas J. Marrie, Lindsay E. Nicolle, Sequential antibiotic therapy: effective cost management and patient care, Can. J. Infect. Dis. 6 (1995).
[5] P.M.M. Bossuyt, J. Dankert, P. Speelman, Implementation in a Large Teaching Hospital, J. Antimicrob. Chemother. (1999) 601–606.
[6] H.F. Helander, L. Fandriks, Surface area of the digestive tract - revisited, Scand. J. Gastroenterol. 49 (2014) 681–689.
[7] T.T. Kararli, Comparison of the gastrointestinal anatomy, physiology, and biochemistry of humans and commonly used laboratory animals, Biopharm. Drug Dispos. 16 (1995) 351–380.
[8] E. Sjögren, B. Abrahamsson, P. Augustijns, D. Becker, M.B. Bolger, M. Brewster, J. Brouwers, T. Flanagan, M. Harwood, C. Heinen, R. Holm, H.P. Juretschke, M. Kubbinga, A. Lindahl, V. Lukacova, U. Münster, S. Neuhoff, M.A. Nguyen, Peer Av, C. Reppas, A.R. Hodjegan, C. Tannergren, W. Weitschies, C. Wilson, P. Zane, H. Lennernäs, P. Langguth, In vivo methods for drug absorption – comparative physiologies, model selection, correlations with in vitro methods (IVIVC), and applications for formulation/API/excipient characterization including food effects, Eur. J. Pharm. Sci. 57 (2014) 99–151.
[9] D. Schmaljohann, Thermo- and pH-responsive polymers in drug delivery, Adv. Drug Deliv. Rev. 58 (2006) 1655–1670.
[10] T. Yoshida, T.C. Lai, G.S. Kwon, K. Sako, pH- and ion-sensitive polymers for drug delivery, Expert Opin. Drug Deliv. 10 (2013) 1497–1513.
[11] Jonathan F. Lovell, Cheng S. Jin, Elizabeth Huynh, Honglin Jin, Chulhong Kim, John L. Rubinstein, Warren C.W. Chan, Weiguo Cao, Lihong V. Wang, Gang Zheng, Porphysome nanovesicles generated by porphyrin bilayers for use as multimodal biophotonic contrast agents, Nat. Mater. 10 (2011) 324–332.
[12] S.K. Jain, T. Haider, A. Kumar, A. Jain, Lectin-conjugated clarithromycin and acetohydroxamic acid-loaded PLGA nanoparticles: a novel approach for effective treatment of *H. pylori*, AAPS PharmSciTech 17 (2016) 1131–1140.
[13] Rita B. Restani, A. Sofia Silva, Rita F. Pires, Renato Cabral, Ilídio J. Correia, Teresa Casimiro, Vasco D.B. Bonifácio, Ana Aguiar-Ricardo, Nano-in-micro POxylated polyurea dendrimers and chitosan dry powder formulations for pulmonary delivery, Part. Part. Syst. Charact. 33 (2016) 851–858.
[14] J. Nagstrup, S. Keller, K. Almdal, A. Boisen, 3D microstructuring of biodegradable polymers, Microelectron. Eng. 88 (2011) 2342–2344.
[15] P. Marizza, S.S. Keller, A. Boisen, Inkjet printing as a technique for filling of microwells with biocompatible polymers, Microelectron. Eng. 111 (2013) 391–395.
[16] L.H. Nielsen, S.S. Keller, K.C. Gordon, A. Boisen, T. Rades, A. Müllertz, Spatial confinement can lead to increased stability of amorphous indomethacin, Eur. J. Pharm. Biopharm. 81 (2012) 418–425.
[17] L.H. Nielsen, S.S. Keller, A. Boisen, A. Müllertz, T. Rades, A slow cooling rate of indomethacin melt spatially confined in microcontainers increases the physical stability of the amorphous drug without influencing its biorelevant dissolution behaviour, Drug Deliv. Transl. Res. 4 (2014) 268–274.
[18] L.H. Nielsen, T. Rades, B. Boyd, A. Boisen, Microcontainers as an oral delivery system for spray dried cubosomes containing ovalbumin, Eur. J. Pharm. Biopharm. (2016), http://www.sciencedirect.com/science/article/pii/S0939641116309626.
[19] L.H. Nielsen, A. Melero, S.S. Keller, J. Jacobsen, T. Garrigues, T. Rades, A. Müllertz, A. Boisen, Polymeric microcontainers improve oral bioavailability of furosemide, Int. J. Pharm. 504 (2016) 98–109.
[20] H.D. Chirra, L. Shao, N. Ciaccio, C.B. Fox, J.M. Wade, A. Ma, T.A. Desai, Planar microdevices for enhanced in vivo retention and oral bioavailability of poorly permeable drugs, Adv. Healthc. Mater. 3 (2014) 1648–1654.
[21] Cade B. Fox, Yuhong Cao, Cameron L. Nemeth, Hariharasudhan D. Chirra, Rachel W. Chevalier, Alexander M. Xu, Nicholas A. Melosh, Tejal A. Desai, Fabrication of sealed nanostraw microdevices for oral drug delivery, ACS Nano 10 (2016) 5873–5881.
[22] P. Marizza, S.S. Keller, A. Müllertz, A. Boisen, Polymer-filled microcontainers for oral delivery loaded using supercritical impregnation, J. Control. Release 173 (2014) 1–9.
[23] V. Linder, B.D. Gates, D. Ryan, B.A. Parviz, G.M. Whitesides, Water-soluble sacrificial layers for surface micromachining, Small 1 (2005) 730–736.
[24] L.A. Feldkamp, L.C. Davis, J.W. Kress, Practical cone-beam algorithm, J. Opt. Soc. Am. A 1 (1984) 612.
[25] Jean Negru, Daniela-Saveta Popa, Laurian Vlase, Dana Iacob, Marcela Achim, Vasile Dorneanu, High-throughput HPLC method for rapid quantification of ketoprofen in human plasma, Farmacia 63 (2015).
[26] L.V Hedges, Distribution, theory for glass's estimator of effect size and related estimators, J. Educ. Stat. 6 (1981) 107.
[27] S. Sawilowsky, New Effect Size Rules of Thumb, Theor. Behav. Found. Educ. Fac. Publ., 2009.
[28] J. Cohen, Statistical power analysis, Curr. Dir. Psychol. Sci. 1 (1992) 98–101.
[29] L.A.E.B. de Carvalho, M.P.M. Marques, J. Tomkinson, Drug–excipient interactions in ketoprofen: a vibrational spectroscopy study, Biopolymers 82 (2006) 420–424.
[30] D.A. LaVan, T. McGuire, R. Langer, Small-scale systems for in vivo drug delivery, Nat. Biotechnol. 21 (2003) 1184–1191.
[31] W.-J. Zhang, C.-Y. Hong, C.-Y. Pan, Efficient fabrication of photosensitive polymeric nano-objects via an ingenious formulation of RAFT dispersion polymerization and their application for drug delivery, Biomacromolecules (2017) acs.biomac.6b01887 http://pubs.acs.org/doi/abs/10.1021/acs.biomac.6b01887.
[32] S. Sant, S.L. Tao, O.Z. Fisher, Q. Xu, N.A. Peppas, A. Khademhosseini, Microfabrication technologies for oral drug delivery, Adv. Drug Deliv. Rev. 64 (2012) 496–507.
[33] P. Marizza, L. Pontoni, T. Rindzevicius, J.F. Alopaeus, K. Su, J.A. Zeitler, S.S. Keller, I. Kikic, M. Moneghini, N. De Zordi, D. Solinas, A. Cortesi, A. Boisen, Supercritical impregnation of polymer matrices spatially confined in microcontainers for oral drug delivery: effect of temperature, pressure and time, J. Supercrit. Fluids 107 (2016) 145–152.
[34] H.D. Chirra, T.A. Desai, Multi-reservoir bioadhesive microdevices for independent rate-controlled delivery of multiple drugs, Small (2012) 3839–3846.
[35] Cade B. Fox, Cameron L. Nemeth, Rachel W. Chevalier, Joshua Cantlon, Derek B. Bogdanoff, Jeff C. Hsiao, Tejal A. Desai, Picoliter-volume inkjet printing into planar microdevice reservoirs for low-waste, high-capacity drug loading, Bioeng. Transl. Med. (2017) 9–16, http://dx.doi.org/10.1002/btm2.10053.
[36] P. Marizza, S.S. Keller, A. Müllertz, A. Boisen, Polymer-filled microcontainers for oral delivery loaded using supercritical impregnation, J. Control. Release 173 (2014) 1–9.
[37] K. Wlodarski, W. Sawicki, K.J. Paluch, L. Tajber, M. Grembecka, L. Hawelek, Z. Wojnarowska, K. Grzybowska, E. Talik, M. Paluch, The influence of amorphization methods on the apparent solubility and dissolution rate of tadalafil, Eur. J. Pharm. Sci. 62 (2014) 132–140.
[38] S. Mallick, The solid state amorphization of poorly water soluble drugs, Indian J. Pharm. Sci. 66 (2004).
[39] G. Tkalec, M. Pantic, Z. Novak, Z. Knez, Supercritical impregnation of drugs and supercritical fluid deposition of metals into aerogels, J. Mater. Sci. 50 (2015) 1–12.
[40] C. Potter, Y. Tian, G. Walker, C. McCoy, P. Hornsby, C. Donnelly, D.S. Jones, G.P. Andrews, Novel supercritical carbon dioxide impregnation technique for the production of amorphous solid drug dispersions: a comparison to hot melt extrusion, Mol. Pharm. 12 (2015) 1377–1390.
[41] P.S. Yadav, V. Kumar, U.P. Singh, H.R. Bhat, B. Mazumder, Physicochemical characterization and in vitro dissolution studies of solid dispersions of ketoprofen with PVP K30 and d-mannitol, Saudi Pharm. J. SPJ Off. Publ. Saudi Pharm. Soc. 21 (2013) 77–84.
[42] Luigi Manna, Mauro Banchero, Davide Sola, Ada Ferri, Silvia Ronchetti, Silvio Sicardi, Impregnation of PVP microparticles with ketoprofen in the presence of supercritical CO2, J. Supercrit. Fluids 42 (2007) 378–384.
[43] M.O. Besenhard, A. Thurnberger, R. Hohl, E. Faulhammer, J. Rattenberger, J.G. Khinast, Continuous API-crystal coating via coacervation in a tubular reactor, Int. J. Pharm. 475 (2014) 198–207.
[44] D.N. Nguyen, L. Palangetic, C. Clasen, G. Van Den Mooter, One-step production of darunavir solid dispersion nanoparticles coated with enteric polymers using electrospraying, J. Pharm. Pharmacol. 68 (2016) 625–633.
[45] D. Sauer, A.B. Watts, L.B. Coots, W.C. Zheng, J.W. McGinity, Influence of polymeric subcoats on the drug release properties of tablets powder-coated with pre-plasticized Eudragit® L 100-55, Int. J. Pharm. 367 (2009) 20–28.
[46] L.H. Nielsen, J. Nagstrup, S. Gordon, S.S. Keller, J. Østergaard, T. Rades, A. Müllertz, A. Boisen, pH-triggered drug release from biodegradable microwells for oral drug delivery, Biomed. Microdevices 17 (2015) 1–7.
[47] H.D. Chirra, T.A. Desai, Emerging microtechnologies for the development of oral drug delivery devices, Adv. Drug Deliv. Rev. 64 (2012) 1569–1578.
[48] S. Sant, S.L. Tao, O.Z. Fisher, Q. Xu, N.A. Peppas, A. Khademhosseini, Microfabrication technologies for oral drug delivery, Adv. Drug Deliv. Rev. 64 (2012) 496–507.
[49] S. Datta, D.J.W. Grant, Crystal structures of drugs: advances in determination, prediction and engineering, Nat. Rev. Drug Discov. 3 (2004) 42–57.
[50] T. Einfalt, O. Planinšek, K. Hrovat, Methods of amorphization and investigation of the amorphous state, Acta Pharma. 63 (2013) 305–334.
[51] J.-S. Choi, M.J. Jin, H.-K. Han, Intestinal absorption characteristics of ketoprofen in rats, Biopharm. Drug Dispos. 27 (2006) 17–21.

From concept to *in vivo* testing: Microcontainers for oral drug delivery

Chiara Mazzoni[a, *, 1], Fabio Tentor [a, *, 1], Sophie Strindberg Andersen[b], Line Hagner Nielsen[a], Stephan Sylvest Keller[a], Tommy Sonne Alstrøm[c], Carsten Gundlach[d], Anette Müllertz[b], Paolo Marizza[a], Anja Boisen[a]

[1]The authors contributed equally to the work.
*Corresponding authors
[a]Department of Micro- and Nanotechnology, Technical University of Denmark, Ørsteds Plads 345C, 2800 Kgs. Lyngby, Denmark
[b]Department of Pharmacy, Faculty of Health and Medical Sciences, University of Copenhagen, Universitetsparken 2, 2100 København Ø, Denmark
[c]Department of Applied Mathematics and Computer Science, Technical University of Denmark, Richard Petersens Plads 324, 2800 Kgs. Lyngby, Denmark
[d]Department of Physics, NEXMAP, Technical University of Denmark, Fysikvej 311, 2800 Kgs. Lyngby, Denmark

Supplementary Information

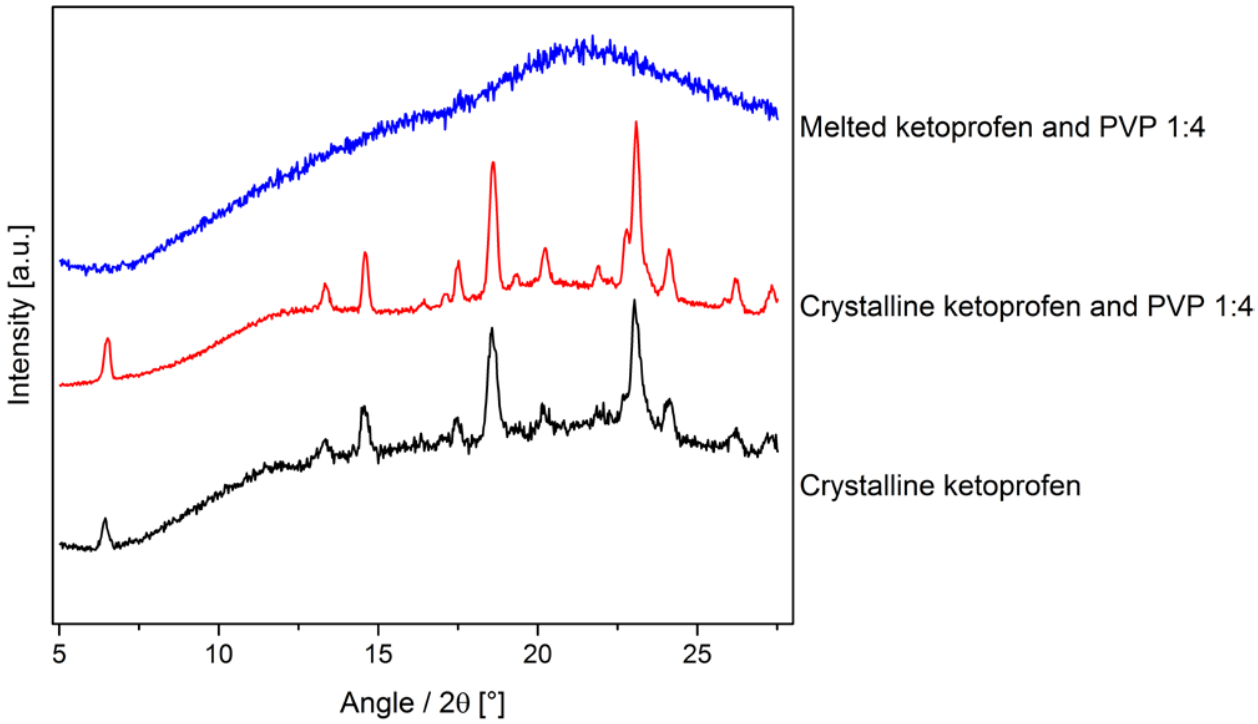

Figure S1: XRPD diffractograms of the control formulation used for the *in vivo* study. Crystalline ketoprofen (**black**), crystalline ketoprofen and PVP 1:4 (**red**) and melted ketoprofen and PVP 1:4 (control for the *in vivo* studies) (**blue**).

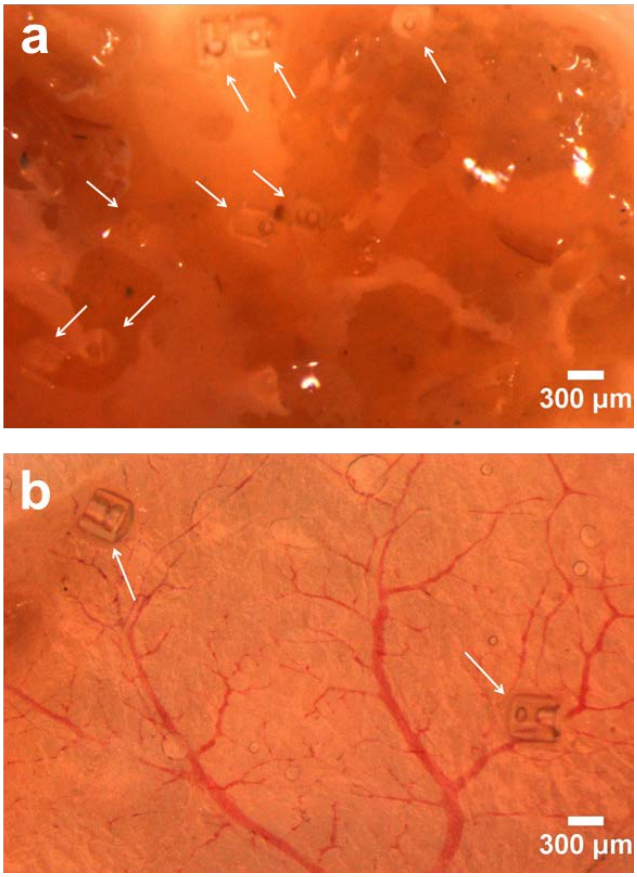

Figure S2: Optical stereoscopy images of the intestinal tissue of oral dosed rats with the D-MCs. D-MCs highlighted with arrows are visible in the intestinal rat tissue, and in (**a**) the engulfment of the D-MCs in the mucus is observed.

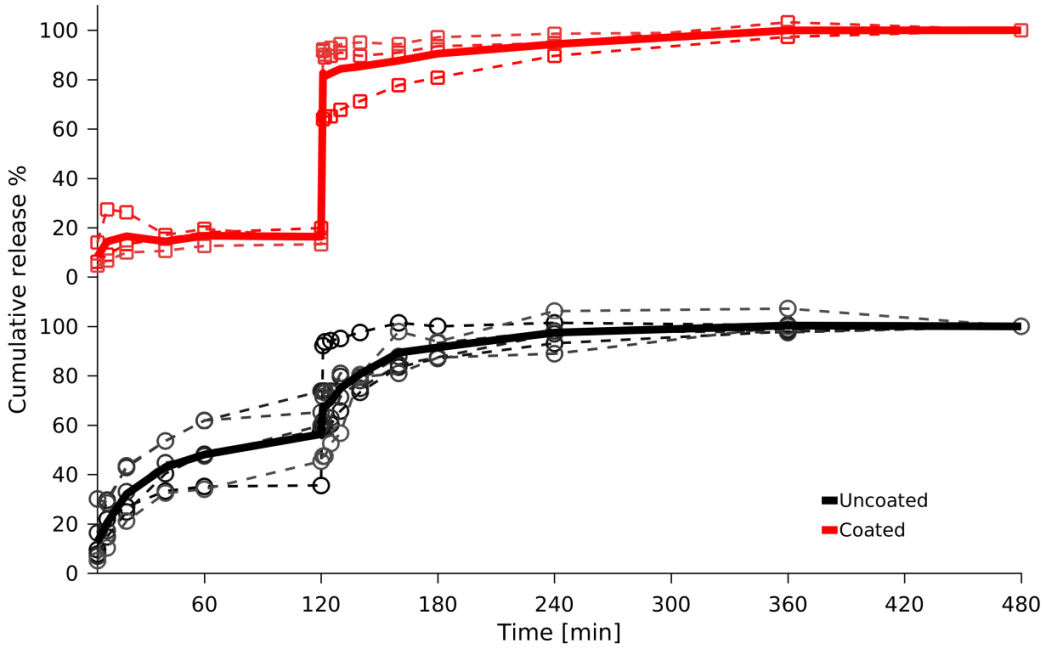

Figure S3: Individual profiles of the *in vitro* cumulative release of ketoprofen. Coated (**red line**) and uncoated (**black line**) D-MCs. For the first 120 min, the chips were placed in FaSSGF and subsequently in FaSSIF for 360 min.

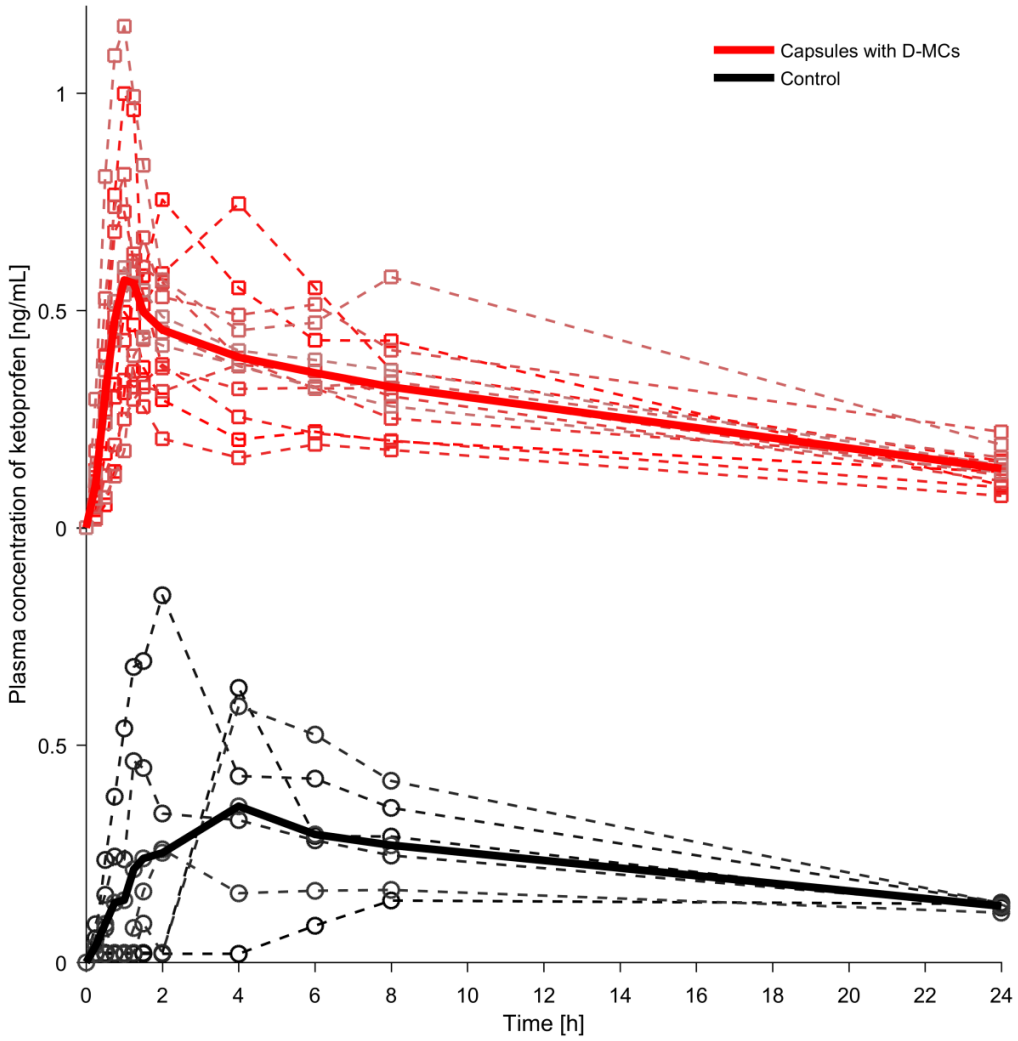

Figure S4: Individual profiles of the *in vivo* plasma concentration of ketoprofen over time. (Red line), capsules with loaded and coated D-MCs**. (Black line)**, control capsules filled with melted ketoprofen and PVP and coated.

Figure S5: Picture of a gelatin capsule filled with loaded and coated D-MCs. Empty D-MCs are positioned outside the capsule for comparison.

Appendix D

Paper IV

Polymeric Lids for Microcontainers for Oral Protein Delivery

C. Mazzoni, R.D. Jacobsen, J. Mortensen, J.R. Jørgensen, L. Vaut, J. Jacobsen, C. Gundlach, A. Müllertz, L.H. Nielsen, A. Boisen

Accepted by Macromolecular Bioscience

Macromolecular Bioscience
www.mbs-journal.de

Polymeric Lids for Microcontainers for Oral Protein Delivery

Chiara Mazzoni, Rasmus Due Jacobsen, Jacob Mortensen, Jacob Rune Jørgensen, Lukas Vaut, Jette Jacobsen, Carsten Gundlach, Anette Müllertz, Line Hagner Nielsen,* and Anja Boisen*

Oral delivery of proteins and peptides is one of the main challenges in pharmaceutical drug development. Microdevices have the possibility to protect the therapeutics until release is desired, avoiding losses by degradation. One type of microdevice is polymeric microcontainers. In this study, lysozyme is chosen as model protein and loaded into microcontainers with the permeation enhancer sodium decanoate (C10). The loaded microcontainers are sealed and functionalized by applying polymeric lids onto the cavity of the devices. The first lid is poly(lactic-*co*-glycolic) acid (PLGA) and on top of this either polyethylene glycol (PEG) or chitosan is applied (PLGA+PEG or PLGA+chitosan, respectively). The functionalization is evaluated in vitro for morphology, drug release, and mucoadhesive properties. These are coupled with in vitro and ex vivo studies using Caco-2 cells, Caco-2/HT29-MTX-E12 co-cultures, and porcine intestinal tissue. PLGA+chitosan shows slower release compared to PLGA+PEG or only PLGA in buffer and the transport of lysozyme across cell cultures is not enhanced compared to the bulk powder. Microcontainers coated with chitosan or PEG demonstrate a three times stronger adhesion during ex vivo mucoadhesion studies compared to samples without coatings. Altogether, functionalized microcontainers with mucoadhesive properties and tunable release for oral protein delivery are developed and characterized.

1. Introduction

Macromolecules such as proteins are used for treatment of diseases such as cancer,[1] rheumatoid arthritis,[2] and psoriasis,[3] and are mainly administered by injections. To increase patient compliance and reduce costs for the healthcare system, it would be beneficial to deliver proteins and peptides via the oral route.[4] Nevertheless, there are certain disadvantages, which are related to the proteins: instability in the gastrointestinal (GI) tract, poor absorption due to large size, hydrophilicity and proteolysis by enzymes found in the GI tract.[5]

For succeeding with oral delivery of proteins, one of the most common strategies is to increase intestinal absorption by the use of permeation enhancers.[5] These compounds allow the passage of proteins across the epithelium by opening the tight junctions. Fatty acids, medium chain glycerides, and chitosan are among the most common examples of permeation enhancers.[5] Sodium decanoate (C10) is a saturated fatty acid and is well known to open tight junctions and can thereby lead to a higher transport of large hydrophilic compounds through the epithelial cell layer.[6,7]

Moreover, in the last decades, hydrogels, nanoparticles, and microparticles have been developed and studied to deliver proteins and peptides orally.[8] The major obstacles for these delivery systems are the instability, polydispersity, and the control of the amount of drug that can be loaded.[8] Microfabricated devices such as planar reservoirs with a diameter of 200 μm and a height of 4–8 μm have been used as carriers for insulin showing an enhanced drug permeability in vitro and in vivo.[9] The authors highlighted that in these microdevices only about 50 ng of insulin was loaded and, thus, an excessive number of microdevices are needed to be administered per day. Microcontainers are polymeric cylindrical microdevices with a diameter and height of ≈300 μm having a volume 100 times larger than the reservoirs, consequently, they have a higher chance of providing a therapeutic dose. The main advantages of the devices compared to traditional particulates are that the devices 1) protect the protein from the GI environment and 2) provide unidirectional release that allows the delivery of the protein to

C. Mazzoni, R. D. Jacobsen, J. Mortensen, L. Vaut, Dr. L. H. Nielsen, Prof. A. Boisen
Department of Health Technology
Technical University of Denmark
Ørsteds Plads 345C, Kgs. Lyngby 2800, Denmark
E-mail: chimaz@dtu.dk; Lihan@dtu.dk
J. R. Jørgensen, Dr. J. Jacobsen, Prof. A. Müllertz
Department of Pharmacy
University of Copenhagen
Universitetsparken, 2, Copenhagen 2100, Denmark
Dr. C. Gundlach
Department of Physics
Technical University of Denmark
Fysikvej 307, Kgs. Lyngby 2800, Denmark
The ORCID identification number(s) for the author(s) of this article can be found under https://doi.org/10.1002/mabi.201900004.

DOI: 10.1002/mabi.201900004

a specific part of the intestine, for example, the small intestine where absorption often occurs.[10] Previously, it has been shown that small molecules, such as furosemide and ketoprofen in microcontainers, coated with pH-sensitive coatings improve the relative oral bioavailability of 220% and 180%, respectively compared to controls.[11,12]

For obtaining optimal performance of the devices, the microcontainers can be functionalized by applying polymeric layers as lids on top of the microcontainers. Poly(lactic-*co*-glycolic) acid (PLGA) has been widely used as degradable carrier for oral protein delivery.[13,14] Insulin-loaded PLGA nanoparticles and microcapsules have been reported to reduce the glucose level substantially in diabetic rats.[15,16] In an aqueous environment, PLGA degrades by hydrolysis to lactic and glycolic acid, both easily metabolized by the body.[13] During this process, the local environment in, for example, the intestine becomes more acidic and, therefore, the solubility of a protein-like insulin can be enhanced.[17,18] Mucoadhesive polymers can prolong the residence time of the carriers at the site of absorption.[19] Since the intestinal mucus turnover time ranges between 30 min and few hours, it can be considered slower than the time needed for absorption.[20] Chitosan, a mucoadhesive polymer, has been used as coating or carrier for micro- and nanoparticles for delivery of proteins improving their oral bioavailability.[8] At the same time as having mucoadhesive properties, it is also a permeation enhancer.[21,22] Polyethylene glycol (PEG) has also been widely utilized for oral delivery of proteins.[8] Depending on the molecular weight and surface concentration of PEG, it has been demonstrated to have either mucoadhesive or mucus penetrating properties.[23] Tobío et al. showed that microparticles of the degradable carrier polylactic acid (PLA) coated with PEG provided a five times higher oral bioavailability of tetanus toxoid than particles without coating. This was explained to be due to the mucus penetrating effect of PEG.[24]

In this study, microcontainers loaded with the model protein lysozyme and C10 were functionalized with polymeric lids to be tested in vitro and ex vivo for oral protein delivery. The microcontainers were functionalized by applying two layers as lids on top of the microcontainers, the first layer was PLGA and on top of this, either PEG or chitosan was applied (PLGA+PEG or PLGA+chitosan, respectively). The functionalized microcontainers were evaluated in vitro for morphology and drug release and, ex vivo for mucoadhesive properties. Furthermore, it was assessed if the functionalization of the microcontainers provided a controlled release and improved lysozyme transport in vitro and ex vivo using cell models and porcine intestinal tissue.

2. Results and Discussion

2.1. Functionalization of Microcontainers

The physical powder mixture of lysozyme and C10 (7:3) was loaded into the microcontainers (**Figure 1**a) with an average load per chip of 1.98 ± 0.36 mg corresponding to each microcontainer loaded with 3.1 ± 0.6 µg powder mixture (Figure 1b). The first functionalization layer was prepared with PLGA to help the dissolution of the protein.[13] It was observed that the polymer was homogeneously distributed over the microcontainers, although, the shape of the lysozyme powder was still visible (Figure 1c). On top of the PLGA layer, either a layer of PEG (Figure 1d,e) or chitosan (Figure 1f,g) was deposited as penetrating/mucoadhesive polymers. In both cases, after applying the second layer, the powder loaded into the microcontainers was completely covered and both coatings were smooth (Figure 1e,g). Moreover, considering the X-ray micro computed tomography (X-ray µCT) images, it was possible to conclude that the two layers were uniformly distributed on the chips (Figure 1d,f). The thicknesses of the different coatings with only one or two layers were measured using an optical profilometer (**Table 1**). Chitosan resulted to be the thinnest among all the layers which is due to the fact that the chitosan solution was prepared in a lower concentration compared to PLGA and PEG solutions and the spraying parameters were different. Moreover, all the measurements showed that the layers were homogeneously distributed within the same chip and among chips ($n = 3$, each measured in three points).

2.2. In Vitro Drug Release from Functionalized Microcontainers

The release of lysozyme from the coated microcontainers showed that for the three different coatings (PLGA, PLGA+chitosan, and PLGA+PEG), the loaded protein was released within 14 h (**Figure 2**). In the insert of Figure 2, it is noticeable that the different coatings resulted in different release profiles. The lysozyme released from the microcontainers coated with PLGA+chitosan reached 70.6 ± 6.6% within the first 2 h of the experiment. Microcontainers coated with only PLGA or PLGA+PEG showed a faster release (92.7 ± 4.6% and 93.3 ± 3.7%, respectively) in the first 2 h. Slower release from the PLGA coating can be achieved by utilizing PLGA standards with either higher molecular weight or larger ratios of lactide.[25] In accordance, it has been shown that coatings of PLGA+chitosan can induce a sustained release due to the low solubility of chitosan at pH 7.4[26,27] as this was also observed here for the microcontainers coated with these two polymers. In the literature, chitosan nanoparticles loaded with lysozyme showed a sustained release due to the swelling of the particles resulting in 20% of lysozyme released over 3 weeks.[28] Chitosan as a lid will also have a tendency to swell due to the hydrogel properties of chitosan[29,30] resulting in a slower diffusion process for lysozyme from the microcontainers causing a sustained release.

2.3. Ex Vivo Mucoadhesion Studies

Mucoadhesion studies applying intestinal porcine tissue were utilized to test if the top layer of the lid (chitosan or PEG) was adding a mucoadhesive feature to the microcontainers. Control of humidity and temperature (80% relative humidity and 37 °C) during the whole experiment allowed for mimicking the physiological environment, avoiding that the tissue dried out during the experiments (Figure S1, Supporting Information).[5] The number of microcontainers adhering to the tissue after 5 min of flow was considered a measure for mucoadhesiveness of the microcontainers. **Figure 3** shows that in the presence of PEG

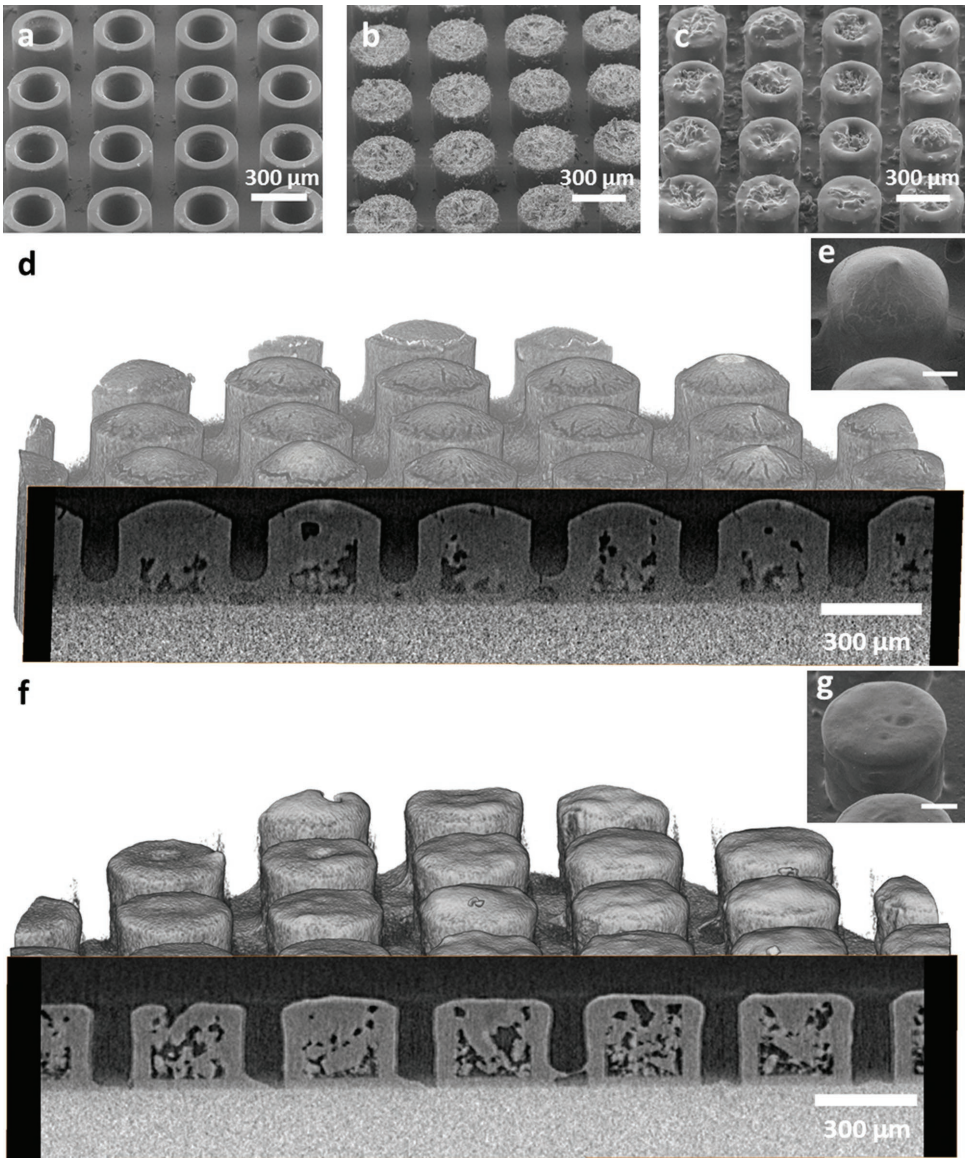

Figure 1. Scanning electron microscope (SEM) images of a) empty microcontainers, b) microcontainers loaded with lysozyme and C10 (7:3 w/w), and c) loaded microcontainers coated with PLGA. X-Ray µCT cross sections and reconstruction of loaded microcontainers coated with PLGA and on top of it either d) chitosan or f) PEG. The same samples are illustrated with SEM pictures in e) and g). The scale bars, where not indicated, correspond to 100 µm.

or chitosan, the percentage of microcontainers adhering to the tissue was higher (40.9 ± 5.5% and 35.7 ± 14.1%, respectively) than for the microcontainers without coating or with only PLGA (13.0 ± 2.3% and 19.3 ± 8.8%, respectively). This means that the number of microcontainers coated with either PEG or chitosan adhering to the tissue is twofold higher compared to the ones only coated with PLGA. If, instead, the number of samples coated with PLGA+PEG or PLGA+chitosan is compared with microcontainers without coating, they resulted to be three times more mucoadhesive. In particular, the number of microcontainers with PLGA+PEG layers that adhered was found to be statistically different from the ones having only one layer of PLGA ($p = 0.0097$). The high variability in these experiments can be caused by the random orientation of the microcontainers and by the use of different pieces of intestinal tissue having different mucus thicknesses that can lead to different adherence values.[31]

Table 1. Thicknesses of the different coatings either as individual coatings or combined with PLGA.

Coating	Thickness [µm]
PLGA	17.1 ± 2.4
PEG	17.0 ± 5.6
PLGA+PEG	32.5 ± 8.0
Chitosan	6.9 ± 1.1
PLGA+chitosan	22.5 ± 3.8

The data represent the mean of three samples measured in three different points of a chip (central and sides) ± standard deviation (SD).

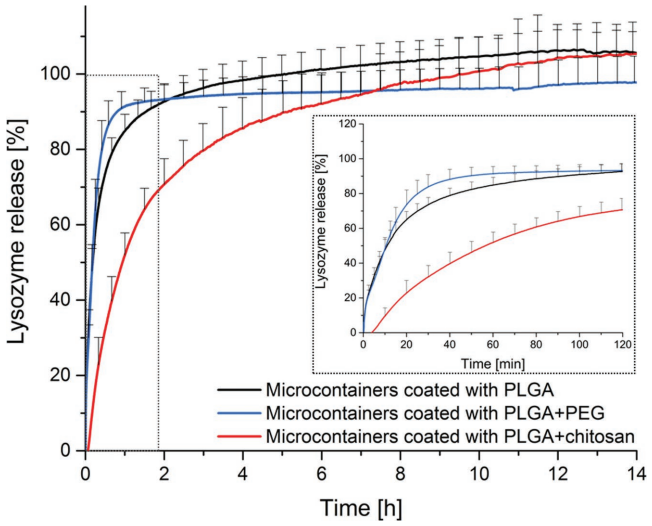

Figure 2. In vitro release of lysozyme from microcontainers with only PLGA, with PLGA+PEG, and with PLGA+chitosan coatings. The release was performed on a µ-DISS profiler in 10 mM phosphate buffered saline (PBS) at pH 7.4 and 37 °C. The data represent mean + SD, $n = 5–6$.

2.4. In Vitro Transport Studies

Transport studies were realized using Caco-2 cell monolayers or Caco-2/HT29-MTX-E12 co-culture monolayers as in vitro models for absorption through the small intestine. The Caco-2 cells are intensively used as an in vitro model for the intestinal epithelial barrier to determine the permeability of drug compounds through the intestinal barrier.[32] However, Caco-2 cells are lacking the goblet cells responsible for mucus production.[33] In vivo, the mucus layer acts as a physical and chemical defense from the luminal content and is important for the prediction of intestinal permeability of compounds, having a great importance for the absorption of proteins.[34] For this reason, the co-cultivation of Caco-2 and HT29 cell lines are widely used since it provides a model constituting the two cell types that are most represented in the intestinal epithelium in humans, enterocytes, and goblet cells.[35]

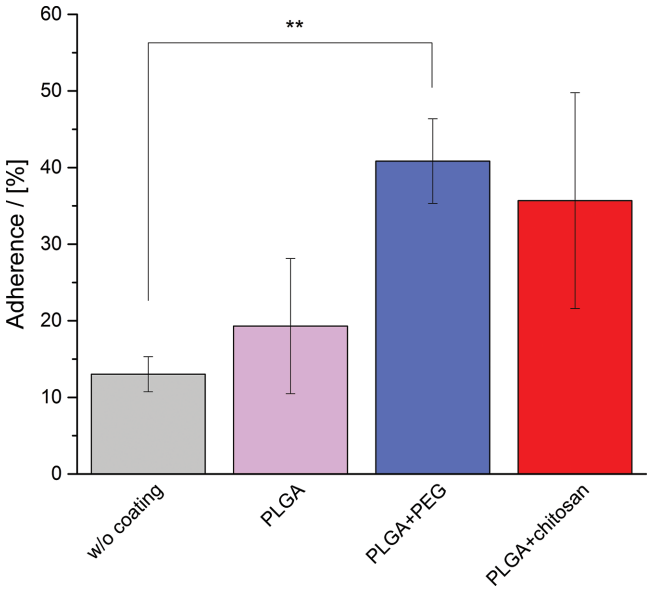

Figure 3. Percentage of microcontainers adhering to intestinal porcine tissue after flow for 5 min with 10 mM PBS at pH 7.4. The microcontainers were loaded with lysozyme and were either without coating, coated with only PLGA, PLGA+PEG, or PLGA+chitosan. The graph represents mean ± SEM ($n = 3$). **, p-value ≤ 0.01.

The percentage of transported lysozyme versus time across the Caco-2 monolayer or the co-culture was calculated. The profiles for the lysozyme confined in the microcontainers are similar to those of the bulk powder (**Figure 4**a). Although, the microcontainers coated with PLGA+chitosan showed a lag-time due to a slower transport of lysozyme. The average flux (Figure 4b) was calculated for each analyzed sample using Equation (1). The microcontainers coated with PLGA and PLGA+PEG displayed flux values of $5.3 \pm 1.4 \times 10^{-6}$ nmol min^{-1} cm^{-2} and $4.9 \pm 1.6 \times 10^{-6}$ nmol min^{-1} cm^{-2}, respectively, hence, there was no significant difference between their flux values (p-value 0.0803). These values are also similar to the bulk powder of lysozyme and C10. The slower onset in lysozyme transport for the chitosan samples (Figure 4a) is likely due to slower release of lysozyme. In addition, the slower onset resulted in a lower flux compared to all the other samples since the flux for microcontainers coated with PLGA+chitosan could be calculated only with two values. This delayed transport can be due to a delayed release of lysozyme from the microcontainers as showed in the in vitro studies (Figure 2) in which after 2 h, only 70.6 ± 6.6% was released. Moreover, it has previously been shown that the presence of chitosan in insulin nanoparticles resulted in a slower transport of insulin across Caco-2 monolayers compared to other formulations.[21] Determination of transepithelial electrical resistance (TEER) before and after the experiments allowed investigation of the integrity of the cell layer. The initial TEER values for all the cells were between 215–255 Ω cm^2 (Figure S2a, Supporting Information). At the end of the experiments, all TEER values, except for the blank, dropped to 90–120 Ω cm^2 (Figure S2a, Supporting Information). This complies with previous findings in the literature, observing that TEER is reduced across Caco-2 cells following treatment with chitosan[36] and especially C10[6,7] as they are both permeation enhancers. Thereby, they are interrupting tight junctions between the cells, but it is a reversible process and studies have shown that the cells recover within 24 h.[7,36] Microcontainers loaded with a protein and C10 (with the same molecular ratio as used in this study) have been tested and they did not show any cytotoxic effect on Caco-2 monolayers and on Caco-2/HT29-MTX-E12 co-culture monolayers (data not shown). Nevertheless, further characterization would be needed in the future to evaluate the cytotoxicity of the coating materials on Caco-2 cell monolayers or Caco-2/HT29-MTX-E12 co-culture monolayers. The transport of lysozyme from the microcontainers release across the Caco-2/HT29-MTX-E12 co-culture was slower than the bulk powder (Figure 4c). The calculated lysozyme flux for PLGA, PLGA+PEG and PLGA+chitosan coated microcontainer were $6.2 \pm 3.5 \times 10^{-6}$, $2.7 \pm 1.2 \times 10^{-6}$, and $3.9 \pm 0.8 \times 10^{-6}$ nmol min^{-1} cm^{-2}, respectively. The flux seems to be highly dependent on the presence of a polymeric coating on the microcontainers. All coated microcontainer samples resulted in a similar low lysozyme flux compared to the relatively high

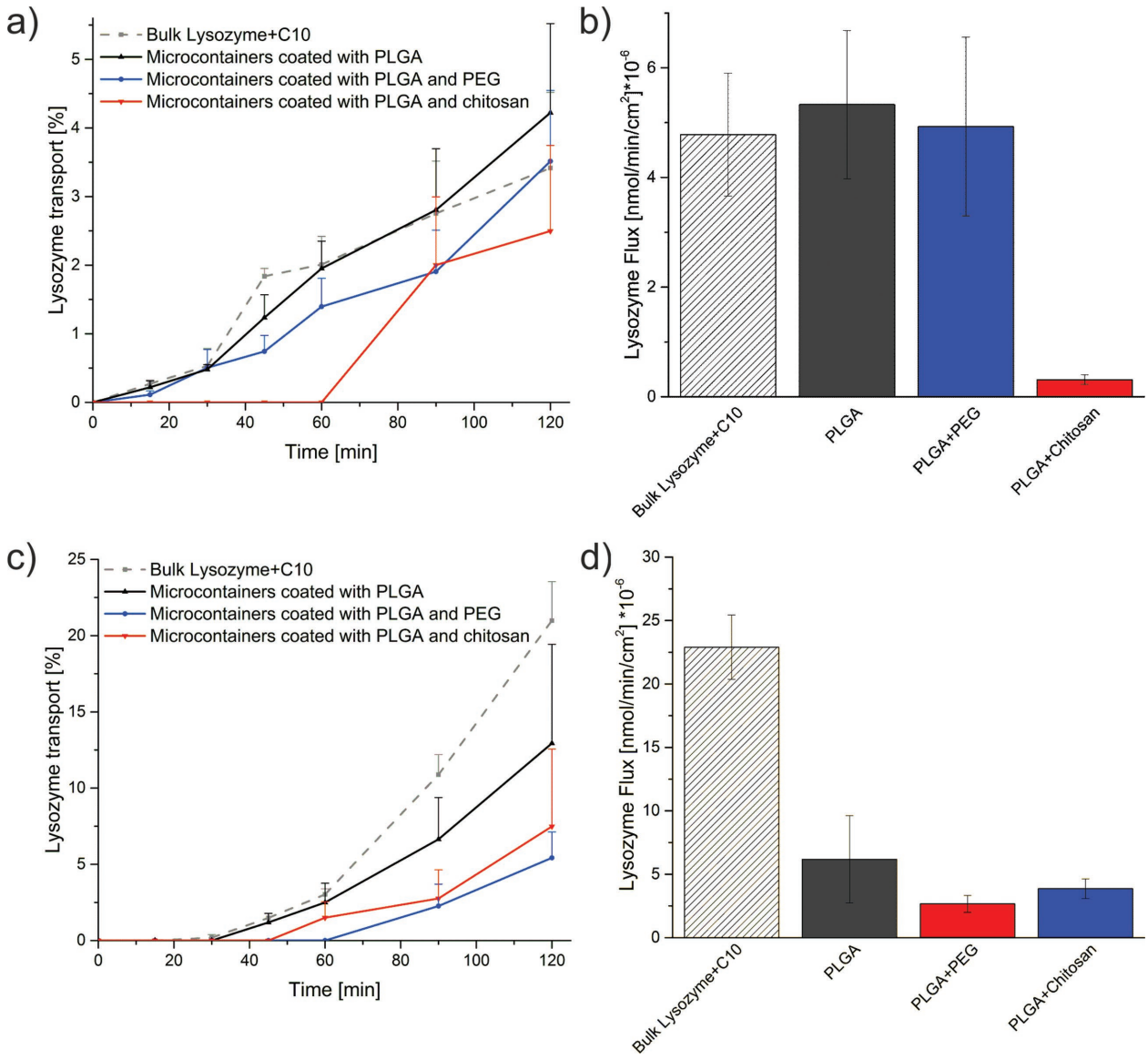

Figure 4. The transport of lysozyme across a) Caco-2 and c) Caco-2/HT29-MTX-E12 cell monolayers is shown for the bulk lysozyme powder and C10 and microcontainers coated with PLGA, PLGA+PEG, or PLGA+chitosan. From these values the lysozyme flux values were calculated and shown in b) for the transport across Caco-2 cell monolayer and in d) for Caco-2/HT29-MTX-E12 cell monolayers. The graphs represent mean + SEM ($n = 3$).

flux seen for the controls ($22.8 \pm 2.5 \times 10^{-6}$ nmol min^{-1} cm^{-2}). These results indicate that the coatings interact with the mucus present in the Caco-2/HT29-MTX-E12 co-culture resulting in a slower transport of lysozyme across the cell monolayers. The initial TEER values for Caco-2/HT29-MTX-E12 cell monolayers were at consistent levels in the range of 345–390 Ω cm^2 (Figure S2b, Supporting Information). TEER values dropped for all the samples at the end of the experiments (2 h), however not significantly for the blank (Figure S2b, Supporting Information). The microcontainers with the chitosan layer showed its permeation enhancing properties having a lower TEER value compared to the other coated with PEG or only PLGA.

The lowering of the TEER values for PLGA+chitosan, in both types of monolayers, highly indicated chitosan interaction with the cell monolayer. The lysozyme flux for the PLGA+chitosan coated microcontainers was observed to be higher across the co-culture than Caco-2 cell monolayers ($p = 0.0101$). A reason for this could be the presence of mucus and PEG-chitosan's known ability to form hydrogels.[37,38] This could allow slower diffusion of lysozyme through the coating in presence of mucus.[5]

2.5. Ex Vivo Transport Studies

Ex vivo transport studies are more representative of the intestinal barrier compared to the use of cell-culture models in which only few types of cells are present compared to the real tissue.[34] Hence, to mimic the in vivo situation as much as possible, intestinal transport studies were also carried out using porcine intestinal tissue in a side-by-side diffusion chamber.

The absorption of lysozyme was insufficient for chitosan coatings and a flux could not be calculated. This is believed to be caused by the slow release from the chitosan coating, due to the formation of the chitosan hydrogel, retaining the lysozyme.[38] This hydrogel behavior was very clear from a visual inspection after the experiment. Moreover, it has been shown that chitosan can bind and cross-link mucin and mucus gel and therefore, delay the diffusion of molecules through the chitosan/mucus gel.[39] From the tissue integrity evaluation at the end of the experiment (Figure S3, Supporting Information), it is noticeable that the P_{app} for PLGA+chitosan is higher than the other samples. It is important to note that, even after 180 min, the concentration of lysozyme in the donor chamber was ten times lower than for the other samples (data not shown) meaning that the lysozyme was not fully dissolved yet. This might be due to the fact that chitosan and C10 worked as permeation enhancers and this might not have any toxicity effect on the cell monolayer even though no lysozyme flux was observed. However, a flux of lysozyme was detected for the other samples and was $3.9 \pm 0.4 \times 10^{-6}$ nmol min^{-1} cm^{-2} for the control (not coated), $7.6 \pm 1.6 \times 10^{-6}$ for PLGA, and $5.3 \pm 0.3 \times 10^{-6}$ nmol min^{-1} cm^{-2} for PLGA+PEG (**Figure 5**). The microcontainers coated only with PLGA showed a higher flux probably due to the lower thickness of the coating compared to samples coated with the second layer of PEG.

3. Conclusion

This work demonstrated that microcontainers can be functionalized by applying two different layers on top of the cavity of the microdevices. Since PLGA is known as a degradable polymer to enhance the solubility of the protein, it has been chosen as first layer. PEG or chitosan represented the second layer as mucoadhesive or mucus penetrating polymers. Both PLGA+PEG and PLGA+chitosan resulted in homogeneous coatings on top of the lysozyme loaded microcontainers. The microcontainers with chitosan coating showed a slower lysozyme release compared to PLGA+PEG or PLGA coatings. With regard to the ex vivo mucoadhesive studies, it was found that the microcontainers coated by chitosan or PEG showed a threefold increase in porcine tissue adhesion, compared to the microcontainers without coatings. The in vitro studies with Caco-2 and Caco2/HT29-MTX-E12 co-culture monolayers and the ex vivo studies did not show transport enhancement and confirmed the results from the release study: chitosan-coated microcontainers result in a slower transport of lysozyme.

In this study, we obtained mucoadhesive microcontainers with tunable release for oral protein delivery. The functionalization will be further tested in vivo for better understanding.

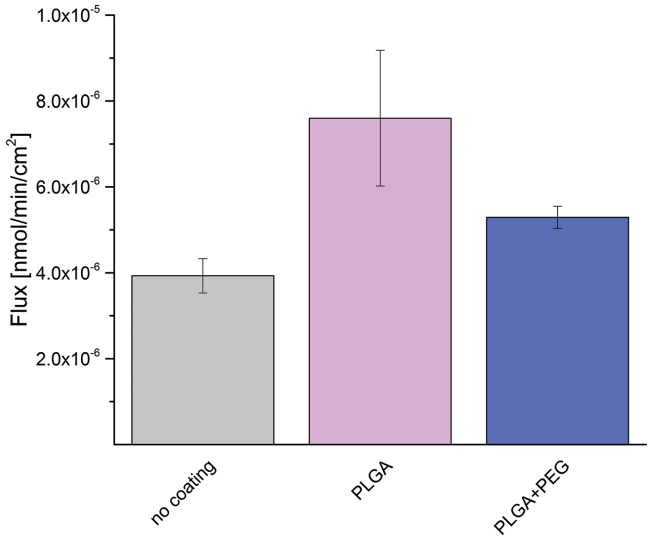

Figure 5. Flux of lysozyme across ex vivo porcine intestinal tissue. Microcontainers without coating, with PLGA, and with PLGA+PEG were tested. The data are represented as mean ± SEM with $n = 4$ (microcontainers with PLGA+chitosan, $n = 3$).

4. Experimental Section

Materials: Silicon (Si) wafers (4-in, b100N n-type) were provided by Okmetic (Vantaa, Finland), and SU-8 2075 and SU-8 developer were purchased from Microresist Technology GmbH (Berlin, Germany). Lyophilized lysozyme (from chicken egg white, 14.8 kDa) (≥40.000 units mg^{-1}, 90% purity), PBS tablets, chitosan (low MW 50–190 kDa, 75–85% deacetylation), PLGA (low MW 7–17 kDa, 50:50 PLA:PGA) were obtained from Sigma-Aldrich (St. Louis, MO, USA). 10x Hank's balanced salt solution (HBSS) and sodium bicarbonate were obtained from Thermo Fisher Scientific (Hampton, NH, USA), whereas PEG (low MW 12 kDa) was purchased from Fisher Scientific (Hampton, NH, USA). *n*-Capric acid C10 was obtained from abcr GmbH (Karlsruhe, Germany). 4-(2-hydroxyethyl)-1-piperazineethanesulfonic acid (HEPES), bovine serum albumin (BSA), and Dulbecco's Modified Eagle's Medium—high glucose, acetonitrile, trifluoroacetic acid (TFA), dichloromethane (DCM), and acetic acid (100.5%) were all acquired from Sigma-Aldrich (St. Louis, MO, USA). D-[1-^{14}C]-mannitol was obtained from PerkinElmer (Waltham, MA, USA). Milli-Q deionized water was provided by a MilliQ Integral Water Purification System for Ultrapure Water, produced by Merck Millipore (Burlington, MA, USA).

Fabrication of Microcontainers: Microcontainers were fabricated in the epoxy-based photoresist SU-8 using a procedure similar to the one described earlier.[40,41] A fluorocarbon coating was deposited on top of the supporting silicon wafer by plasma polymerization to ease the detachment of microcontainers from the chip.[11] The dimensions of the microcontainers were measured using an Alpha-Step IQ Stylus Profilometer (KLA-Tencor Corporation, Milpitas, USA) and optical microscopy. The fabricated microcontainers had an inner diameter of 232 ± 1 µm and a height of 255 ± 6 µm (mean ± SD, $n = 4$) (Figure 1a). After fabrication, the wafers were cut into squared chips of 1.2×1.2 cm containing 625 microcontainers using an Automatic Dicing Saw from DISCO (Kirchheim b. München, Germany).

Loading of Lysozyme into Microcontainers: To facilitate the loading of lysozyme, the received powder was lightly ground in a mortar to obtain a fine powder. Lysozyme was carefully mixed with C10 (7:3 w/w ratio). The ratio between lysozyme and C10 was chosen as it was found that this quantity of C10 ensured the opening of the tight junctions without cytotoxicity effects on the cell layer (data not shown). A shadow mask was attached on top of the chip to cover the areas in between the microcontainers and to avoid excess powder in these spaces.[42] The fine powder of lysozyme was evenly distributed on top of the mask and pressed into the cavity of the microcontainers with a brush. The shadow mask was removed together with the excess of powder resulting in filled microcontainers. The chips with microcontainers were weighted before and after filling to assess the amount of loaded powder.

Table 2. Parameters used for spray coating PLGA, chitosan, and PEG onto the cavity of microcontainers.

	PLGA	Chitosan	PEG
Shaping air [kPa]	0.03	0.01	0.03
Nozzle speed [mm s^{-1}]	10	25	10
Distance between the nozzle and the sample [mm]	50	25	50

Functionalization of Microcontainers: After loading, the coatings were applied onto the cavity of the microcontainers to functionalize them. The coating was performed by spray coating with an ExactaCoat Ultrasonic Spray System (Sonotek, USA) with an accumist nozzle operating at 120 kHz. The polymer solutions used were: PLGA (0.7%) in DCM (w/v), PEG (0.7%) in DCM (w/v), or chitosan (0.5%) in acetic acid (0.1 M, w/v). The PLGA lid was sprayed followed by either PEG or chitosan on top (PLGA+PEG or PLGA+chitosan, respectively). Microcontainers only with a PLGA lid were also investigated. During the procedure, the flow rate was kept at 0.1 mL min^{-1}, together with a generator power of 1.3 W. Each chip was coated with two alternating spray paths having an offset of 1 mm, resulting in a total of 60, 120, or 70 passages for PLGA, chitosan, or PEG, respectively. The shaping air, the speed of the nozzle, and the distance between the nozzle and the sample are described in **Table 2**. For the aqueous acidic solution used for the chitosan coating, the plate underneath the chip was set to a temperature of 40 °C during the spraying process.

Morphology Characterization: The samples PLGA+PEG and PLGA+chitosan were subjected to X-ray μCT investigations using a commercial Zeiss Xradia versa 410 system (Pleasanton, USA) to assess the coating morphology. The samples were mounted on a pin such that undisturbed 360° access to the sample was obtained. The pre-voltage was kept at 60 kV and the power at 10 W. The 4X optical objective was chosen resulting in an efficient pixel size of 2.83 μm, 3201 projection angles were measured over 360°. The exposure time for each projection was 4 s and the total scanning time 5 h and 2 min. All collected data were reconstructed by the commercial software connected to the system which relies on a Feldkamp, Davis, and Kress algorithm,[43] based on filtered back-projection algorithm. Three areas from each sample were analyzed to obtain a more representative image of the whole chip.

The loading and coating processes were investigated using a Tabletop Microscope TM3030 (Hitachi High-Technologies Europe GmbH, Krefeld, Germany). The samples were observed at a 30° tilt using 15 kV and secondary electrons (SE) detector.

Flat silicon chips with a layer of SU-8 on top were sprayed with each polymer solution for thickness measurements as described in the "Functionalization of Microcontainers" section. However, these were only coated on one half, by placing a flat half chip on top. The thickness measurements were performed with a KLA-Tencor Alpha-Step IQ stylus profilometer (Milpitas, CA, USA) with a scan speed of 50 μm s^{-1} and force of 15.3 mg. Each chip was measured in three different places (middle and sides).

In Vitro Drug Release from Functionalized Microcontainers: The release of lysozyme from the spray coated microcontainers was studied using a μ-DISS profiler (pION INC, Woburn, MA) connected to a temperature controlled water bath (Struers Kebo Lab, Rødovre, Denmark). The release of lysozyme from the coated microcontainers (with PLGA, PLGA+PEG, and PLGA+chitosan) was performed attaching each chip to a cylindrical magnetic stirrer and covering it with PBS (10 mL of 10 mM) at pH 7.4 at 100 rpm. The temperature was 37 °C and the absorbance was measured at 280 nm. The path length of the UV probes was 20 mm and each channel was calibrated with concentrations ranging from 0.03 to 0.3 mg mL^{-1}. The percentage of release was calculated from the known amount of powder loaded per chip. These experiments were replicated five to six times for microcontainers coated with PLGA, PLGA+PEG, or PLGA+chitosan.

Ex Vivo Mucoadhesion Studies: An ex vivo setup similar to the one described in literature[44,45] was used to perform the experiments for investigating the mucoadhesion of the coated microcontainers. Porcine intestine was obtained from healthy experimental control pigs (50–55 kg, 15–16 weeks of age, LYD pigs). Immediately after euthanasia of the pigs, the intestines were excised using a scalpel and placed in ice. Within 2 h, the tissues were frozen and on the day of the experiment, a 5 cm piece was cut longitudinally and placed on the supporting slide with the apical side facing upward. The mucosal side visually looked intact including the mucus layer as the intestine was frozen without preparation.

A pump (Watson Marlow, Falmouth, UK) was used to apply a peristaltic flow of PBS buffer (10 mM) at pH 7.4. The used setup was temperature and humidity controlled with a temperature of 37 °C and relative humidity of 80% (Figure S1, Supporting Information). Initially, the loosely adhering mucus was washed away for 1 min with a flow of 10 mL min^{-1}. After coating the chips, the microcontainers were gently manually scraped off the silicon chip. A defined amount of microcontainers (177 ± 35) were applied onto a spatula to ease the placement of them on the middle of the porcine intestinal tissue (in the flow path). Therefore, the orientation of the microcontainers on the tissue was random. Subsequently, a flow of 10 mL min^{-1} was applied for 5 min, after which the intestine was left to dry for 24 h. The remaining microcontainers were counted using a Leica S9E stereo microscope (Leica, Wetzlar, Germany) to determine the percentage of microcontainers that adhered to the intestinal tissue at the end of the experiment. This experiment was repeated with three different pieces of tissue for every type of sample (empty microcontainers, microcontainers with PLGA, PLGA+PEG, and PLGA+chitosan coatings).

In Vitro Transport Studies: The Caco-2 (HTB-37) cell line and HT29-MTX-E12 cell line were acquired by American Type Culture Collection (Manassas, VA, USA) and Inserm (Paris, France), respectively. The Caco-2 and the HT29-MTX-E12 cells were used in the number of passages of 37–43 and 65–71, respectively and co-culture monolayers were seeded in a 1:1 ratio of the two cell lines. All the cells were cultured as described by Natoli et al.,[46] and transport experiments were performed on polarized cells after 21 days on polycarbonate Transwell filters with a surface area of 4.67 cm^2 and 0.4 μm pore size (Corning Costar from Sigma-Aldrich, St. Louis, MO, USA). In vitro transport studies were carried out in six well plates, and before the experiment, each plate was left at room temperature for 20 min. Subsequently, TEER was measured using an Epithelial Volt/Ohm Meter (EVOM) (World Precision Instruments, Sarasota, FL, USA) with Endohm chambers for each well and all wells were afterward washed twice with HBSS buffer (1X HBSS, HEPES (10 mM), BSA (0.05% w/v), sodium bicarbonate (0.04% w/v)) with a pH of 7.4. Following this, HBSS buffer was added on the apical side (1.5 mL) and to the basolateral side (2.6 mL). Each chip was then gently placed upside down directly onto the cell layers. The experiment was initiated when the plates were put on a table shaker set at 75 rpm and 37 °C. Samples were taken (100 μL), and the volume was replaced with pre-heated HBSS, from the basolateral side at specific time points of 15, 30, 45, 60, 90, and 120 min. A single sample was also taken from the apical side after 120 min to normalize the release of proteins in the data analysis. After the 2 h runtime, the chips were gently removed. The cells were washed twice with HBSS buffer and TEER values were measured again. All samples were frozen at –20 °C and analyzed with the RP-HPLC methods described in "Reversed-Phase High-Performance Liquid Chromatography (RP-HPLC) method." The lysozyme flux (F) [mol cm^{-2} s^{-1}] was calculated according to Equation (1).

$$F = \frac{dQ}{dt} \cdot \frac{1}{A} \tag{1}$$

where dQ/dt [mol s^{-1}] is the rate of lysozyme permeation and A is the area of the inserts (4.67 cm^2). All the experiments were done in triplicates.

Ex Vivo Transport Studies: Ex vivo transport studies were performed using a modular EM-CSY-8 Ussing chamber system (Physiologic

Instruments, San Diego, CA, USA) including a temperature-controlled metal rack for mounting Ussing chambers in series. Ussing chambers containing a vertical port were assembled and mounted onto the rack. A slider was inserted between each pair of chambers and a volume of HBSS buffer (2 mL) at pH 7.4 was added to each chamber. The metal rack was pre-heated to equilibrate the system until the buffer in the chambers reached 35–37 °C. Moreover, humidified airflow was applied to each chamber. A piece of porcine intestine was carefully stripped to remove the serosa and the longitudinal and circular muscle layers of the intestine.[47] After equilibration, the buffer was removed, the chambers were dried, and the slider was taken out. A small cut of stripped intestine was carefully stretched and mounted into the slider by impaling the edges of the intestine on a circle of small metal pins around the aperture. Loaded and coated microcontainers were scraped off and gently applied onto the apical side of the intestine before the slider was re-inserted into the Ussing chambers. Pre-heated HBSS buffer (2 mL) pH 7.4 was then added to each chamber. Samples were taken from the receptor side (100 µL) at 30 min time intervals from 0 to 180 min. A single sample was also taken from the donor side (100 µL) at 0 and 180 min. All samples were analyzed with RP-HPLC described in "Reversed-Phase High-Performance Liquid Chromatography (RP-HPLC) method" and the flux was calculated as described in the "In Vitro Transport Studies" section. Following each ex vivo transport experiment, the integrity of the porcine intestine was evaluated by the flux of radioactive D-[1-^{14}C]-mannitol. A HBSS buffer with D-[1-^{14}C]-mannitol (0.1 mM) was prepared, and the solution (2 mL) was added to the apical side and regular HBSS buffer was added to the basolateral side (2 mL). Three samples (of each 100 µL) were taken at 0 and 60 min from both the apical and basolateral side. Three samples were also taken from the original D-[1-^{14}C]-mannitol (0.1 mM) HBSS buffer solution. Ultima Gold Scintillation fluid (2 mL) was added to each sample, vortexed, and analyzed by a scintillation analyzer (PerkinElmer, Tri-Carb 2910 TR). The apparent permeability coefficient (P_{app}) [cm s^{-1}] has been calculated according to Equation (2).

$$P_{app} = \frac{dQ}{dt} \cdot \frac{1}{A \cdot C_0} = \frac{F}{C_0} \quad (2)$$

where dQ/dt [mol s^{-1}] is the rate of lysozyme permeation, A is the area of the inserts (0.78 cm^2), C_0 [mol cm^{-3}] is the initial donor concentration of D-[1-^{14}C]-mannitol, and F is described in Equation (1).

All the experiments were repeated four times per sample type except for the microcontainers coated with PLGA and chitosan which were tested in triplicate.

Reversed-Phase High-Performance Liquid Chromatography Method: Samples obtained from the in vitro and ex vivo transport studies were analyzed by RP-HPLC on a Prominence Ultra-Fast Liquid Chromatography (UFLC) instrument system (Shimadzu, Japan). The column used was a Kinetex 5 µm XB-C18 (100 Å, 100 × 4.6 mm) (Phenomenex, USA). The mobile phases were acetonitrile with TFA (0.1%, v/v) (solvent A) and MilliQ deionized water with TFA (0.1%, v/v) (Solvent B) at 30 °C and solvent A had a steady gradient from 29% to 71% over 15 min at a flow rate of 1.4 mL min^{-1}, and the absorbance was measured at 280 nm. RP-HPLC has been used also to verify the integrity of the protein after grinding and leaving it at room temperature for 1 week (data not shown).

Statistical Analysis: Data is expressed as mean ± standard error of the mean (SEM) for ex vivo mucoadhesion studies and ex vivo and in vivo transport studies. Mean ± standard deviation (SD) has been used in all the other data analysis. *p*-values are calculated using the unpaired *t*-test in GraphPad Prism (GraphPad Software, CA, USA) and were considered statistically significant when below 5% ($p < 0.05$).

Supporting Information

Supporting Information is available from the Wiley Online Library or from the author.

Acknowledgements

R.D.J. and J.M. contributed equally to this work. The authors would like to acknowledge the Center for Intelligent Drug Delivery and Sensing Using Microcontainers and Nanomechanics (IDUN) whose research is funded by the Danish National Research Foundation (DNRF122) and Villum Fonden (Grant No. 9301). The 3D Imaging Centre at the Technical University of Denmark is gratefully acknowledged. Associate Professor Stephan Sylvest Keller is acknowledged for the help with fabrication of the microcontainers and fruitful discussions regarding the spray coating technique. Laboratory technicians Lene Grønne Pedersen and Mette Frandsen from University of Copenhagen are both acknowledged for their help regarding the cell cultivation.

Conflict of Interest

The authors declare no conflict of interest.

Keywords

microdevices, mucoadhesion, oral drug delivery, polymeric coating, protein

Received: January 3, 2019
Revised: March 20, 2019
Published online:

[1] D. Peer, J. M. Karp, S. Hong, O. C. Farokhzad, R. Margalit, R. Langer, *Nat. Nanotechnol.* **2007**, *2*, 751.
[2] P. C. Taylor, *Curr. Opin. Pharmacol.* **2003**, *3*, 323.
[3] M. Patel, A. Day, R. B. Warren, A. Menter, *Dermatol. Ther. (Heidelb)* **2012**, *2*, 16.
[4] M. Morishita, N. A. Peppas, *Drug Discov. Today* **2006**, *11*, 905.
[5] A. M. Wagner, M. P. Gran, N. A. Peppas, *Acta Pharm. Sin. B* **2018**, *8*, 147.
[6] T. Lindmark, N. Schipper, L. Lazorová, A. G. De Boer, P. Artursson, *J. Drug Target.* **1998**, *5*, 215.
[7] A. C. Chao, J. V. Nguyen, M. Broughall, A. Griffin, J. A. Fix, P. E. Daddona, *Int. J. Pharm.* **1999**, *191*, 15.
[8] D. J. McClements, *Adv. Colloid Interface Sci.* **2018**, *253*, 1.
[9] C. B. Fox, C. L. Nemeth, R. W. Chevalier, J. Cantlon, D. B. Bogdanoff, J. C. Hsiao, T. A. Desai, *Bioeng. Transl. Med.* **2017**, *2*, 9.
[10] B. F. Choonara, Y. E. Choonara, P. Kumar, D. Bijukumar, L. C. du Toit, V. Pillay, *Biotechnol. Adv.* **2014**, *32*, 1269.
[11] L. H. Nielsen, A. Melero, S. S. Keller, J. Jacobsen, T. Garrigues, T. Rades, A. Müllertz, A. Boisen, *Int. J. Pharm.* **2016**, *504*, 98.
[12] C. Mazzoni, F. Tentor, S. A. Strindberg, L. H. Nielsen, S. S. Keller, T. S. Alstrøm, C. Gundlach, A. Müllertz, P. Marizza, A. Boisen, *J. Controlled Release* **2017**, *268*, 343.
[13] F. Danhier, E. Ansorena, J. M. Silva, R. Coco, A. Le Breton, V. Préat, *J. Controlled Release* **2012**, *161*, 505.
[14] C. Snider, S.-Y. Lee, Y. Yeo, G. J. Grégori, J. P. Robinson, K. Park, *Pharm. Res.* **2008**, *25*, 5.
[15] S. Sun, N. Liang, H. Piao, H. Yamamoto, Y. Kawashima, F. Cui, *J. Microencapsul.* **2010**, *27*, 471.
[16] B. S. Kim, J. M. Oh, H. Hyun, K. S. Kim, S. H. Lee, Y. H. Kim, K. Park, H. B. Lee, M. S. Kim, *Mol. Pharmaceutics* **2009**, *6*, 353.
[17] B. S. Zolnik, D. J. Burgess, *J. Controlled Release* **2007**, *122*, 338.
[18] O. Siddiqui, Y. Sun, J.-C. Liu, Y. W. Chien, *J. Pharm. Sci.* **1987**, *76*, 341.
[19] S. K. Lai, Y.-Y. Wang, J. Hanes, *Adv. Drug Delivery Rev.* **2009**, *61*, 158.

[20] H. Schneider, T. Pelaseyed, F. Svensson, M. E. V. Johansson, *Sci. Rep.* **2018**, *8*, 5760.
[21] A. M. M. Sadeghi, F. A. Dorkoosh, M. R. Avadi, M. Weinhold, A. Bayat, F. Delie, R. Gurny, B. Larijani, M. Rafiee-Tehrani, H. E. Junginger, *Eur. J. Pharm. Biopharm.* **2008**, *70*, 270.
[22] I. A. Sogias, A. C. Williams, V. V. Khutoryanskiy, *Biomacromolecules* **2008**, *9*, 1837.
[23] Y.-Y. Wang, S. K. Lai, J. S. Suk, A. Pace, R. Cone, J. Hanes, *Angew. Chem. Int. Ed.* **2008**, *47*, 9726.
[24] M. Tobío, A. Sánchez, A. Vila, I. Soriano, C. Evora, J. Vila-Jato, M. Alonso, *Colloids Surf., B* **2000**, *18*, 315.
[25] G. Mittal, D. K. Sahana, V. Bhardwaj, M. N. V. Ravi Kumar, *J. Controlled Release* **2007**, *119*, 77.
[26] N. Ahmad, M. A. Alam, R. Ahmad, S. Umar, F. Jalees Ahmad, *J. Microencapsul.* **2018**, *35*, 1.
[27] K. Tahara, T. Sakai, H. Yamamoto, H. Takeuchi, Y. Kawashima, *Int. J. Pharm.* **2008**, *354*, 210.
[28] A. M. Piras, G. Maisetta, S. Sandreschi, S. Esin, M. Gazzarri, G. Batoni, F. Chiellini, *Int. J. Biol. Macromol.* **2014**, *67*, 124.
[29] F. Ahmadi, Z. Oveisi, S. M. Samani, Z. Amoozgar, *Res. Pharm. Sci.* **2015**, *10*, 1.
[30] M. R. Rekha, C. P. Sharma, *Protein and Peptide Delivery* (Ed: C. Van Der Walle), Elsevier, Amsterdam **2011**, pp. 165–194.
[31] M. P. D. Gremião, F. C. Carvalho, M. L. Bruschi, R. C. Evangelista, M. Palmira, D. Gremião, *Brazilian J. Pharm. Sci.* **2010**, *46*.
[32] H. Sun, E. C. Chow, S. Liu, Y. Du, K. S. Pang, *Expert Opin. Drug Metab. Toxicol.* **2008**, *4*, 395.
[33] T. Lea, in *The Impact of Food Bioactives on Health* (Eds: K. Verhoeckx, P. Cotter, I. López-Expósito, C. Kleiveland, T. Lea, A. Mackie, T. Requena, D. Swiatecka, H. Wichers), Springer International Publishing, Cham **2015**, pp. 103–111.
[34] C. R. Kleiveland, in *The Impact of Food Bioactives on Health* (Eds: K. Verhoeckx, P. Cotter, I. López-Expósito, C. Kleiveland, T. Lea, A. Mackie, T. Requena, D. Swiatecka, H. Wichers), Springer International Publishing, Cham **2015**, pp. 135–140.
[35] A. Wikman-Larhed, P. Artursson, *Eur. J. Pharm. Sci.* **1995**, *3*, 171.
[36] T.-H. Yeh, L.-W. Hsu, M. T. Tseng, P.-L. Lee, K. Sonjae, Y.-C. Ho, H.-W. Sung, *Biomaterials* **2011**, *32*, 6164.
[37] S. Lu, K. S. Anseth, *Macromolecules* **2000**, *33*, 2509.
[38] S. Yan, T. Wang, X. Li, Y. Jian, K. Zhang, G. Li, J. Yin, *RSC Adv.* **2017**, *7*, 17005.
[39] S. Kootala, L. Filho, V. Srivastava, V. Linderberg, A. Moussa, L. David, S. Trombotto, T. Crouzier, *Biomacromolecules* **2018**, *19*, 872.
[40] P. Marizza, S. S. Keller, A. Boisen, *Microelectron. Eng.* **2013**, *111*, 391.
[41] L. H. Nielsen, S. S. Keller, K. C. Gordon, A. Boisen, T. Rades, A. Müllertz, *Eur. J. Pharm. Biopharm.* **2012**, *81*, 418.
[42] Z. Abid, C. Gundlach, O. Durucan, C. von Halling Laier, L. H. Nielsen, A. Boisen, S. S. Keller, *Microelectron. Eng.* **2017**, *171*, 20.
[43] L. A. Feldkamp, L. C. Davis, J. W. Kress, *J. Opt. Soc. Am. A* **1984**, *1*, 612.
[44] K. D. Madsen, C. Sander, S. Baldursdottir, A. M. L. Pedersen, J. Jacobsen, *Int. J. Pharm.* **2013**, *448*, 373.
[45] K. V. R. Rao, P. Buri, *Int. J. Pharm.* **1989**, *52*, 265.
[46] M. Natoli, B. D. Leoni, I. D'Agnano, A. Felsani, *Toxicol. Vitr.* **2012**, *26*, 1243.
[47] L. L. Clarke, *Am. J. Physiol. Gastrointest. Liver Physiol.* **2009**, *296*, G1151.

Supporting Information

for *Macromol. Biosci.,* DOI: 10.1002/mabi.201900004

Polymeric Lids for Microcontainers for Oral Protein Delivery

Chiara Mazzoni,* Rasmus Due Jacobsen, Jacob Mortensen, Jacob Rune Jørgensen, Lukas Vaut, Jette Jacobsen, Carsten Gundlach, Anette Müllertz, Line Hagner Nielsen,* and Anja Boisen

Supporting Information

Polymeric Lids for Microcontainers for Oral Protein Delivery

Chiara Mazzoni[1,*] , Rasmus Due Jacobsen[1#], Jacob Mortensen[1#], Jacob Rune Jørgensen[2], Lukas Vaut[1], Jette Jacobsen[2], Carsten Gundlach[3], Anette Müllertz[2], Line Hagner Nielsen[1,*], Anja Boisen[1]

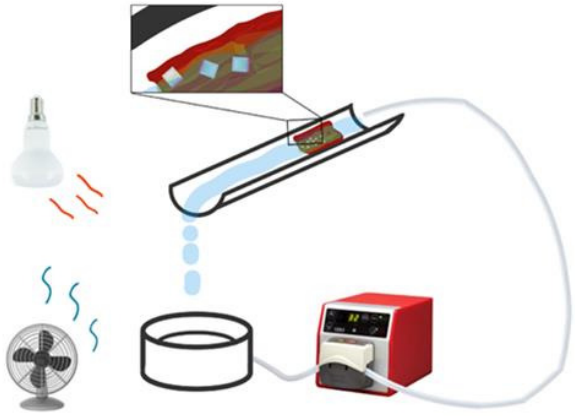

Figure S1: Schematic representation of the ex vivo mucoadhesion setup. Pig intestine is placed on a slide and flushed with a peristaltic pump. The temperature and humidity are controlled.

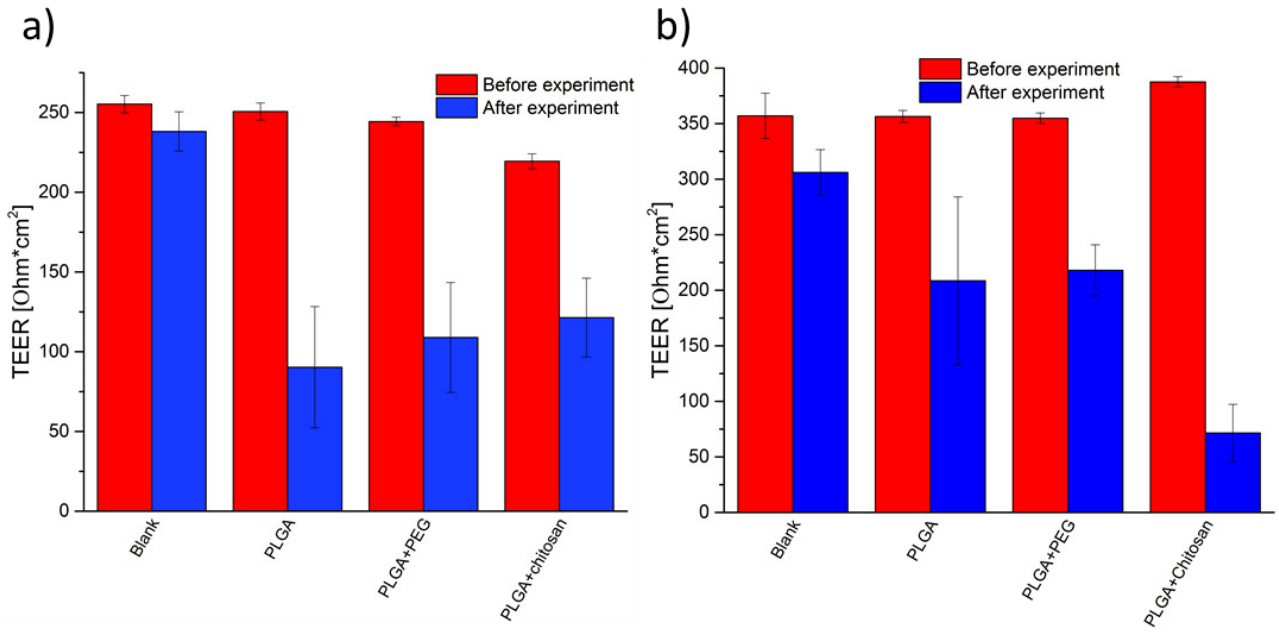

Figure S2: TEER values measured before and after the experiments for the blank, microcontainers coated with PLGA, PLGA+PEG and PLGA+chitosan. These were done with a) Caco-2 cell monolayer and b) Caco-2/HT29-MTX-E12 cell monolayers (mean ± SD, n = 3).

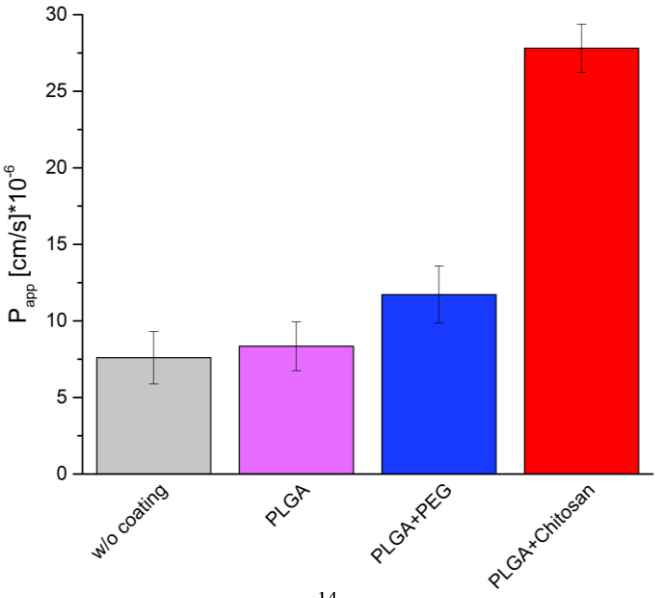

Figure S3: P_{app} of D-[1-^{14}C]-mannitol calculated after the ex vivo transport studies comparing the microcontainers without coating with the ones with only PLGA, PLGA+PEG and PLGA+chitosan. All the values are represented as mean ± SD, n = 2-4.

Microcontainers are polymeric cylindrical microdevices designed for oral drug delivery. They have an external diameter and a height of approximately 300 µm. Contrary to the omni-directional release that is characteristic for oral drug formulations like tablets, capsules and particulate systems, the unidirectional release provided by microcontainers avoids loss of the drug in the lumen. In this project, the work focused on two main aspects i) loading techniques of drugs into microcontainers for enhancing oral delivery of poorly water soluble drugs and ii) coating the cavity of microcontainers in order to functionalize these for increasing the oral absorption of proteins. This project showed a promising potential for microcontainers as oral delivery system for poorly soluble drugs and proteins.

Danmarks Tekniske Universitet

DTU Health Tech
Department of Health Technology
Ørsteds Plads, Building 345C
DK-2800 Kgs. Lyngby
Denmark

Email: healthtech-info@dtu.dk
www.healthtech.dtu.dk